THESIS

COMPETITIVENESS OF STRUCTURAL SYSTEMS IN MEDIUM-HEIGHT REINFORCED CONCRETE BUILDINGS

RINCHEN

GRADUATE SCHOOL, KASETSART UNIVERSITY
2008

THESIS APPROVAL

GRADUATE SCHOOL, KASETSART UNIVERSITY

Master of Engineering (Civil Engineering)

DEGREE

Civil Engineering	Civil Engineering
FIELD	**DEPARTMENT**

TITLE: Competitiveness of Structural Systems in Medium-Height Reinforced Concrete Buildings

NAME: Mr. Rinchen

THIS THESIS HAS BEEN ACCEPTED BY

Kitjapat P. **THESIS ADVISOR**

(Mr. Kitjapat Phuvoravan, Ph.D.)

Piya Chotickai **THESIS CO-ADVISOR**

(Assistant Professor Piya Chotickai, Ph.D.)

B. Vardhanabhuti **THESIS CO-ADVISOR**

(Mr. Barames Vardhanabhuti, Ph.D.)

DEPARTMENT HEAD

(Associate Professor Korchoke Chantawarangul, Ph.D.)

APPROVED BY THE GRADUATE SCHOOL ON May 20, 2008

Vinai Artkongharn. **DEAN**

(Associate Professor Vinai Artkongharn, M.A.)

THESIS

COMPETITIVENESS OF STRUCTURAL SYSTEMS IN MEDIUM-HEIGHT REINFORCED CONCRETE BUILDINGS

RINCHEN

A Thesis Submitted in Partial Fulfillment of
the Requirements for the Degree of
Master of Engineering (Civil Engineering)
Graduate School, Kasetsart University
2008

Rinchen 2008: Competitiveness of Structural Systems in Medium-Height Reinforced Concrete Buildings. Master of Engineering (Civil Engineering), Major Field: Civil Engineering, Department of Civil Engineering.
Thesis Advisor: Mr. Kitjapat Phuvoravan, Ph.D. 138 pages.

Structural system is the integral part of the building in resisting the lateral loads arising from earthquake and wind. In this study, five different structural systems namely rigid frame, shearwalled-frame, framed-tube, braced-tube and outrigger are incorporated into the hypothetical 25-story reinforced concrete building in sequence to examine the response of each under the effect of earthquake and wind. Seismic analyses based on response spectrum and linear time history analysis, and the dynamic effects due to wind are considered. Structural responses in terms of natural periods, story shear, story moment, story deflection and story drift ratio, obtained from the analyses, are compared among different structural systems. Because of the symmetrical plan of the building adopted in this study, analysis of eigenproblem yielded nearly equal natural periods for two consecutive modes of vibration. The seismic story shear and story moment are marked by irregular variation while wind story shear and story moment are smooth over the height of building. However, the story displacement and story drift profile are similar, differing only in magnitude, for both earthquake and wind. Structural systems having shorter periods are governed by the seismic responses. Conversely, structural systems with longer periods are governed by the wind responses. Hence, the use of same approximate periods, stipulated in many codes, does not provide same level of safety for both wind and earthquake. Cross-wind accelerations at roof level are higher than along-wind acceleration, indicating that cross-wind has significant influence on human comfort criteria. Besides structural behaviour, cost forms another important factor in the evaluation of performance of structural systems.

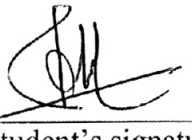

Student's signature

Kitjapat P.

Thesis Advisor's signature

12 / May / 2008

ACKNOWLEDGEMENTS

I am indebted to many people who have contributed to the success of this research. In this regard, I would like to extend my gratitude and sincere appreciation to my thesis advisor Dr. Kitjapat Phuvoravan for his valuable technical guidance, encouragement and insight provided during this research. My appreciation is also due to Assistant Professor Dr. Piya Chotickai and Dr. Barames Vardhanabhuti for their suggestions. I thank Binay Charan Shrestha, my colleague and a graduate student from Nepal, for graciously sharing his wealth of resource materials with me. Support and encouragement received from many friends are gratefully acknowledged.

I express my gratitude to Thailand International Cooperation Agency (TICA) for providing the scholarship to undertake this research. Thanks are also to Dr Trakool Aramraks, and the staff of the International Graduate Program in Civil Engineering (IPCE), Kasetsart University, Bangkhen for rendering all the support and assistance.

A few more people deserved to be thanked for assisting me in my endeavor to pursue higher studies which culminated into the completion of this research. In this regard, I would like to extend my gratitude to my parents for their incessant advice and unconditional love throughout my life. Without your counsel, I doubt I would have achieved this level of thinking and understanding. Thanks are also to my father-in-law Sonam Dorji and my late mother-in-law Neten Dema for their financial assistance during my school. Mother-in-law's advice, counsel, and warm smile will be sorely missed. During my childhood, my grandma Sangay Dema had caressed, nurtured, and brought out the idea to put me in school. Thanks for this great idea and care. Thanks are also to my brothers and sisters for their support and encouragement during this study.

Lastly, I thank my beloved wife Sonam Yangdon and my loving son, Jigme Namgyel Zigs for their love, support, sacrifice and understanding.

Rinchen

April 2008

TABLE OF CONTENTS

LIST OF TABLES

LIST OF TABLES (Continued)

LIST OF FIGURES

LIST OF FIGURES (Continued)

LIST OF FIGURES (Continued)

LIST OF ABBREVIATIONS

ACI	=	American Concrete Institute
ASCE	=	American Society of Civil Engineers
AS	=	Australian Standard
BSR	=	Bhutan Schedule of Rates
CQC	=	Complete Quadratic Combination
DBE	=	Design Basis Earthquake
DOFs	=	Degree Of Freedoms
Eq.	=	Equation
FEMA	=	Federal Emergency Management Agency
IS	=	Indian Standard
LATBSDC	=	Los Angeles Tall Buildings Structural Design Council
MCE	=	Maximum Considered Earthquake
Nu	=	Ngultrum (Currency of Bhutan)
NZS	=	New Zealand Standard
NEHRP	=	National Earthquake Hazards Reduction Program
OPC	=	Ordinary Portland Cement
SI	=	Spectrum Intensity
SRSS	=	Square Root of Sum of Squares
2D	=	Two Dimension
3D	=	Three Dimension

COMPETITIVENESS OF STRUCTURAL SYSTEMS IN MEDIUM-HEIGHT REINFORCED CONCRETE BUILDINGS

INTRODUCTION

Structural system is to the building what skeleton is to the human body. It comprises of both horizontal and vertical structural elements that acting jointly support and transmit to the ground the loads arising from earthquake motions, wind, gravity and lateral earth pressure. Its role becomes increasingly important with the increase in building height. Thus, the vital criteria for structural systems are adequate reserve of strength against failure, adequate lateral stiffness, and efficient performance during the service life of the building.

Historically, the structural systems for the early high-rise buildings were exclusively of steel since very little knowledge about the properties of concrete was known then. However, by the turn of the century, with the advancement of research on concrete, its use in structural systems became prevalent.

Nowadays, concrete is widely used in the construction of medium-height buildings, especially in developing countries. It has become the favorite material for builders of medium-height buildings, since it possesses superior properties with regard to fire resistance, sound absorption, insulation, damping and mouldability. Advances in formwork design, concrete mix, pumping techniques and use of admixtures have further contributed to the ease of working with concrete in medium-height buildings.

With the increase in building height, the need to provide stiff and strong structures to counteract the forces of nature became necessary. This has led to radical development in structural systems. Based on the arrangement of structural elements, wide varieties of structural systems are available; each designed to suit the requirements of individual building.

The behavior of structural systems towards wind or earthquake forces is predominantly characterized by the lateral sway motion. Some differences, however, exist with regard to the lateral response of buildings. In the case of structural response to earthquake, significant contribution of higher modes of vibration can be expected. However, for wind, the higher modes of vibration have negligible influence on building responses, and the responses are generally described in terms of fundamental mode of vibration.

While the lateral force on building due to wind increases nonlinearly with the increase in building height, the significance of seismic forces with the increase in building height is not easily discernable. This is because seismic forces are very much related to the mass and the natural period of vibration of structures. On one hand, the mass increases with the increase in building height resulting in the increase of lateral forces. On the other hand, the seismic load decreases with the increase of building periods. As height increases, it generally results in lengthening of periods. Moreover, for wind load, serviceability issues such as motion perception may govern the design in addition to the strength, while for seismic load, serviceability issues are rarely taken into consideration and the design is based on strength requirements.

To determine the efficiency of structural systems, it is not only important to understand their behavior but also it is useful to know the relative cost of materials for structural systems. This is because the quantity of materials required for lateral load resistance increases nonlinearly with the increase in building height. Material requirements also differ among different structural systems.

Statement of the Problem

Though the wealth of knowledge exist in relation to the individual structural system under the effect of single lateral loading arising from either earthquake motion or wind, the research on the behavior of different structural systems under the effect of both wind and earthquake is rare. Many researchers have focused their attention on either very tall buildings or low-rise buildings, and that too, on the narrow aspect of

the behavior, thus overshadowing the global behavior of the structure. Further, too much attention is given to the analysis that the adequacy of the structural member is seldom checked before commencing the next cycle of analysis. In most cases, the analysis results are reported based on the inadequate structural members. Moreover, in a quest to prove the mathematical prowess, some researchers have attempted to describe the structural behavior in complicated mathematical terms, thus obscuring the understanding of true behavior of real structures.

Additionally, many codes stipulate the use of approximate fundamental natural period to determine the static force due to earthquake and dynamic effects due to wind. Since the nature of loading is different, the use of same period both for earthquake and wind load computation may not be appropriate.

Further, the superior performance of the structural systems with regard to deflection and lateral load resistance does not translate into the least cost of materials. Nevertheless, in some cases, the efficiency of the structural systems is evaluated on the basis of analytical performance while disregarding the quantity of materials required for the structural systems.

Towards this end, in this study, an effort is being made to describe the behavior of different structural systems of medium-height reinforced concrete building under the effect of lateral load arising from both earthquake and wind. The subtle differences with regard to responses of individual structural system towards these forces are being pointed out. The merits and demerits of the use of approximate fundamental time period, stipulated in many codes, with regard to the computation of wind and earthquake load are highlighted. The various response quantities of the building are reported based on the adequate member sizes. Finally, different structural systems are assessed for their performance based on their resistance to lateral load, and the cost of structural materials.

OBJECTIVES

This research is being carried out with the following objectives:

1. To investigate the behavior of different structural systems under wind and seismic loading

2. To compare the seismic and wind responses of different structural systems

3. To assess the performance of structural systems based on the lateral load resistance and the cost of materials

Scope

This study focuses on the behavior of hypothetical 25-story reinforced concrete buildings with different structural systems under the effect of wind and earthquake loading. Five different structural systems: rigid frame, shearwalled-frame, framed-tube, braced-tube and outrigger systems are incorporated into the above building separately to examine the behavior of each structural system.

Seismic analysis as per Indian Standard IS 1893 (2002) and dynamic effect due to wind as per Indian Standard IS 875: Part 3 (2004) are used to investigate the responses of each structural system. Second-order elastic analysis is performed to obtain the necessary responses for the comparison of behavior of different structural systems. The adequacy of structural members for structural systems is checked with the requirements of Indian Standard IS 456 (2000).

Different structural systems are assessed for their performance based on their behavior under the effect of lateral loads arising from wind and earthquake, and the cost of structural materials required for each structural system.

LITERATURE REVIEW

This section of the thesis explains the important concepts that are prerequisites to the understanding of the subsequent parts of the thesis. In particular, this part of the thesis covers the reasons for the choice of Indian Standards for this study. This is followed by the brief background to five structural systems that are selected for the study. Thereafter, structural modelling and relevant issues including geometric modelling, material modelling and, gravity and horizontal loading due to wind and earthquake are described. Subsequently, the structural analyses with particular emphasis on the P-Delta effect are explained. The serviceability issues such as deflection, drift and human comfort criteria are outlined. Finally, the economy of structural systems are described.

1. Background to the use of Indian Standards

Exhaustive references to Indian Standards have been made in this study. This is because this study has been carried out with the intention that medium-height reinforced concrete building similar to the one in this study may be constructed in Bhutan in the distant future. Although Bhutan has few building standards, they are not fully developed right now. This has required the use of standards belonging to other countries for the structural design of buildings. The choice of Indian Standards in preference to other countries standards may partly be attributed to the fact that most of the construction materials in Bhutan are imported from India, thus rendering easy use of the standards. The other reasons could be due to the geological setting of the country. Since Bhutan lies on the Himalayas, which is considered to be one of the most seismically active regions of the world, the country has been considered to fall under the seismic zone V (most seismically active zone) as per the Indian Standard Criteria for Earthquake Resistant Design of Structures (2002). This has required all buildings to be designed for severest case of earthquake (zone V) in Bhutan. In line with the above stated reasons, Indian Standards have been chosen for this study too. Apart from Indian Standards, other relevant standards are also used as supplements.

2. Structural Systems

Structural systems comprise of both horizontal and vertical structural elements that acting jointly support and transmit to the ground the loads arising from earthquake motions, wind, gravity and lateral earth pressure. Its role becomes increasingly important with the increase in building height. Thus, the vital criteria for structural systems are adequate reserve of strength against failure, adequate lateral stiffness, and efficient performance during the service life of the building.

The determination of the structural forms of a building involves the selection and arrangement of the major structural elements to resist most efficiently the various combinations of gravity and horizontal loadings. The choice of structural form is strongly influenced by the internal planning, the material and method of construction, the external architectural treatment, the location and routing of service systems, the nature and magnitude of the horizontal loading, and the height and proportion of the building (Smith and Coull, 1991).

With regard to horizontal loading, a high-rise building is essentially a vertical cantilever (Smith and Coull, 1991). As height increases, the lateral force begins to dominate the structural systems and becomes increasingly important in the overall building system (Tarnath, 1988).

Strength, rigidity and stability are the three main factors to consider in the design of all structures. For high-rise building, rigidity and stability requirement are often the dominant factors in the design. There are basically two ways to satisfy these requirements in a structure. The first is to increase the size of the members beyond and above the strength requirements. However, this approach has its own limits, beyond which it becomes either impractical or uneconomical to increase the sizes. The second and more elegant approach is to change the form of the structure into something more rigid and stable to limit the deformation and increase stability (Tarnath, 1988).

Based on the arrangement of structural elements, wide varieties of structural systems have evolved over the years. In fact, there are so many structural systems, each designed to suit the requirements of individual building, that it is difficult to classify them into distinct categories (Tarnath, 1998). Nonetheless, Gunel and Elgin (2007) have broadly classified the structural systems into the following:

1) Rigid frame systems
2) Braced frame and shear-walled frame systems
3) Outrigger systems
4) Braced-tube systems
5) Bundled-tube systems

Complex structural systems can be formed by the combination of different structural systems given above. General background to a few selected structural systems that seem relevant to medium-height reinforced concrete buildings, and those included in this study, are described hereunder. The detailed descriptions along with the analytical formulation for various structural systems under general lateral loading can be found elsewhere (Smith and Coull, 1991; Tarnath, 1988, 1998).

2.1 Rigid frame systems

Rigid frame systems consist of columns and beams joined by moment-resisting connections (Smith and Coull, 1991). Rigid frame systems are ideally suited for reinforced concrete structures owing to the inherent joint rigidity developed as a result of monolithic construction (Smith and Coull, 1991; Gunel and Elgin, 2007).

The horizontal stiffness of a rigid frame is governed by the bending stiffness of the columns, beams, rigidity of joint, and the axial rigidity of columns (Smith and Coull, 1991). The strength and stiffness are proportional to the dimension of the beam and the column, and inversely proportional to the column spacing (Gunel and Elgin, 2007). Thus in order to obtain an efficient frame action, closely spaced columns is mandatory.

Under lateral loading, rigid frame systems are governed by two modes of deformation: shear deformation due to lateral sway of the frames and the bending deformation due to axial extension and shortening of columns (Figure 1). Usually shear deformation predominates in high-rise rigid frame structures.

For a building in high seismic areas, design of beam-column joints becomes an important issue in this type of structural systems.

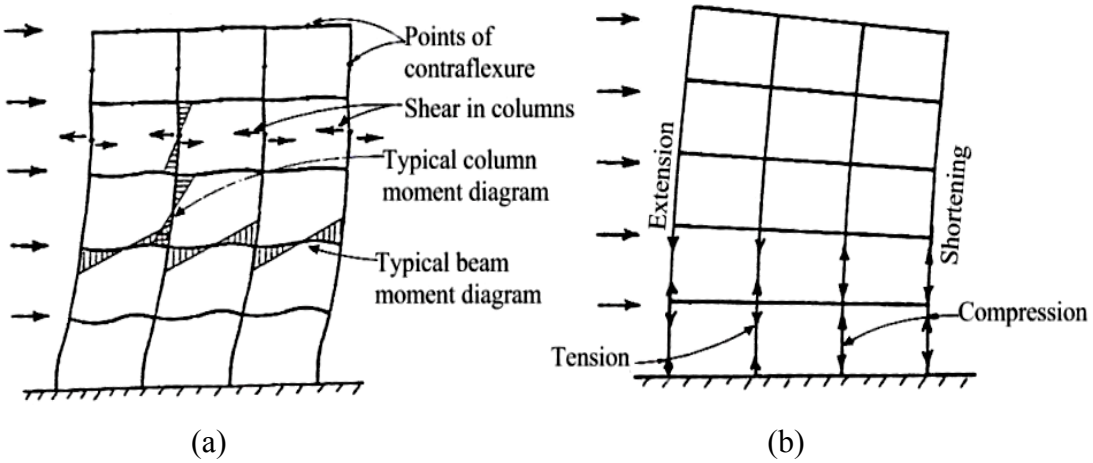

Figure 1 Rigid frame system; a) Shear deformation; b) Bending deformation
Source: Smith and Coull (1991)

2.2 Shear-walled frame systems

Shear-walled frame systems resist the lateral load by a combined action of shear wall and rigid frames (Figure 2). A shear wall deflects predominantly in a bending mode whereas a rigid frame bends in a shear mode (MacLeod, 1970). As the structural elements are not free to deform independently, a considerable horizontal interaction develops in the structural systems. The degree of interaction depends on the relative stiffness of the walls and frames, and the height of the structure (Smith and Coull, 1991).

The linear sway of the moment frame, when combined with the parabolic sway of the shearwall results in an enhanced stiffness because the wall is restrained by

the frame at the upper levels while at the lower levels the frame is restrained by the wall (Tarnath, 1998).

However, the behaviour of shearwalled-frame is drastically altered if the stiffness of the walls and the frames are abruptly changed instead of using the same stiffness throughout the height of the building. Actual behavior of complex shearwalled-frame can only be captured from the numerical analysis (Tarnath, 1998).

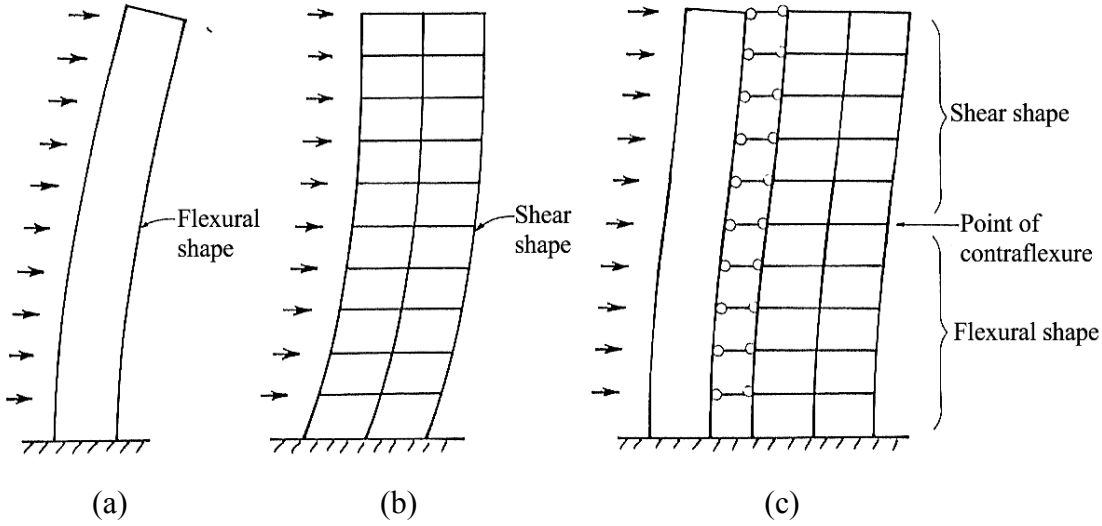

Figure 2 Shearwalled-frame system; a) Wall under uniform loading; b) Frame under uniform loading; c) Wall-frame under uniform loading

Source: Smith and Coull (1991)

2.3 Framed-tube systems

The primary characteristic of a framed-tube system is the employment of closely spaced perimeter columns interconnected by deep spandrels, so that the whole building works as a huge vertical cantilever to resist overturning moments. The efficiency of this system is derived from the great number of rigid joints acting along the periphery, creating a large tube. Exterior tube carries all the lateral loading. The gravity loading is shared between the tube and the interior columns or walls, if they exist (Gunel and Ilgin, 2007).

Normally, the strong bending direction of the columns is aligned along the face of the building in contrast to typical rigid frame building (Smith and Coull, 1991).

The primary resistance to lateral load is provided by the overall bending of the tube, which introduces tensile and compressive forces in the tube's windward and leeward faces. However, due to the flexibility of the beam, the deformation of the corner columns is more than the interior columns (Tarnath, 1988; Smith and Coull, 1991). Thus the axial stresses in columns are not uniform but somewhat parabolic in shape with maximum stress at corner column (Figure 3).

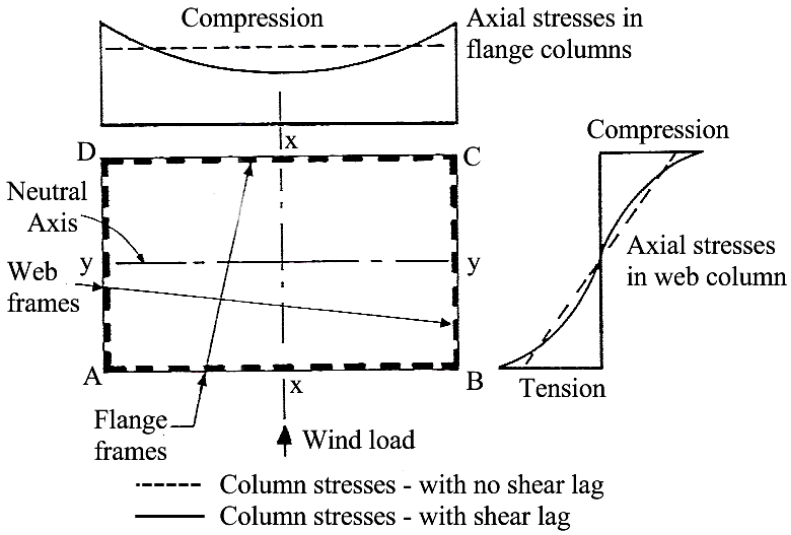

Figure 3 Axial stress distributions in columns in frame-tube system
Source: Smith and Coull (1991)

2.4 Braced-tube systems

This system is essentially the modification of framed-tube system with the addition of multi-story diagonal bracings to the face of the tube. The rigidity and the efficiency of the framed-tube are significantly improved by reducing the excessive axial loads on the corner columns (Gunel and Ilgin, 2007). A stiffer, much more efficient structure is realized with the addition of diagonals (Tarnath, 1998).

In reinforced concrete building, diagonals are created by filling the window openings by reinforced concrete shear walls to achieve the same effect as a diagonal bracing (Figure 4).

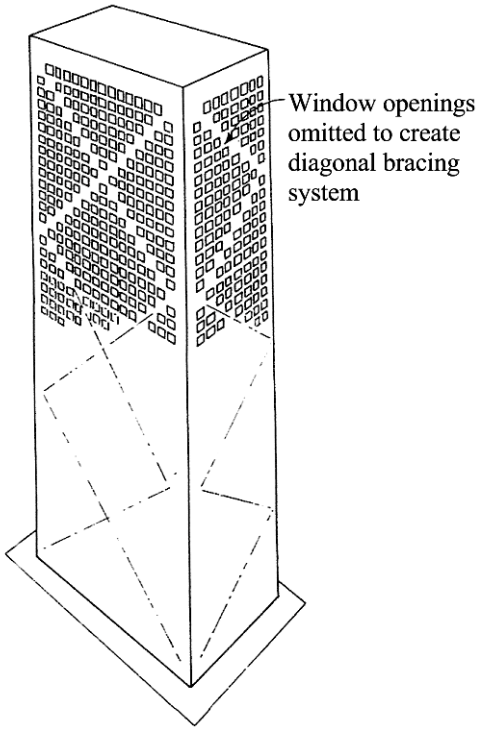

Figure 4 Concrete braced-tube systems
Source: Smith and Coull (1991)

2.5 Outrigger systems

The outrigger system comprises a central core, including either braced frames or shear walls, with horizontal "outrigger" trusses or girders connecting the core to the external columns (Figure 5). Often the external columns are interconnected by exterior belt girder. The outriggers and belt girder are often two stories deep to achieve the adequate stiffness (Gunel and Ilgin, 2007).

When an outrigger-braced structure is loaded laterally, the column-restrained outriggers resist the rotation of the core, causing tension in the windward columns and compression in the leeward columns. The effective structural depth of

the building is greatly increased, thus augmenting the lateral stiffness of the building and reducing the lateral deflections and moments in the core (Smith and Coull, 1991).

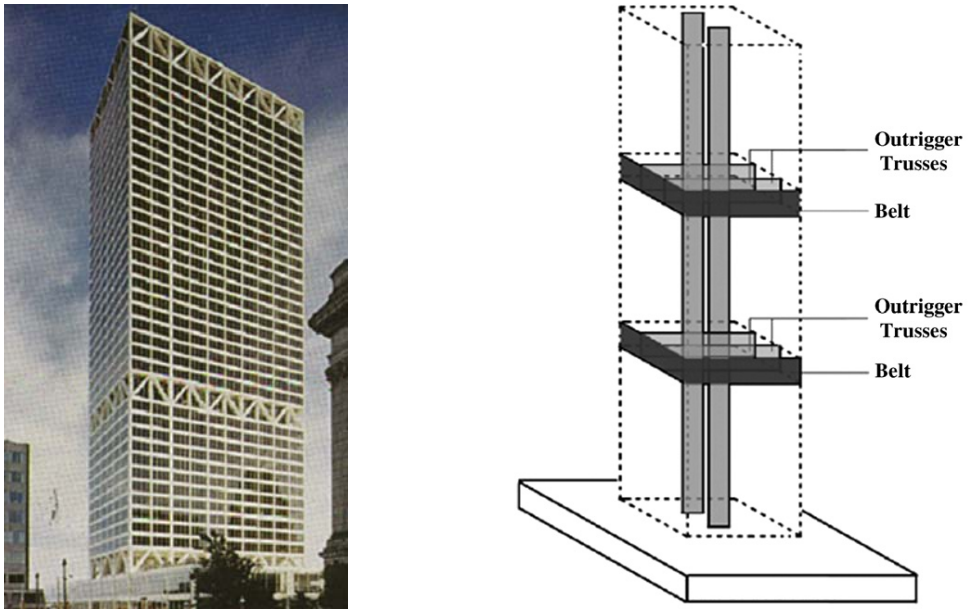

(a) (b)

Figure 5 Outrigger system; a) Building with outrigger; b) outriggers and belts
Source: Gunel and Ilgin (2007)

3. Structural Modelling

Structural modeling refers to the mathematical idealization of real physical structures for the purpose of determining member forces and displacements resulting from applied loads and any imposed displacements or P-Delta effects.

A three-dimensional mathematical model of the physical structure is generally required that represents the spatial distribution of the mass and stiffness of the structure to an extent that is adequate for the calculation of the significant features of its dynamic response. In addition to the designated elements and components of the lateral force resisting systems, all other elements and components that in combination represent more than 15 percent of the total initial stiffness of the building, or a

particular story, are needed to be included in the mathematical model (LATBSDC, 2005).

Thus, the essential requirements for the analytical model of structures are the inclusion of sufficient details of geometry, material, support and loading such that the mathematical model reflects the near-true behavior of the physical structure.

3.1 Geometric modeling of structural members

Nowadays, three-dimensional beam elements (3D beam elements) having 12 Degree of Freedoms (DOFs) with 6 DOFs (three translations and three rotations) at each node are used for modelling beams and columns (Figure 6).

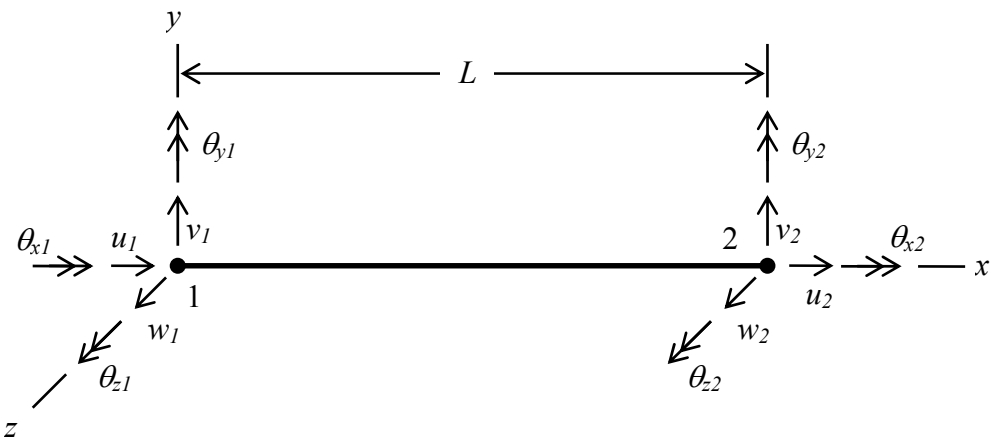

Figure 6 3D beam element on the x-axis of rectangular coordinate systems
Source: Adapted from Cook *et al*. (2002)

To allow the beam element to stretch as well as bend, axial translations are added to the array of nodal DOFs of 2D beam element. The bending stiffness terms are modified to account for transverse shear deformation, thus producing a Timoshenko beam element. The general stiffness matrix of the 3D beam element is (Cook *et al.*, 2002):

$$
[\mathbf{k}] = \left[\begin{array}{cccccc:cccccc}
X & 0 & 0 & 0 & 0 & 0 & -X & 0 & 0 & 0 & 0 & 0 \\
 & Y_1 & 0 & 0 & 0 & Y_2 & 0 & -Y_1 & 0 & 0 & 0 & Y_2 \\
 & & Z_1 & 0 & -Z_2 & 0 & 0 & 0 & -Z_1 & 0 & -Z_2 & 0 \\
 & & & S & 0 & 0 & 0 & 0 & 0 & -S & 0 & 0 \\
 & & & & Z_3 & 0 & 0 & 0 & Z_2 & 0 & Z_4 & 0 \\
 & & & & & Y_3 & 0 & -Y_2 & 0 & 0 & 0 & Y_4 \\
\hdashline
 & & & & & & X & 0 & 0 & 0 & 0 & 0 \\
 & & & & & & & Y_1 & 0 & 0 & 0 & -Y_2 \\
 & & & & & & & & Z_1 & 0 & Z_2 & 0 \\
 & & & \text{Symmetric} & & & & & & S & 0 & 0 \\
 & & & & & & & & & & Z_3 & 0 \\
 & & & & & & & & & & & Y_3
\end{array}\right]
\begin{array}{c}
u_1 \\ v_1 \\ w_1 \\ \theta_{x1} \\ \theta_{y1} \\ \theta_{z1} \\ u_2 \\ v_2 \\ w_2 \\ \theta_{x2} \\ \theta_{y2} \\ \theta_{z2}
\end{array}
\tag{1}
$$

where

$$
X = \frac{EA}{L} \qquad Y_1 = \frac{12EI_z}{(1+\phi_y)L^3} \qquad Y_2 = \frac{6EI_z}{(1+\phi_y)L^2}
$$

$$
Y_3 = \frac{(4+\phi_y)EI_z}{(1+\phi_y)L} \qquad Y_4 = \frac{(2-\phi_y)EI_z}{(1+\phi_y)L} \qquad \phi_y = \frac{12EI_z k_y}{AGL^2}
$$

$$
S = \frac{GK}{L} \qquad Z_1 = \frac{12EI_y}{(1+\phi_z)L^3} \qquad Z_2 = \frac{6EI_y}{(1+\phi_z)L^2} \tag{2}
$$

$$
Z_3 = \frac{(4+\phi_z)EI_y}{(1+\phi_z)L} \qquad Z_4 = \frac{(2-\phi_z)EI_y}{(1+\phi_z)L} \qquad \phi_z = \frac{12EI_y k_z}{AGL^2}
$$

A/k_y is the effective shear area for transverse shear deformation in the y direction, in which k_y = 1.2 for a solid rectangular cross-section, and k_y = 1.11 for circular section. Similarly, A/k_z is the effective shear area for transverse shear deformation in the z direction. As element becomes more and more slender, ϕ approaches zero. The θ_x DOF account for twist about the x axis, for which the stiffness coefficient is GK/L, where G is the shear modulus given by:

$$G = \frac{E}{2(1+\nu)} \tag{3}$$

where E is elastic modulus, and ν is poisson's ratio of a material. K is a property of the shape and size of the cross section. K becomes equal to J, the polar moment of inertia of the cross-sectional area about its centroid only for a circular cross section, solid or tube. For thin-walled cross-sections, K is a small fraction of J (Cook *et al*., 2002). Further details about the 3D beam elements can be found in Cook *et al.* (2002).

The super elements (Figure 8d) are generally used for modelling shearwalls. Super elements are developed from 24 DOFs shell elements which has 6 DOFs at each node: three translations and three rotations (Figure 7c). The shell element, in turn, is formed by the combination of the membrane element (Figure 7a) and plate bending element (Figure 7b).

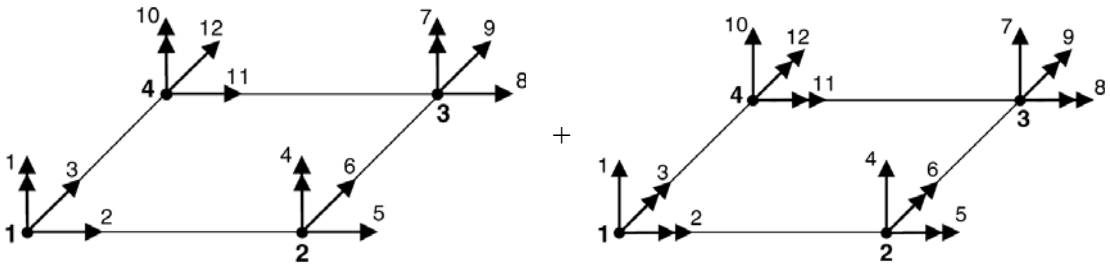

(a) 12 DOFs membrane element (b) 12 DOFs plate bending element

||

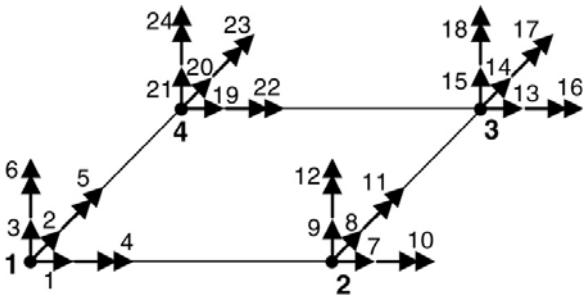

(c) 24 DOFs shell element

Figure 7 Formation of flat quadrilateral shell element

Source: Adapted from Kim *et al*. (2005)

The stiffness matrix for a rectangular shell element has a dimension of 24 x 24 (Liu and Quek, 2003), making it too complicated to reproduce here. With regard to the finite element formulation, reference may be made to Cook *et al*. (2002) and Liu and Quek (2003).

The problem with modelling the building structures using plane stress elements for shearwalls was that, drilling degree of freedoms (DOFs) were required in the plane stress elements for the connection of shearwall and frames. Otherwise, beams could not be rigidly connected to shearwalls, resulting in the underestimation of the lateral stiffness of a building structure. For this reason, improvement in the behaviour of plane stress element was necessary (Kim *et al.*, 2005). This has led to the use of 24 DOFs shell elements to model shearwalls in buildings (Figure 7c).

However, to capture the realistic behaviour of shearwalls, it became necessary to use a refined finite element model in the analysis. But this method of subdividing the whole building structure into a finer mesh resulted in large number of elements causing tremendous amount of analysis time and computer memory cost. This made this procedure inefficient (Kim *et al*., 2005).

To overcome this problem, Kim *et al*. (2005) developed a three-dimensional super element from the assemblage of several shell elements by statically condensing the inactive DOFs, and using stiff fictitious beams to enforce the compatibility at the boundary of super elements. Figure 8 shows the formulation procedure for the super element from the assemblage of shell elements and the use of stiff fictitious beam. The mathematical formulation for the same can be found in Kim *et al*. (2005).

The super elements used for modelling shearwalls, available in many of the commercial structural analysis software are based on this concept.

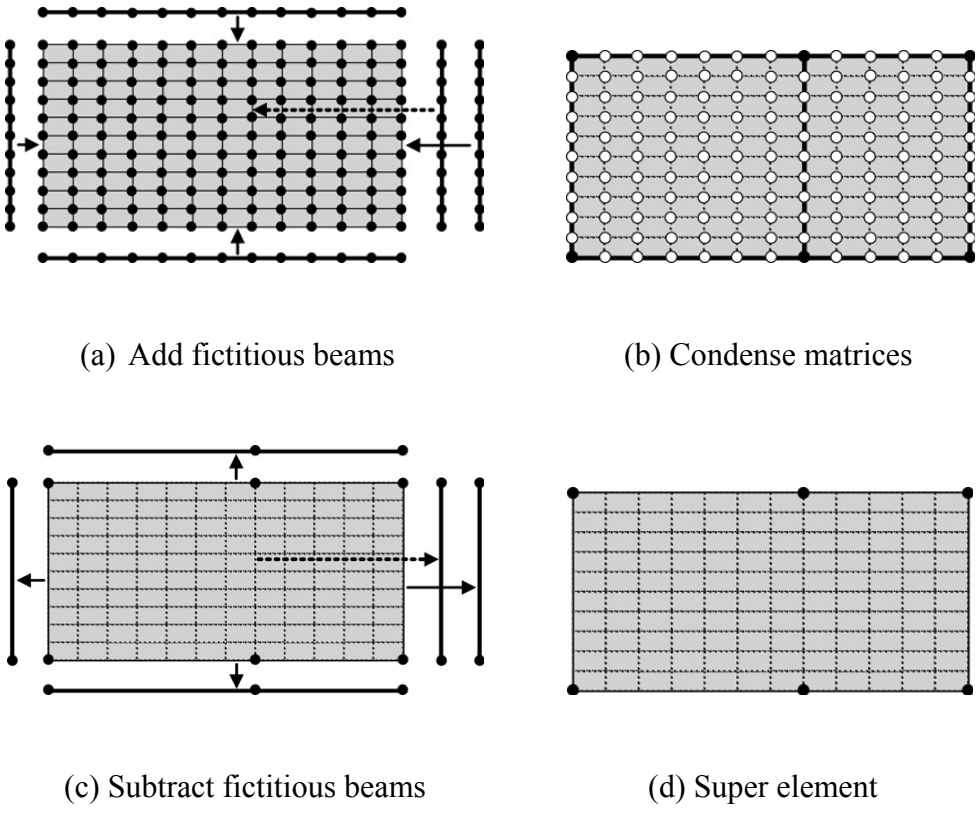

(a) Add fictitious beams (b) Condense matrices

(c) Subtract fictitious beams (d) Super element

Figure 8 Procedure for development of super element
Source: Kim *et al.* (2005)

With regard to the modelling of floor slabs, ASCE 7 (2005) permits the floor slabs to be idealized as rigid diaphragm so long as the length-to-breadth ratios of floor plan is 3 or less and have no horizontal irregularities. The idealization of monolithic concrete floor slab as rigid diaphragm is further supported by IS 1893 (2002). This option has been adopted by many available structural analysis software due to the inherent advantages of minimum computing time.

3.2 Stiffness of reinforced concrete members

Under seismic load reversals, reinforced concrete members suffer from flexural cracking. Due to this, the stiffness properties in the reinforced concrete members are smaller than the properties of the uncracked sections. This reduction in

flexural stiffness is to be reflected in the analysis to obtain accurate results (ASCE 7, 2005; ACI 318, 2005; Sadjadi *et al*., 2007).

Ideally, the member stiffness needs to reflect the degree of cracking and inelastic action that has occurred along each member. However, the complexities involved in selecting different stiffness for all members of a frame make analysis inefficient in design offices (ACI 318, 2005). Thus, the current practice is to reduce the moment of inertia of concrete members by certain amount to account for the cracking in reinforced concrete members due to flexural tensile stresses (Paulay and Priestley, 1992; ACI 318, 2005).

The problem, however, arises when dealing with the flexural stiffness at ultimate and service load, especially for the dynamic analysis. On one hand, flexural stiffness at ultimate load is required. On the other hand, analysis of deflections, vibrations, and building periods are needed at various service load levels to determine the serviceability of the structure. The seismic base shear is also based on the service load periods of vibration. The magnified service loads and deflections by a second-order analysis should also be computed using service loads. Therefore, moments of inertia of the structural members in the service load analyses should be representative of the degree of cracking at the various service load levels investigated. Unless a more accurate estimate of the degree of cracking at design service load level is available, it would be satisfactory to use 1/0.70=1.43 times the moments of inertia given for ultimate load, for service load analyses (ACI 318, 2005).

Because of this complexity, many software do not have the provision to account for the moment of inertia for ultimate load and service load separately during the analysis. Thus, some compromise has to be made in the choice of flexural stiffness of structural members during mathematical modeling.

3.3 Fixity of supports

The behaviour of the structure would be altered if there is soil-structure interaction at the base of the structure especially during earthquake motions. IS 1893: Part 1 (2002) defines soil-structure interaction as "effects of the supporting foundation medium on the motion of structure." The degree of soil-structure interaction depends on the type of soil beneath the structure. Considerable soil-structure interaction can be expected if the soil under the base of the building is soft. However, the soil-structure interaction may not be considered in the seismic analysis for structures supported on rock or rock-like material (IS 1893, 2002). For the purpose of determining seismic loads, it is permitted to consider the structure to be fixed at the base (ASCE 7, 2005).

Thus, the choice of the support conditions for the structure is essentially governed by the condition of soil on which the structure is founded. The assumption of fixed support may be justified if the structure is built on stiff soil or rock. For the high-rise buildings, in some cases, mat foundation is provided on top of piles, which adds considerable stiffness against foundation rotation. This also results in rigid base.

3.4 Structural analysis

Structural analysis refers to the determination of internal forces, stresses and deformation of a real physical structure under prescribed loads, based on the idealized mathematical model of a structure.

Despite the fact that computer analysis of structure has advanced significantly, linear elastic analysis is still the preferred method of analysis as it is simple and allows the superposition of actions and deflections of various load cases. Although nonlinear methods of analysis have been developed, their use at present for high-rise building is more for research than for the design office (Smith and Coull, 1991; FEMA450, 2003). However, realistic inclusion of P-Delta effects is crucial for establishing the onset of collapse because collapse is ultimately P-Delta related (Wilson, 2002; LATBSDC, 2005; ASCE 7, 2005).

Fundamentally, the dynamic behavior of the structure in the linear elastic range is described by the dynamic equilibrium equation (Chopra, 2001):

$$\boldsymbol{m}\ddot{\boldsymbol{u}} + \boldsymbol{c}\dot{\boldsymbol{u}} + \boldsymbol{k}\boldsymbol{u} = \boldsymbol{p}(t) \tag{4}$$

where $\boldsymbol{m}$ = mass matrix, $\boldsymbol{c}$ = damping matrix, $\boldsymbol{k}$ = stiffness matrix, $\ddot{\boldsymbol{u}}$ = acceleration vector, $\dot{\boldsymbol{u}}$ = velocity vector, $\boldsymbol{u}$ = displacement vector and $\boldsymbol{p(t)}$ = time dependant force vector. For a structure excited by the ground motion, Eq. (4) gets specialized to:

$$\boldsymbol{m}\ddot{\boldsymbol{u}} + \boldsymbol{c}\dot{\boldsymbol{u}} + \boldsymbol{k}\boldsymbol{u} = -\boldsymbol{m}\boldsymbol{\iota}\ddot{u}_g(t) \tag{5}$$

where $\boldsymbol{\iota}$ = influence vector and $\ddot{u}_g(t)$ = ground acceleration. For the static analysis, Eq. (4) simplifies to:

$$\boldsymbol{k}\boldsymbol{u} = \boldsymbol{p} \tag{6}$$

The details of the derivation and applications can be found elsewhere (Chopra, 2001).

3.4.1 Eigenproblem

Often the natural frequencies and the corresponding modes of vibration are required during various stages of analysis. This requires the solution of the eigenvalue problem (Chopra, 2001):

$$[\boldsymbol{k} - \omega_n^2 \boldsymbol{m}]\phi_n = 0 \tag{7}$$

where $\boldsymbol{k}$ and $\boldsymbol{m}$ are defined above, ω_n and ϕ_n are the natural circular frequencies and the corresponding mode shapes respectively.

The eigenvalue (ω_n) are the roots of the characteristic polynomial of the determinant of [$\boldsymbol{k}$-$\omega^2\boldsymbol{m}$]. Various methods to extract the eigenpair (ω_n, ϕ_n) from Eq. (7) can be found elsewhere (Chopra, 2001). It has been demonstrated that load-dependent Ritz vectors produce more accurate results when used for a seismic

dynamic analysis than if the exact free-vibration mode shapes are used. The natural period of vibration, T_n is related to ω_n by:

$$T_n = \frac{2\pi}{\omega_n} \tag{8}$$

and the natural cyclic frequency of vibration is denoted by:

$$f_n = \frac{1}{T_n} \tag{9}$$

The natural period, T_n and natural frequency, f_n are essential parameters that are required for the computation of earthquake forces and dynamic effects of wind on the structures.

As evident from Eq.(7), the vibration properties of the structure are dependent on the mass and stiffness of the structures. Hence, it is essential to estimate the mass and stiffness of the structure with a high degree of accuracy. In this context, the major assumption required is to estimate the amount of live load to be included as added mass. For regular symmetric structures, which have equal stiffness in all directions, the periods associated with the lateral displacements result in pairs of identical periods (Wilson, 2002).

3.4.2 Gravity loading

Gravity loading is primarily due to the self-weight of the structure, superimposed dead loads and the live loads due to use and occupancy of the building. In determining dead loads for purposes of design, the actual weights of materials and constructions are used. Live loads used in the design is the maximum loads expected by the intended use or occupancy but in no case be less than the minimum uniformly distributed unit loads required by the standards. Given the fact that not all floors are loaded fully at the same time, many codes allow certain reduction of live loads for the design of vertical structural members.

Gravity loads form one of the most important loads because they exist throughout the life of the structures. Details of the self-weight of materials and live loads can be found in Part 1 and Part 2 of Indian Standard IS 875 (1987).

3.4.3 Seismic analysis

During earthquake, base of the building moves with the ground while the upper part of the building lags behind in motion because of its flexibility. As a result, stresses are induced in the structural members. To address this issue, the current state of knowledge in earthquake engineering recognizes five types of procedures for seismic analysis (Table 1).

Table 1 Procedures for seismic analysis

Static Analysis	Dynamic Analysis
Equivalent Lateral Force Analysis	Response Spectrum Analysis
Non-linear Static Analysis	Linear Time History Analysis
(Pushover Analysis)	Nonlinear Time History Analysis

While the Equivalent Lateral Force, Response Spectrum and Linear Time History Analysis deal with the linear elastic behaviour, Pushover and Nonlinear Time History Analysis address non-linear behaviour of the structures by taking account of the hysteretic behaviour of the materials. Considerable effort is required for nonlinear analysis. At present, they are generally limited to research than for the routine design.

Indian Standard IS 1893 (2002) contains provisions for both the static analysis and the dynamic analysis of buildings. Static analysis using equivalent lateral force procedure is restricted to regular buildings having height less than 40 m and irregular buildings having height less than 12 m in seismic Zone V, the most seismically active zone. Dynamic analysis using response spectrum and time history

analysis can be implemented for those buildings falling outside the scope of static analysis.

At the core of seismic analysis is the use of response spectra plot such as Figure 9, in which the spectral acceleration is plotted for wide range of fundamental natural period of the structures. Figure 9 has been adapted from IS 1893 (2002).

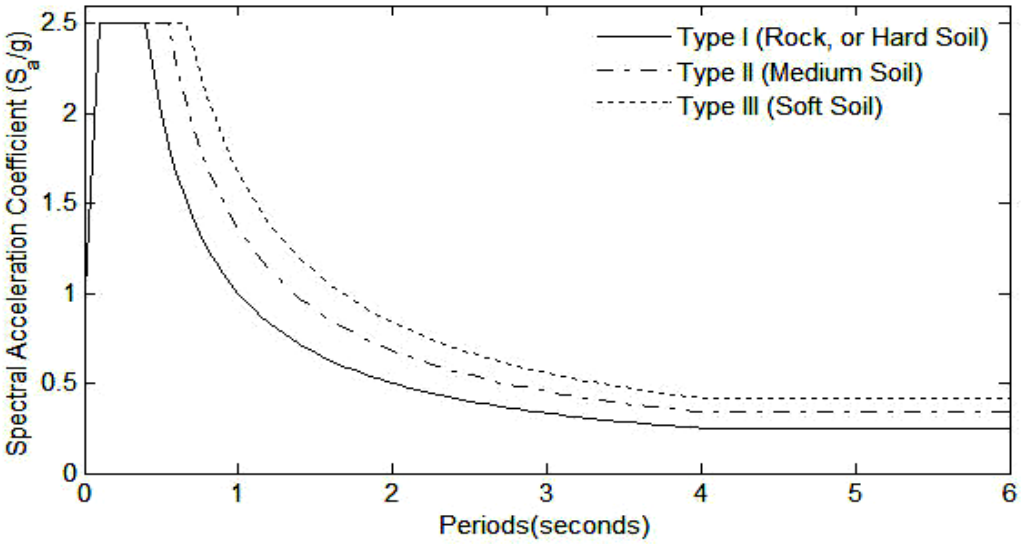

Figure 9 Response spectra for rock and soil sites for 5% damping

For the static analysis using equivalent force procedure, the static forces in the structure are derived from the design seismic base shear (V_b) given by:

$$V_b = A_h W \tag{10}$$

where W = Seismic weight of the building, equal to full dead load plus fraction of live load, and A_h= Design horizontal seismic coefficient, given by:

$$A_h = \frac{ZI}{2R}\left(\frac{S_a}{g}\right) \tag{11}$$

where Z = Zone factor, I = Importance factor, R = Response reduction factor, S_a/g = Spectral acceleration coefficient, read from Figure 9 corresponding to fundamental natural period of the structure. The lateral forces are distributed along the height of the structures using Eq. (12):

$$Q_i = V_b \frac{W_i h_i^2}{\sum_{j=1}^{n} W_j h_j^2} \tag{12}$$

where Q_i = Design lateral force at floor i, W_i = Seismic weight of floor i, h_i = Height of floor i measured from base, and n = Number of storys in the building. Section A.1.1 of Appendix A may be referred for further details.

Fundamentally, the static loading using equivalent lateral force procedure is formulated with the assumption that the first mode of vibration dominates the higher modes in the earthquake response. This is true for short period structures. Accordingly, the equations are derived on the basis of horizontal displacement of the first mode of vibration increases either linearly or quadratically with height (FEMA450, 2003). In the case of IS 1893 (2002), quadratic variation of displacement has been adopted as depicted by Eq.(12).

In the dynamic analysis using response spectrum, the contributions from the higher modes of vibration are taken into account by combining the maximum response quantities (member forces, displacements, story forces, story shears, and base reactions) from each mode of vibration to obtain the peak responses. The number of modes to be used in the analysis is determined by the requirement that the sum total of modal masses of all modes considered is at least 90 percent of the total seismic mass.

According to Indian Standard (IS1893, 2002), response spectrum analysis is characterized mainly by four parameters: modal mass (M_k), modal participation factors (P_k), mode shape coefficient (ϕ_{ik}) and modal natural period (T_k). Modal mass (M_k) is a part of the total seismic mass of the structure that is effective in

mode k of vibration, while modal participation factor (P_k) of mode k of vibration is the amount by which mode k contributes to the overall vibration of the structure. Similarly, mode shape coefficient (ϕ_{ik}) is the ratio of the amplitude of mass i to the amplitude of one of the masses of the system when vibrating in normal mode k, and the modal natural period (T_k) is the time period of vibration in mode k.

IS 1893 (2002) allows either standard design spectrum given in the standard (Figure 9) or site-specific design spectrum to be used for carrying out response spectrum analysis.

To obtain the peak response quantities, two methods of modal combinations: *square-root-of-sum-of-squares* (SRSS) and *complete quadratic combination* (CQC) rules are provided in IS 1893 (2002). The general form of SRSS combination rule is

$$\lambda = \left[\sum_{k=1}^{r} \left(\lambda_k \right)^2 \right]^{1/2} \tag{13}$$

in which λ = peak response quantity, λ_k = absolute value of quantity in mode k, and r = number of modes being considered. The general form of CQC combination rule is given by:

$$\lambda = \left[\sum_{i=1}^{r} \sum_{j=1}^{r} \lambda_i \rho_{ij} \lambda_j \right]^{1/2} \tag{14}$$

in which λ = peak response quantity, λ_i = response quantity in mode i (including sign), λ_j = response quantity in mode j (including sign), and ρ_{ij} = cross-modal coefficient, given by (Chopra, 2001):

$$\rho_{ij} = \frac{8\sqrt{\zeta_i \zeta_j}\left(\beta\zeta_i + \zeta_j\right)\beta^{3/2}}{\left(1-\beta^2\right)^2 + 4\zeta_i\zeta_j\beta\left(1+\beta^2\right) + 4\left(\zeta_i^2 + \zeta_j^2\right)\beta^2} \tag{15}$$

where ζ_i, ζ_j = modal damping ratio (in fraction) in i^{th} and j^{th} mode, respectively, β = the frequency ratio (= ω_i/ω_j), ω_i = circular frequency in i^{th} mode, and ω_j = circular frequency in j^{th} mode. For equal modal damping, ζ for all modes of vibration, Eq. (15) reduces to:

$$\rho_{ij} = \frac{8\varsigma^2(1+\beta)\beta^{3/2}}{(1-\beta^2)^2 + 4\varsigma^2\beta(1+\beta)^2} \tag{16}$$

SRSS rule is applicable to buildings having well-separated modes while CQC rule to closely-spaced modes. Modes are considered to be closely-spaced if the natural frequencies differ from each other by 10 percent or less of the lower frequency (IS 1893, 2002). As stated by Chopra (2001), CQC rule is applicable to a wider class of structures as it overcomes the limitation of the SRSS rule.

Section A.1.2 of Appendix A may be referred for the detailed procedures for response spectrum analysis.

The standard (IS 1893, 2002), however, does not provide enough information with regard to the use of Time History Method. It only directs the user to use appropriate ground motion and perform analysis using accepted principles of dynamics. On the other hand, ASCE 7 (2005) contains detailed information with regard to the time history analysis.

The time history analysis is a higher tier of dynamic analysis that involves simulating the response time histories of the building using step-by-step integration of the response in the time domain. In other words, it is an analysis of the dynamic response of the structure at each increment of time, when its base is subjected to a specific ground motion time history. Accelerograms at the ground surface are required for input into the analyses. All accelerograms selected for the analyses must be compatible with the design earthquake scenario, the seismo-tectonic environment of the region, the geology of the area and geotechnical details in relation to the overlying soil sediments of the sites (Lam *et al.*, 2007).

There are two basic procedures for developing acceleration time histories: selecting a suite of past recorded earthquake ground motion, and synthetically developing or modifying one or more ground motions. The response spectrum properties of the accelerograms must be checked to ensure that they are consistent with the specified level of seismic hazard. Multiple accelerograms must be applied to the analyses to cover the variability (Lam *et al.*, 2007). Appropriate acceleration histories can be obtained from records of events having magnitudes, fault distance, and source mechanism that are consistent with those that control the maximum considered earthquake (ASCE 7, 2005).

Once a suite of ground motion has been selected, these commonly are manipulated to represent the target linear response spectrum using either *scaling* or *spectrum matching*. *Scaling* involves applying a constant factor to individual pairs of horizontal ground motion records to make their response match the design spectrum at a single period or over a range of periods. *Spectrum matching* is a process whereby individual ground motion records are manipulated to adjust the linear response spectrum of the motion so it matches the target design response spectrum. Resulting motions should be compared with original motions to ensure the original character of the motion is not modified excessively (Moehle *et al*., 2007).

A simple way to modify a strong-motion record is to multiply the amplitude of the acceleration history throughout by a certain factor α (Malhotra, 2003). Varieties of scaling methods exist, and all methods attempt to match the design response spectrum. A few of the scaling methods are outlined in Section A.2 of Appendix A for references.

In order to apply scaling factor to any ground motion to match with the response spectra of Figure 9 (IS 1893, 2002), it is essential to understand the background to it. When S_a is multiplied by zone factor, Z, the product S_aZ corresponds to Maximum Considered Earthquake (MCE). When S_aZ is divided by 2, that is $S_aZ/2$, it corresponds to Design Basis Earthquake (DBE). Since the ground motions are compared with design response spectrum (ASCE 7, 2005), the scaling of

ground motion is with respect to $S_aZ/2$. This is self-evident from Eq.(11). The factor I/R are normally applied to the responses (bending moments, axial forces, shears, etc) rather than at the beginning of the analysis (ASCE 7, 2005).

Since time history analysis are highly dependent on the characteristics of the individual ground motion records, subtle changes in these records can lead to significant differences with regard to the predicted response of the structure (FEMA450, 2003). Therefore, time history analyses should be paralleled by a lower-tier of analyses for benchmarking purposes (Lam *et al.*, 2007).

Application of nonlinear time history analysis even to the simplest structures demands great deal of effort in modeling material and geometric nonlinearity and requires large, high speed computers and complex software. Even so, it takes prohibitively long to analyze the structure having multi degree of freedom systems. The extra complexity and the cost inherent in the use of time history analysis rather than response spectrum are seldom justified. As a result this procedure is rarely used in the design process (FEMA450, 2003). So, equivalent lateral force and response spectrum analysis has proven to be the most widely used method for the seismic analysis of structure.

The major advantage of using the forces obtained from a dynamic analysis as the basis for a structural design is that the vertical distribution of forces maybe be significantly different from the forces obtained from an equivalent static load analysis. Consequently, the use of dynamic analysis produces structural designs that are more earthquake resistant than structures designed using static loads (Wilson, 2002).

3.4.4 Dynamic effects of wind

The wind on earth's surface is turbulent in nature that gives rise to randomly varying wind pressures above the surface of the earth. For structural engineering purposes, the velocity of wind can be considered as having two

components; a mean velocity component whose value increases with height and a turbulent velocity fluctuations (Figure 10).

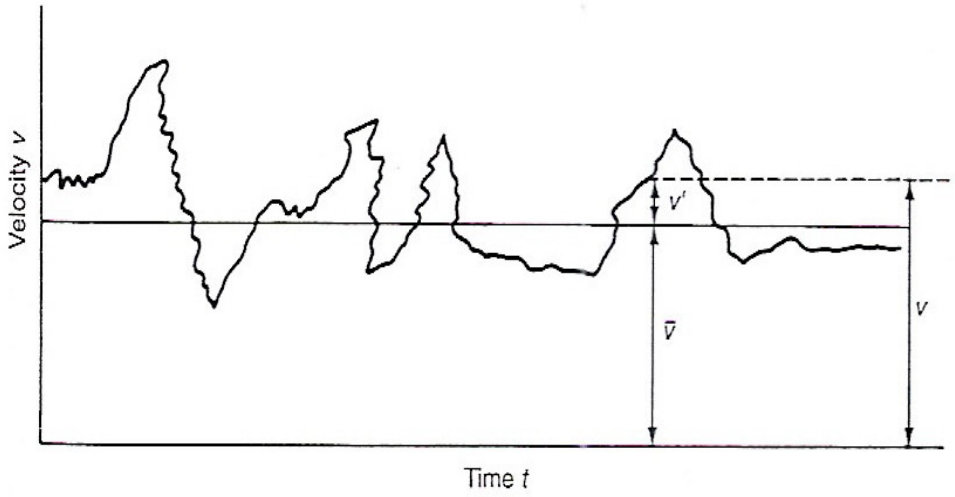

Figure 10 Variation of wind velocity with time
Source: Tarnath (1998)

Thus, the velocity at any instant v_t can be represented as the summation of the mean velocity and the instantaneous value of velocity fluctuation about the mean value as (Tarnath, 1998):

$$v_t = \overline{v} + v' \tag{17}$$

where v_t = velocity at instant t, $\overline{v}$ = mean velocity, and v'= instantaneous velocity fluctuation about the mean velocity, $\overline{v}$. The longest averaging time used in structural engineering practice is one hour. As the averaging time decreases, the maximum speed of wind increases (Tarnath, 1998).

The wind pressure at any height above the mean ground level is obtained by the following relationship between wind pressure and wind speed AS/NZS 1170.2 (2002):

$$p_z = \frac{1}{2}\rho V_z^2 \tag{18}$$

where ρ is the density of air, generally assumed as 1.2 kg/m^3 at sea level, and p_z and V_z are wind pressure and wind speed respectively at height z.

Wind speed, V_z at any height z above the ground is derived from the basic wind speed, V_b which are generally measured at 10 m high above the ground. IS 875: Part 3 (2004) defines the basic wind speed, V_b as the peak gust wind speed averaged over a period of 3 seconds, with a return period of 50 years.

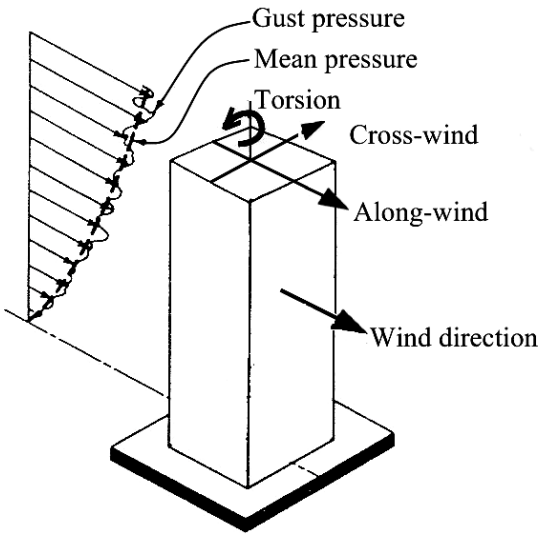

Figure 11 Wind pressure distribution and response directions
Source: Adapted from Tarnath (1998) and Mendis *et al.* (2007)

Flexible structures respond dynamically to the effects of wind, particularly if the frequencies of the fluctuating wind pressure are within 20% of the fundamental frequencies of the structures. Under the action of wind, tall buildings oscillate simultaneously in the along-wind, cross-wind and torsional directions. It has been recognized that for many high-rise buildings the cross-wind and torsional response may exceed the along-wind response. Nevertheless, most existing codes and standards provide little guidance for the critical cross-wind and torsional responses (Zhou *et al*., 2003).

Dynamic response in the along-wind direction arises from turbulence buffeting, while that in the cross-wind direction result from either due to vortex shedding or turbulence buffeting (Mendis *et al*., 2007). Turbulence intensity, or gustiness, describes the turbulence of the wind flow (Simiu and Scanlan, 1996). It is defined as $\sigma_v(z)/\overline{V}(z)$, where $\sigma_v(z)$ = standard deviation of wind speed, and $\overline{V}_z(z)$ = mean wind speed at height *z*. It decreases with the increase in height above the ground.

According to current state of knowledge in wind engineering, three methods are employed for evaluating the wind loads on structures. They are static analysis, dynamic analysis and wind tunnel tests. Static analysis, which ignores the dynamic effect of wind, is generally limited to the regular and rigid low-rise buildings. Dynamic analysis are used for flexible buildings having regular shapes with fundamental frequency less than 1 Hz. Wind tunnel tests are usually carried out for tall buildings or buildings having unusual configurations. Because the contribution from higher mode of vibration is rarely significant for wind loading (Simiu and Scanlan, 1996; AS/NZS, 2002), forces due to dynamic affects of wind are derived based on the fundamental mode of vibration.

Indian standard IS 875: Part 3 (2004) addresses both static and dynamic wind loading on structures. In practice, static analysis is normally appropriate for structures up to 50 m in height (Mendis *et al*., 2007) or rigid structures having fundamental frequency greater than 1 Hz (IS 875, 2004; ASCE 7, 2005). IS 875: Part 3 (2004) stipulates that the dynamic effects of wind be taken into account while designing the buildings if:

1) Height to minimum lateral dimension ratio is more than 5; or
2) Natural frequency in the first mode of vibration is less than 1 Hz

The standard (IS 875) provides calculation procedures for both along-wind and cross-wind response by using the dynamic response factor. This

factor approximately accounts for the quasi-static and resonant components of the wind loading.

Along-wind load on a structure on a strip area A_e, at any height z is given by (IS1875: Part 3, 2004):

$$F_z = C_f A_e p_z C_{dyn} \tag{19}$$

where F_z = along-wind equivalent static load on the structure at any height z corresponding to strip area A_e, C_f = force coefficient for the building which accounts for variation of pressure over the building and is function of geometry of building, and C_{dyn} = dynamic response factor for along-wind loading.

The equivalent cross-wind static force per unit height (W_e) as a function of z is given by:

$$W_e(z) = 0.6 V_h^2 d C_{dyn} \tag{20}$$

where V_h = wind speed at top of the building, d = lateral dimension of the building parallel to the wind stream, and C_{dyn} = dynamic response factor for cross-wind loading.

As observed from Eq.(19) and Eq.(20), the whole task of accounting dynamic effects of wind is thus reduced to determining the dynamic response factor, C_{dyn}. The static design wind pressure is simply multiplied by the dynamic response factor to convert the static wind loading to dynamic wind loading. However, the procedures for evaluating dynamic response factors for along-wind and cross-wind are different (Section C.1.1 and C.1.2; Appendix C). Even more so is the complexity involved in the interaction of two responses that many codes simply ignore the cross-wind effect.

It is noted that many of the expressions given in IS 875: Part 3 (2004) are essentially same as those given in AS/NZS 1170.2 (2002). The IS 875,

however, have no provisions for the combination of along-wind and cross wind loading. On the other hand, AS/NZS1170.2 (2002) gives the combination rule for along-wind and cross-wind response as:

$$\varepsilon_t = \varepsilon_{a,m} + \sqrt{\left[(\varepsilon_{a,p} - \varepsilon_{a,m})^2 + \varepsilon_{c,p}^2\right]} \tag{21}$$

where ε_t = dynamic action effect (such as axial load, bending moment, shear, etc), $\varepsilon_{a,m} = \varepsilon_{a,p}/[C_{dyn}(1+2g_v I_h)$, $\varepsilon_{a,p}$ = action effect derived from the peak along-wind response, $\varepsilon_{c,p}$ = action effect derived from the peak cross-wind response, C_{dyn} = dynamic response factor, g_v = peak factor, and I_h = turbulence intensity (refer Section C.1.1 of Appendix C for definition of terms).

Expression (21) is not directly amenable to design. Considerable effort is required for the response combinations. As an approximation to the above combination rule, AS/NZS1170.2 also provides combination rule for loads instead of responses in the commentary section as follows:

1) Mean along-wind load + 0.75 (peak-mean) along-wind ± 0.75 (peak-mean) cross-wind

2) Mean along-wind load + 1.0(peak-mean) along-wind

3) (Peak-mean) cross-wind

This approximate combination rule for loading has been adopted for this study instead of the response combination given by Eq.(21). The detailed procedures with regard to the computation of both along-wind and cross-wind load are provided in the IS 875: Part 3 (2004). Excerpts from IS 875: Part 3 (2004) are included in Section C.1.1 and C.1.2 of Appendix C.

3.4.5 P-Delta effect

ASCE 7 (2005) defines P-Delta effect as “The secondary effect on shears and moments of structural members due to the action of the vertical loads

induced by horizontal displacement of the structure resulting from various loading conditions." P-Delta effect is the second-order effect of gravity loading (Smith and Coull, 1991) and is essentially a stability problem (Tarnath, 1998). It has been termed the *P-Delta effect* because the additional overturning moment on the building are equal to the sum of story weights "P" times the lateral displacements "Delta" (Wilson, 2002).

For most building structures, the P-Delta effect occurs in the columns because of gravity load. Columns in buildings are subjected to simultaneous bending caused by lateral loads, and axial compression due to gravity loads. Hence, they are in effect "beam-column" (Tarnath, 1998). The column axial forces being compressive make the structure more flexible against lateral loads. Gravity load considered for P-Delta effect consists of dead load plus fraction of live load.

The concept of P-Delta effect can be illustrated by a simple cantilever subjected to vertical load, P_g due to gravity and horizontal load, F due to earthquake or wind as in Figure 12.

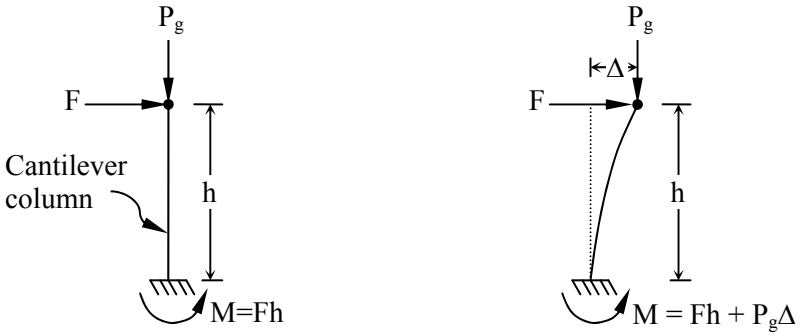

a) Undeformed Configuration b) Deformed Configuration

Figure 12 Illustration of P-Delta effect

When the building is subjected to horizontal forces, the resulting horizontal displacements lead to additional overturning moments because the gravity load P_g is also displaced. Therefore, in addition to the overturning moments produced by lateral force F, the secondary moment $P_g\Delta$ must also be resisted. This moment

increment in turn produces additional lateral displacement, and hence Δ increases further.

Of the many methods available, three methods are widely used to account for the P-Delta effect in buildings. These are moment magnifier method, iterative P-Delta analysis method and Non-iterative P-Delta analysis method.

In the traditional moment magnifier method, moments obtained from first-order elastic analysis are multiplied by the moment magnifier that is the function of factored axial force and the critical buckling load for the column. The problem is usually classified into sway frame and non-sway frame. The frame is considered non-sway if the increase in the lateral moments resulting from P-Delta effects does not exceed 5 percent of the first-order moments (ACI 318, 2005). The details of this method are given in ACI 318 (2005).

In the Iterative P-Delta analysis method, an initial first-order analysis of the structure is made with the external horizontal loading. The resulting horizontal deflections are then used in conjunction with the gravity loading to compute at each floor level an equivalent increment of horizontal load. This increment is added to the initial horizontal load and the analysis is repeated. The resulting increased deflections are then used in conjunction with the gravity loads to compute another set of equivalent horizontal increments, which again are added to the initial horizontal load for a reanalysis. The iterations are continued until increases in the deflections become negligible (Smith and Coull, 1991).

The third method is the Non-iterative P-Delta analysis method, in which the second-order effects are accounted for by directly modifying first-order stiffness matrix so that, when analyzed for the actual horizontal loading, the resulting values of drift and member forces include the P-Delta effects. The matrix equation for this case is given by (Smith and Coull, 1991):

$$\{H\} = [K - K_G]\{\Delta^*\} \tag{22}$$

in which $\{H\}$ = vector of the actual horizontal loading, K = first order stiffness matrix, K_G = geometric stiffness matrix and is the function of the gravity loading, and $\{\Delta^*\}$ = vector of the total lateral displacements, which includes P-Delta effects. The details of the formulation for last two methods are given elsewhere (Smith and Coull, 1991; Wilson, 2002).

However, the use of traditional moment magnifier method, especially in the case of heavy gravity loading or of a flexible structure, has been discouraged by Smith and Coull (1991) because of the deterioration of accuracy. Moreover, the inclusion of P-Delta effect in the analysis stage eliminates the need to determine the column effective length factors, since the P-Delta effects automatically produce the required design moment amplifications (Wilson, 2002).

Normally, the maximum moment in columns occurs at the ends. However, in a very slender columns or columns bent in single curvature, maximum moment may occur between its ends (ACI 318, 2005). This is the local p-delta effect.

The decision as to whether to include P-Delta effect in the analysis is provided by the stability ratio, θ given by (ASCE 7, 2005):

$$\theta = \frac{P_x \Delta}{V_x h_{sx} C_d} \tag{23}$$

where P_x = total vertical design load at and above level x with load factor ≤ 1.0, Δ = design story drift occurring simultaneously with V_x, V_x = seismic shear force acting between level x and x-1, h_{sx} = story height below level x, C_d = deflection amplification factor, whose value ranges from 1.25 to 6 depending on the efficiency of the seismic force resisting system. The higher value of C_d refers to more ductile systems.

ASCE 7 (2005) states that if the stability ratio, θ computed from Eq. (23) is less than 0.10, inclusion of P-Delta effects may be waived. The standard (ASCE 7, 2005) also imposes the maximum limit on stability coefficient, θ as:

$$\theta_{\max} = \frac{0.5}{\beta C_d} \leq 0.25 \tag{24}$$

where β = ratio of shear demand to shear capacity for the story between levels *x* and *x-1*. β is permitted to be conservatively taken as 1.0. Where the stability coefficient, θ is greater than 0.10 but less than or equal to $\theta_{\max}$, the incremental factor related to P-delta effects on displacement and the member forces are to be determined by rational analysis. Where θ is greater than $\theta_{\max}$, the structure is potentially unstable and should be redesigned. FEMA450 (2003) encourages the inclusion of P-Delta effect in the analysis as it effectively checks the stability of a structure based on its initial stiffness.

Because high-rise building design results in larger computer analysis models as compared to low-rise building design, the most important thing to keep in mind is fundamental behavior and to provide "sanity checks" along the way that ensure analytical modeling is accurately depicting the real structural behavior (Zils and Viise, 2003).

4. Serviceability Criteria

4.1 Deflection and drift criteria

Control of deflection and story drift is imperative for high-rise buildings with the view to limiting damage and cracking of non structural members such as the façade, internal partitions and ceilings (Mendis, *et al*., 2007).

Story drift refers to the horizontal deflection at the top of the story relative to the bottom of the story. Story drift ratio or interstory drift ratio is the story drift divided by the story height (ASCE 7, 2005). One simple parameter that affords an estimate of the lateral stiffness of a building is the drift index, which is defined as the ratio of the maximum deflection at the top of the building to the total height of the building (Smith and Coull, 1991).

Several codes specify a wind drift criteria of H/500 for high-rise buildings (Zils and Viise, 2003; Scott *et al*., 2005), where H is the height of building. At the same time, an inter-story drift of H/350 is also commonly used (Scott *et al*., 2005). However, IS 1893 (2002) stipulates the maximum story drift ratio of 1/250 but the maximum wind drift criteria of H/500 is specified in IS 456 (2000).

4.2 Acceleration and occupant comfort criteria

For most high-rise buildings, serviceability considerations may govern the design. Acceptability criteria for vibrations in buildings are frequently expressed in terms of acceleration limits for a one or five year return period wind speed and are based on human tolerance to vibration discomfort in the upper levels of buildings (Mendis *et al*., 2007). However, for checking motion perception, 10 year wind is generally used in USA (ASCE 7, 2005). Figure 13 shows the allowable horizontal acceleration versus fundamental natural frequency of a building for various return periods.

Generally, horizontal accelerations vary inversely proportional to the generalized mass and square root of damping, and are less significantly correlated to the stiffness and the period of structure (Eq.(C12) and (C13) of Appendix C). As a result, often the most cost-effective way to reduce building accelerations is by maximizing generalized mass (Zils and Viise, 2003). Scott *et al*. (2005) states that stiffening the building is often the least effective response if acceleration is an issue. Although accelerations are reduced, the motions become more perceptible at higher frequencies. However, Mendis *et al*. (2007) argues that increasing the mass and stiffness is in direct conflict with earthquake design optimization where loads are minimized in buildings by reducing both the mass and stiffness. He states that increasing the damping results in reduction of both the wind and earthquake responses.

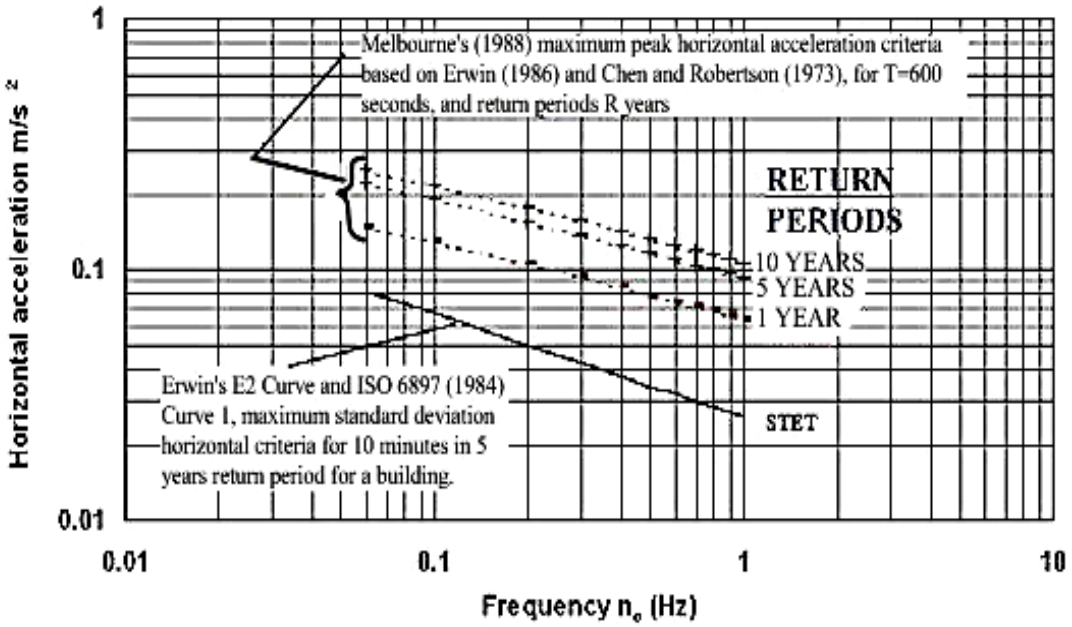

Figure 13 Horizontal acceleration criteria for occupancy comfort in buildings
Source: Mendis *et al*. (2005)

There are as yet no generally accepted international standards for comfort criteria, and the design is usually based on published data. A considerable amount of research has, however, been carried out into the important physiological and psychological parameters that affect human perception to motion and vibration in the low frequency range of 0-1Hz encountered in high-rise buildings. These parameters include the occupant's expectancy and experience, their activity, body posture and orientation, visual and acoustic cues, and the amplitude, frequency, and accelerations for both the translational and rotational motions to which the occupant is subjected (Mendis *et al*., 2007) . Table 2 gives some guidelines on general human perception levels.

Table 2 Human perception levels

Level	Acceleration (m/sec^2)	Effect
1	<0.05	Humans cannot perceive motion
2	0.05-0.1	a) Sensitive people can perceive motion; b) Hanging objects may move slightly
3	0.1-0.25	a) Majority of people will perceive motion; b) Level of motion may affect desk work; c) Long-term exposure may produce motion sickness
4	0.25-0.4	a) Desk work becomes difficult or almost impossible; b) Ambulation still possible
5	0.4-0.5	a) People strongly perceive motion; b) Difficult to walk naturally; c) Standing people may lose balance
6	0.5-0.6	Most people cannot tolerate motion and are unable to walk naturally
7	0.6-0.7	People cannot walk or tolerate motion
8	>0.85	Objects begin to fall and people may be injured

Source: Mendis *et al*. (2007)

5. Economy of Structural Systems

The size and density of structural elements in a modern high-rise building are strikingly less than in the buildings of former centuries. The available rentable floor space are determined by the structural plan density index, defined as the total area of all vertical structural elements divided by the gross floor area of the footprint of the building at the ground level. Contemporary high-rise building has structural plan density index in the range of 2 to 3 percent compared to monumental structures such as pyramids of Egypt which has structural plan density close to 100 percent. Maximum economy is achieved by maintaining this index around 2.5 percent (Tarnath, 1988).

To determine the efficiency of structural systems, it is not only important to understand their behavior but also it is useful to know the relative cost of materials for structural systems. The structural system of a high-rise building often has a more pronounced effect than a low-rise building on the total building cost and the architecture (Zils and Viise, 2003). The cost of structural materials required for lateral-load resistance increases nonlinearly with the increase in building height (Figure 14). Material requirements also differ among different structural systems.

The structural cost usually accounts for 20 to 30 percent of the cost of a high-rise building. However, some of the factors which determine efficiency and economy are rather vague and not well defined by codes and standards (Scott *et al*., 2005). The overall cost of a multi-story building may come down considerably if the structural system is designed efficiently.

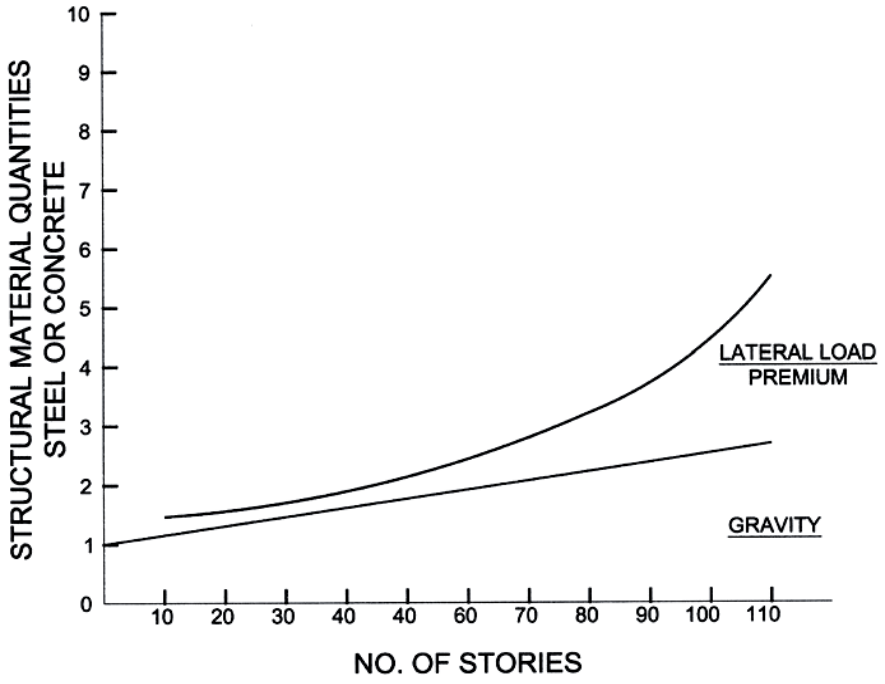

Figure 14 High-rise premium

Source: Zils and Viise (2003)

RESEARCH METHODOLOGY

The research for this study commenced with the detailed review of literature, followed by the analytical modelling of selected five structural systems. Structural analysis with particular emphasis on wind and earthquake loads was conducted to obtain building responses in terms of vibration modes, story shear, moment, displacment and story drift. Human comfort criteria based on the maximum horizontal accelerations at the roof level was checked. Lastly, costs of structural materials for each structural system was estimated based on the rate of materials collected in Bhutan. Structural systems were compared based on their behaviour towards wind and earthquake, horizontal acceleraion at roof and cost of structural materials.

This part of the thesis covers the detailed description of analytical modelling of five structural systems along with the necessary assumptions with regard to geometric and material modelling. Structural analyis for wind and earthquake loads are described next. Lastly, outline of expected results, member design and stuctural cost estimation are provided. The details of each stage of this study is described henceforward.

1. Literature Review

Literatures on different structural systems, wind and earthquake loads on structures, analysis requirements, and additional criteria both for strength and serviceability limit states pertaining to the medium-height reinforced concrete buildings were reviewed thoroughly. Indian standards relating to concrete, seismic and wind loading were reviewed, although Australian standards on wind loading and American standards on concrete and loadings were given equal importance. Deficiencies in Indian standards were supplemented from American and Australian standards. The review provided both knowledge and insight into the behavior of structural systems and, additional requirements with regard to analysis and design of high-rise buildings.

2. Collection of Relevant Data

Part of this study involved the comparison of cost of different structural systems in medium-height reinforced concrete building. Should the buildings similar to the one in this study be built in Bhutan, it would be essential to use the cost of materials in the context of Bhutan. Towards this end, necessary information pertaining to the cost of materials especially cement, sand, crushed stones and steel reinforcement were collected in Bhutan, and subsequently used in this study.

3. Mathematical Models

The building chosen for this study is the hypothetical 25-story reinforced concrete building having uniform story height of 3.6 m with total building height of 90 m and plan dimension of 27 m by 27 m (Figure 15). The floor system is 125 mm thick reinforced concrete solid slab on grid of beams.

Five types of structural systems: rigid frame, shear-walled frame, framed-tube, braced-tube and outrigger systems were incorporated in sequence into the same building to study their behavior. In terms of the lateral stiffness and mass distribution, the building is symmetrical in plan with respect to two orthogonal axes. Square plan is chosen to facilitate the computation of various response parameters. It is important to note that if the centre of mass and center of rigidity do not match, then torsional response results.

This building is not meant to represent any physical building. As such, some details such as openings for doors, windows, ducts and lift core are deliberately left out from the models. The idea here is to compare the global behavour of the structural systems, not on the behavioural effect due to minute details.

3.1 Description of Cases of models

Three cases of analytical models are considered: Case 1, Case 2 and Case 3, with each case consisting of five different structural systems, namely rigid frame, shearwalled-frame, framed-tube, braced-tube and outrigger. The categorization of models into Case 1, Case 2 and Case 3 is based on the use of different sections of structural members. The plan of each structural system for Case 2 and Case 3 is shown in Figure 15 through Figure 18. Plan of structural systems for Case 1 is same as those of Case 2 and Case 3, except that the column sizes were same throughout. Figure 19, Figure 20 and Figure 21 shows typical frame elevations of structural systems.

In Case 1 models, beams size of 350 x 550 mm and column size of 750 x 750 mm were assumed throughout the building height for all five structural systems. The beam depth of 550 mm was arrived at after considering the deflection limit under gravity load, and the column size of 750 x 750 mm was adopted after checking the adequacy of sections for five structural systems. Since the column sections were all same irrespective of structural systems, this had resulted in framed-tube system being very flexible, and the choice of the above column section was in fact governed by it for Case 1. This case of analytical models was in fact to act as baseline to observe how effectively the geometric modification of some structural systems could bring about the drastic changes in their lateral load resisting capability.

In Case 2 models, beam and column sections were modified with the intention of fully mobilizing the capacity of each structural systems for lateral load resistance while ensuring that they met the strength and serviceability requirements. Table 3 shows the member sizes used for the Case 2 models. Normally, the beam and column sections were kept same for braced-tube and framed-tube system with the exception of additional diagonal bracing on four faces of the building in the case of braced-tube system. However, in this study, for comparison purpose, the column and beam sections for braced-tube systems were made different from those of framed-tube system. The adequacy of the column sections for each structural system was checked

and same section was used throughout the building height. Certain uniformity in the choice of frame section was maintained to ease modelling task and subsequent design.

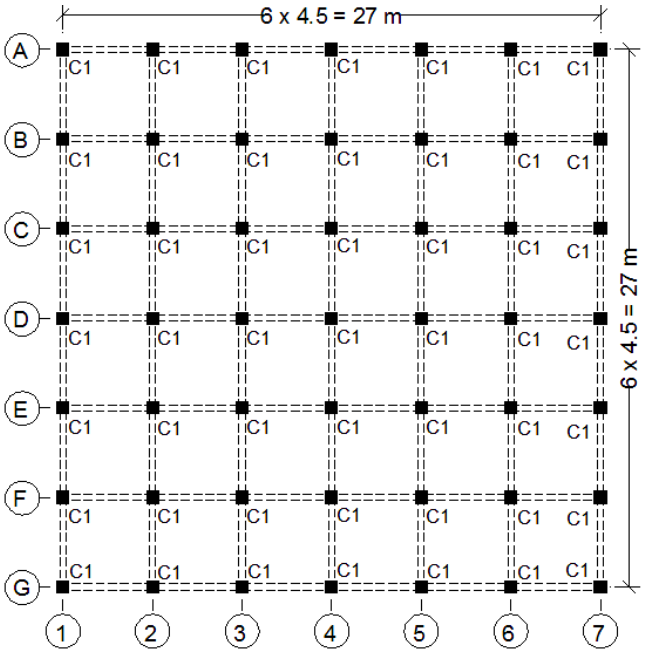

Figure 15 Rigid frame system plan

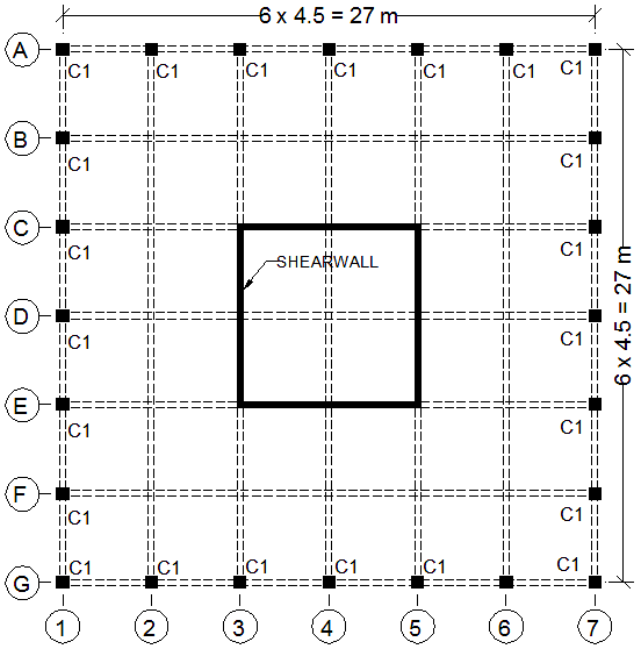

Figure 16 Shearwalled-frame and outrigger system plan

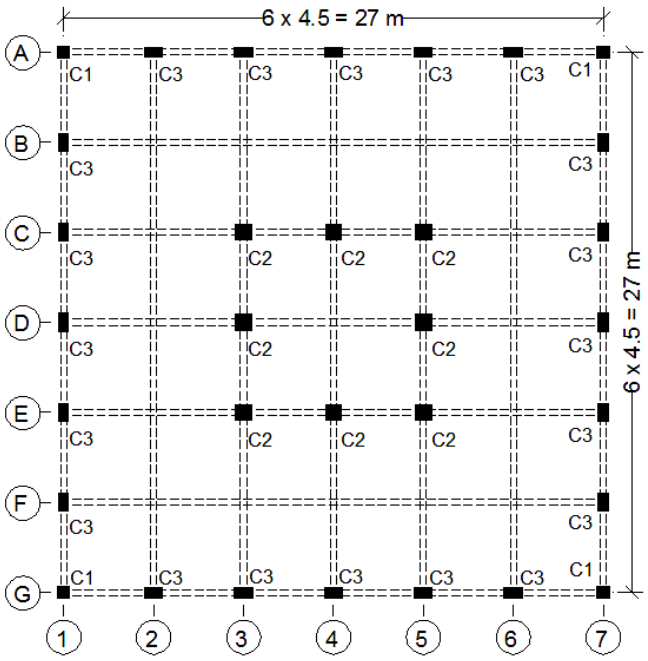

Figure 17 Framed-tube system plan

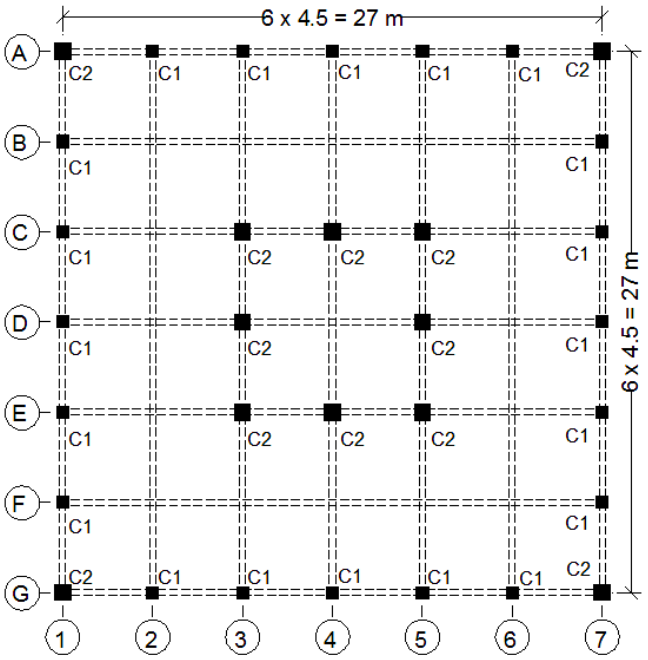

Figure 18 Braced-tube system plan

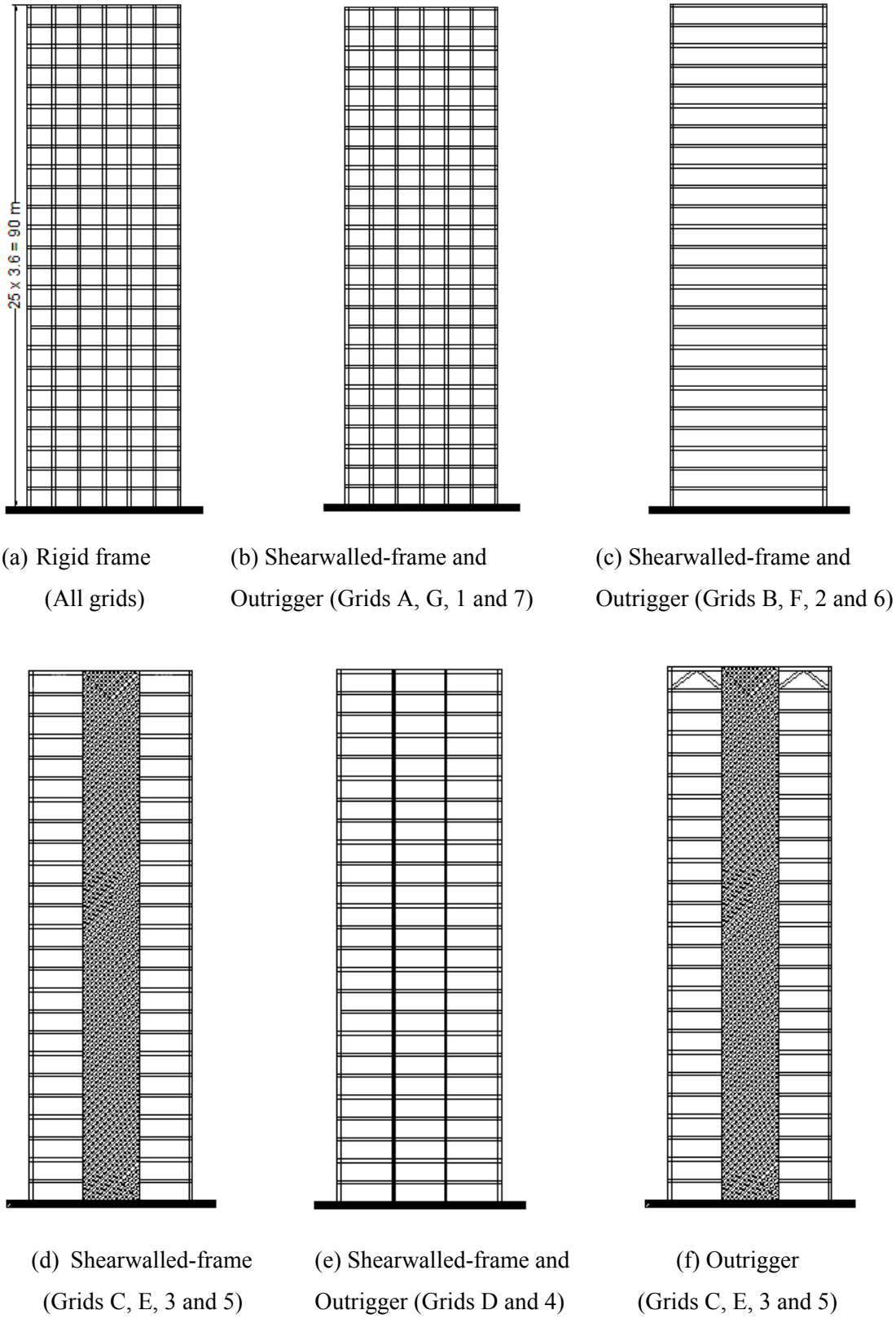

(a) Rigid frame (All grids)

(b) Shearwalled-frame and Outrigger (Grids A, G, 1 and 7)

(c) Shearwalled-frame and Outrigger (Grids B, F, 2 and 6)

(d) Shearwalled-frame (Grids C, E, 3 and 5)

(e) Shearwalled-frame and Outrigger (Grids D and 4)

(f) Outrigger (Grids C, E, 3 and 5)

Figure 19 Typical frame elevation of rigid frame, shearwalled-frame and outrigger systems

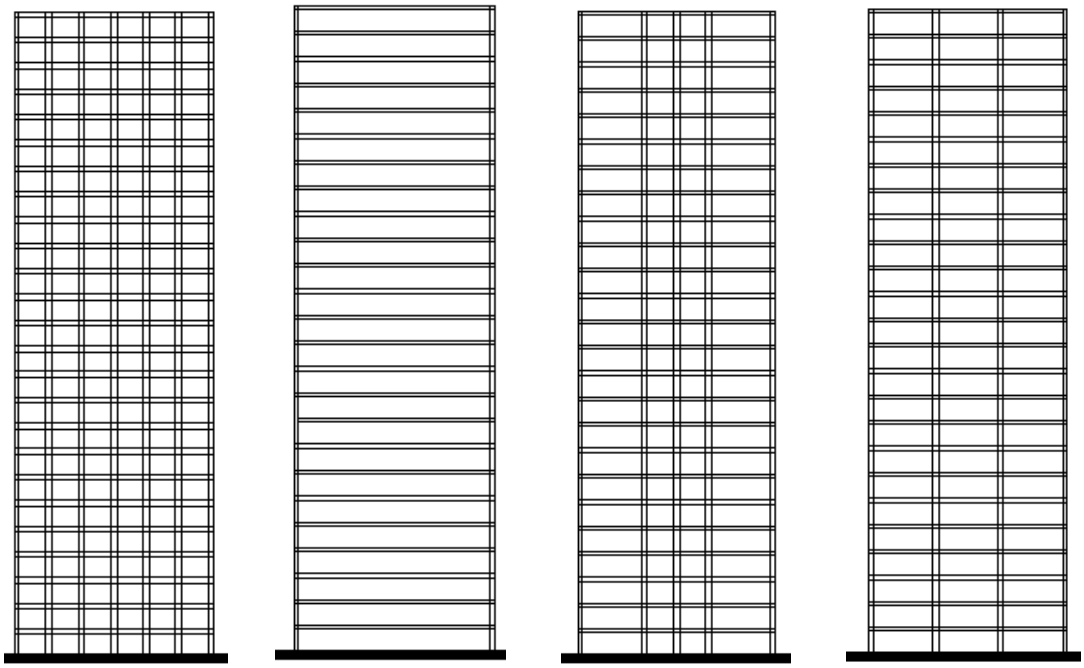

Figure 20 Typical frame elevation of framed-tube systems

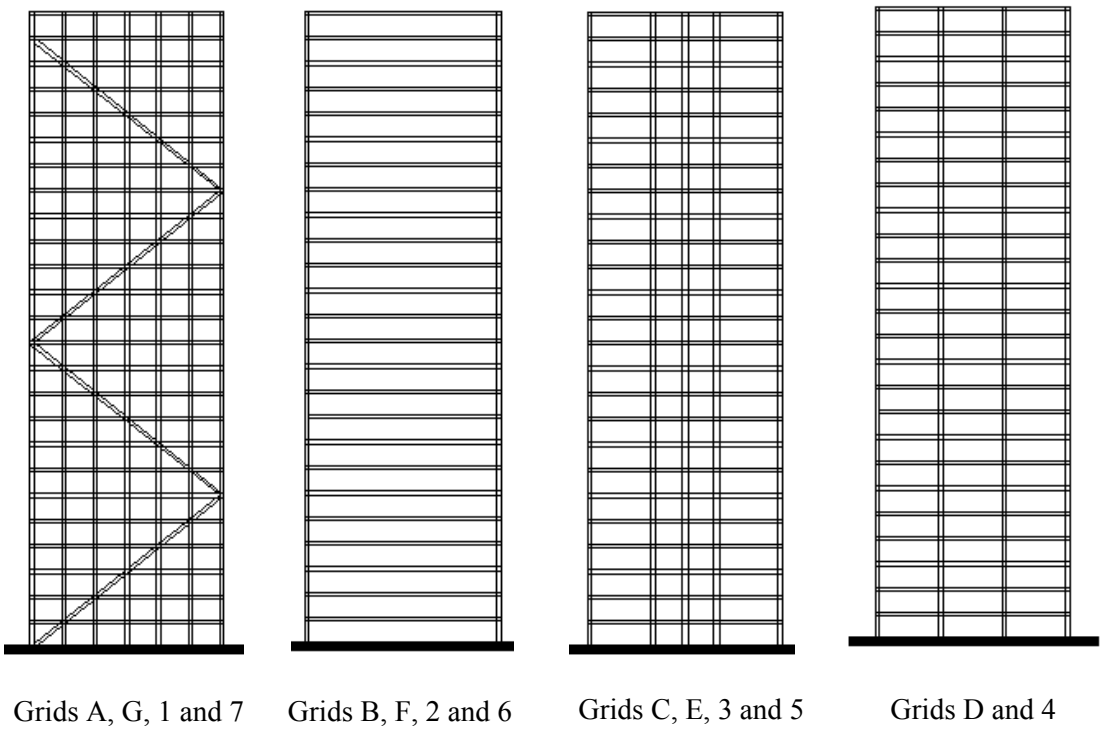

Figure 21 Typical frame elevation of braced-tube systems

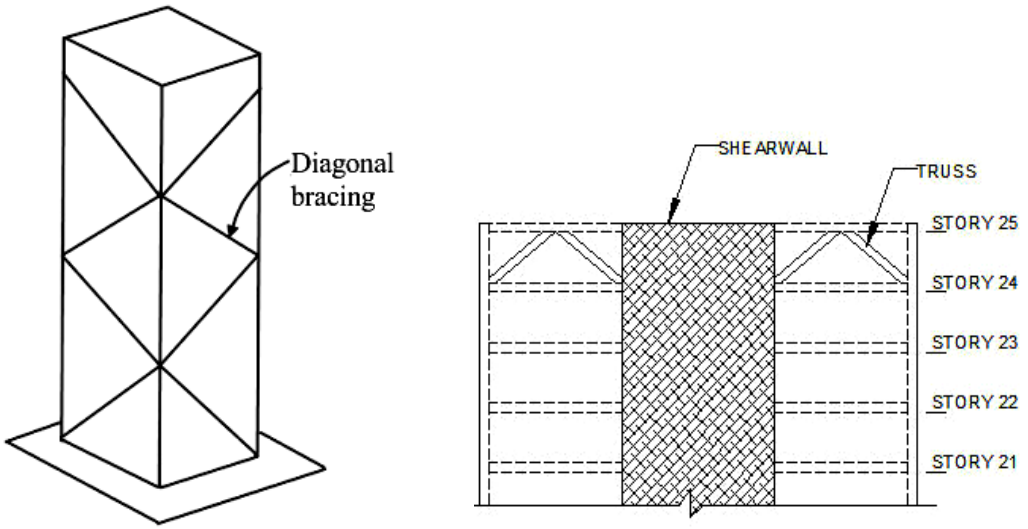

Figure 22 a) 3D elevation of diagonal bracing for braced-tube; b) Outrigger truss for outrigger system

Table 3 Member sizes (in mm) for Case 2 models

Structural Systems	Columns		Beams
	Designation	All Storys	All Floors
Rigid Frame	C1	600 x 600	350 x 550
Shearwalled Frame	C1	600 x 600	350 x 550
Framed-Tube	C1	600 x 600	350 x 550[1]
	C2	800 x 800	350 x 800[2]
	C3	900 x 500	
Braced-Tube	C1	600 x 600	350 x 550
	C2	800 x 800	
Outrigger	C1	600 x 600	350 x 550

[1] Interior beams [2] Peripheral beams (i.e. beams along grid A, G, 1 and 7)

In Case 3 Models, instead of using same sections throughout the building height, column sections were modified with the intention to satisfy strength, serviceability, and minimum cost criteria. Hence, column C1 was reduced to 500 x

500 mm, C2 to 600 x 600 mm and C3 to 700 x 500 mm for all models from 16th story upwards. However, this reduction of column sections resulted in roof deflection of 186 mm for rigid frame system for wind load, which marginally exceeded the maximum allowable deflection of 180 mm (i.e. H/500). Thus, column C1 for rigid frame system was increased to 650 x 650 mm from the 15th story downwards to satisfy the maximum deflection criteria.

Table 4 Member sizes (in mm) for Case 3 models

Structural Systems	Columns			Beams
	Designation	1st Story-15th Story	16th Story-25th Story	All Floors
Rigid Frame	C1	650 x 650	500 x 500	350 x 550
Shearwalled Frame	C1	600 x 600	500 x 500	350 x 550
Framed-Tube	C1	600 x 600	500 x 500	350 x 550[1]
	C2	800 x 800	600 x 600	350 x 800[2]
	C3	900 x 500	700 x 500	
Braced-Tube	C1	600 x 600	500 x 500	350 x 550
	C2	800 x 800	600 x 600	
Outrigger	C1	600 x 600	500 x 500	350 x 550

[1] Interior beams [2] Peripheral beams (i.e. beams along grid A, G, 1 and 7)

Apart from columns and beams described above, some additional members were required as part of structural system for some structural systems. For instance, shearwall in the form of core was used for shearwalled-frame and outrigger systems (Figure 16), and outrigger truss (Figure 22b) was provided along grid C, E, 3 and 5 at 25th story for outrigger systems. Multistory diagonal bracing was provided on the four faces of the braced-tube system (Figure 21, Figure 22a). The details of additional structural members are given in Table 5. They were kept same throughout the height of the building and for all the three cases considered.

Table 5 Additional structural members for all cases of analytical models

Structural Members	Size (mm)	Structural Systems
Shearwall	350 (thickness)	Shearwalled-Frame, Outrigger
Bracing[1]	350 x 500	Braced-Tube
Outrigger truss[1]	350 x 500	Outrigger

[1] Composite member

Multistory diagonal bracing for braced-tube was formed by encasing 2 numbers of ISMB400 structural steel section in rectangular concrete section of 350 x 500 mm, while the outrigger truss is formed by encasing 2 numbers of ISMB350 in rectangular concrete section of 350 x 500 mm. Section properties of steel section can be found in SP6 (1964).

To accurately predict the response of each structural system, due care was given to create a detailed and efficient models of the structures by taking into account all necessary geometric and strength characteristics of columns, beams, slabs and walls. 3D beam elements (Figure 6) having 12 DOFs with 6 DOFs each node were used to generate the structural frames, while shell elements having 24 DOFs with 6 DOFs at each corner node were used for modelling structural walls. These shell elements were indeed super elements in that the deformation along the boundary was automatically satisfied even if the meshing was coarser. Each face of the shearwalls over the height of one story was modelled using 10 x 5 number of shell elements. The parametric study was carried out to arrive at the choice of 10 x 5 number of shell elements. The detail of the parametric study is provided in Section B.1 of Appendix B. Non-structural members such as external curtain walls, internal partition walls and utilities were not explicitly modelled but their weights were taken into account.

In the analytical models, slab was considered as a rigid diaphragm in its own plane. This assumption is appropriate since the inplane stiffness of floor slab is

very large and the building width-to-depth ratio is 1, thus fulfilling the conditions stipulated in many codes (IS 1893, 2002; ASCE 7, 2005).

The models were considered to be fixed at the base. The fixed support is justified since the soil in Bhutan is generally stiff. Moreover, for high-rise buildings, because of the need to cater for the overall stability, pile foundations are required to anchor the building to the ground, which generally acts as stiff base.

3.2 Material properties

The material properties are assumed to be identical throughout the height of the structure and are based on IS 456 (2000). The details of the materials used for the analysis are shown in Table 6.

Table 6 Properties of materials

Items	Values
Characteristic strength of concrete at 28 days, f_{ck}	35 N/mm^2
Elastic modulus of concrete, $E = 5000\sqrt{f_{ck}}$	29580.4 N/mm^2
Poisson's ratio, ν	0.2
Unit weight of reinforced concrete	24 kN/m^3
Characteristic strength of reinforcement, f_y	415 N/mm^2
Flexural stiffness of beams and structural walls	$0.5I_g$
Flexural stiffness of columns and composite members	$1.0I_g$

The stiffness contribution from the structural steel in composite members was taken into account in the analytical models by transforming the steel section to concrete section through modular ratio, n, where n is the ratio of elastic modulus of steel to elastic modulus of concrete. The flexural stiffness of beams and structural walls (I_g) were reduced by 50% to reflect the stiffness reduction of the concrete members due to flexural cracking. However, full stiffness was used for the column as

per ACI 318 (2005). The background to the reduction of flexural stiffness in flexural members was given in Section 3.2 under Literature Review.

4. Structural Analysis

4.1 Gravity loading

Self-weight of the structural members including beams, columns, and slabs were calculated based on unit weight of 24 kN/m^3. Superimposed dead load (partitions, finishes, services) of 2 kN/m^2, curtain wall load of 2.8 kN/m along the periphery of the building, and the floor live load of 4 kN/m^2 (office floors) were considered in accordance with IS 875: Part 2 (1987). Since not all floors were loaded fully at the same time, live load reduction as per IS 875: Part 2 (1987) was taken into account while designing the columns. However, for the sake of simplification, live load pattern had been omitted from the consideration.

4.2 Seismic analysis

Earthquake loading for the structural models was based on Indian Standard IS 1893 (2002). As the height of the building in this study is 90 m, which exceeded the codal requirement of 40 m to qualify for the static analysis, it has necessitated the dynamic analysis. The detailed background to seismic analysis was provided in Section 3.4.3 under Literature Review.

The response spectrum analysis was performed to determine the responses of each structural system. At the same time, static analysis using equivalent lateral force procedure was carried out to benchmark the base shear from the response spectrum analysis. Section A.1.1 and A.1.2 of Appendix A may be referred for the procedure of equivalent lateral force static analysis and response spectrum analysis. Linear time history analysis was also carried out for Case 3 models to investigate how each structural system behaves towards the particular ground motion. Seismic weight

of the building was computed using full dead load plus 50 percent of live load for all floors.

For this study, seismic zone V, soil type II (Medium soil), importance factor of 1, response reduction factor of 3, and damping of 5 percent of the critical (IS 1893, 2002) were used for the analysis of all structural systems. The response reduction factor of 3 was chosen to be consistent in seismic loading for different structural systems since the standards included response reduction factor only for limited cases of buildings. Likewise, natural period of vibration from rational analysis was used instead of approximate time period (Eq. (A1) and Eq.(A2) ; Appendix A) for the computation of various seismic responses. This was done because the standards provided approximate time period formula only for moment resisting frames. Moreover, the intention in this study was to compare the behaviour of different structural systems. So it was essential to use the accurate time period from rational analysis.

For response spectrum analysis, eight modes of vibration were considered to achieve the sum total of modal masses of all modes at least 90 percent of the total seismic mass. Complete Quadratic Combination (CQC) rule was used to combine the response quantities from each mode of vibration. CQC rule was suitable in this study since in many cases vibration modes were symmetric due to building being regular and symmetrical. As required by the code, where base shear from response spectrum analysis was less than the base shear from static analysis, all the response quantities were scaled up by the factor of $V_{b,s}/V_{b,d}$ where $V_{b,s}$ and $V_{b,d}$ are the base shear from static and response spectrum analysis respectively. Torsional response was ignored in this study.

A linear time history analysis was performed on Case 3 models using the horizontal acceleration of Bhuj earthquake, which was recorded at the seismic station at Ahmedabad, India. Figure 23 shows the time histories of ground acceleration, ground velocity, and ground displacement of this earthquake. Only one ground motion was used for this study to observe how different structural systems behave

towards the typical ground motion. The ground motion was scaled up by a factor of α = 1.8, which was derived using Malhotra's (2003) method (Section A.2.3, Appendix A), to match with the design response spectra of the standard (IS1893, 2002). The details of the derivation of scale factor are included in Section A.3 of Appendix A.

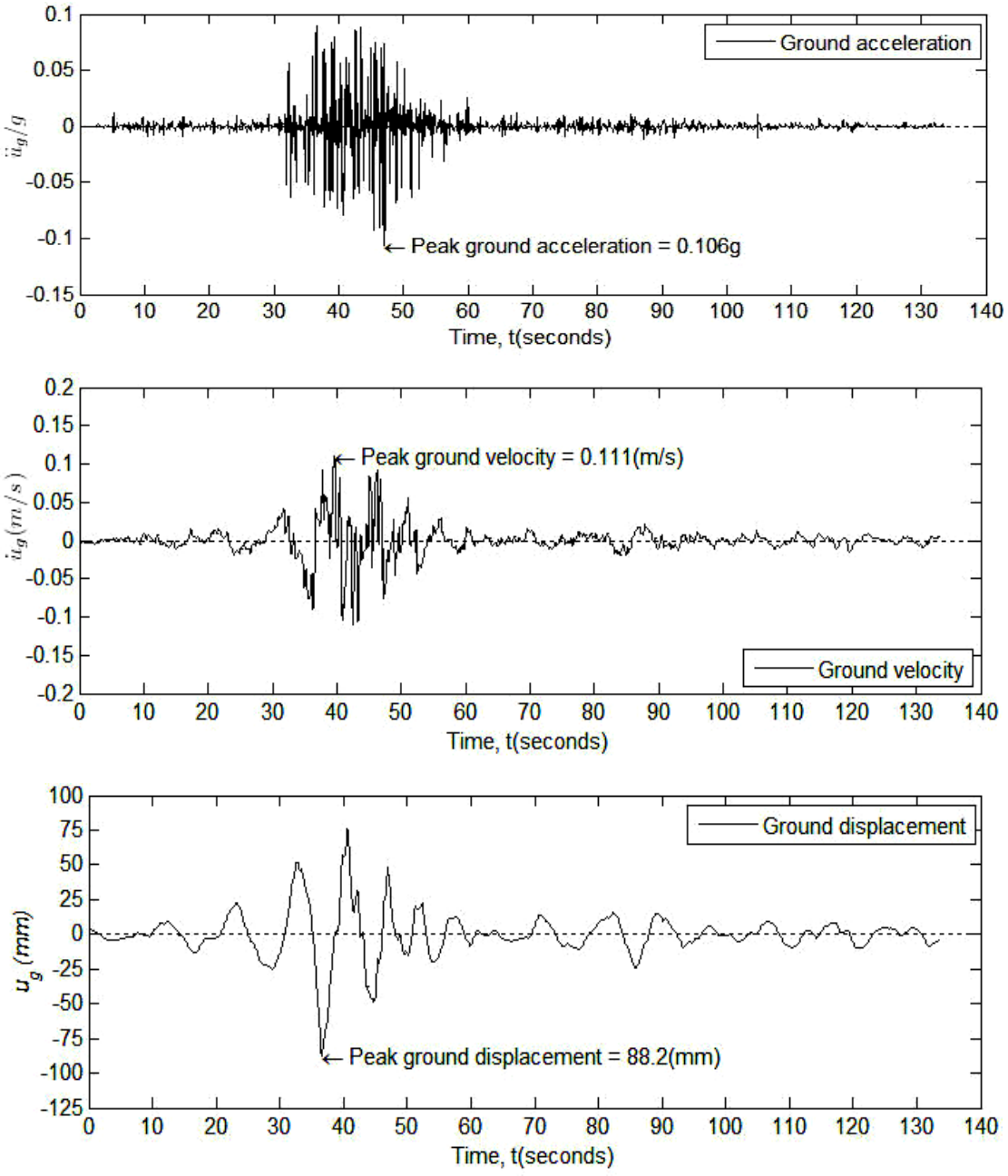

Figure 23 N 78 E component of horizontal ground motion recorded at the Ahmedabad, India, during the Bhuj earthquake of January 26, 2001

The scaling method proposed by Malhotra (2003) was chosen since it provided better results compared to spectrum intensity (Section A.2.1, Appendix A). Ground motion records of Bhuj earthquake, India was selected for this study since parameters required for Malhotra's scaling method were readily available (Malhotra, 2003).

To check the suitability of the selected ground motion, response spectra of the scaled ground motions are usually developed and compared with the standard design response spectra.

As such, design response spectra for the scaled as well as the original Bhuj earthquake ground motion were constructed and compared with the standard design response spectra of Figure 9 for the medium soil. Figure 24 shows both the scaled and unscaled response spectra of Bhuj earthquake along with the design response spectra of IS 1893 (2002).

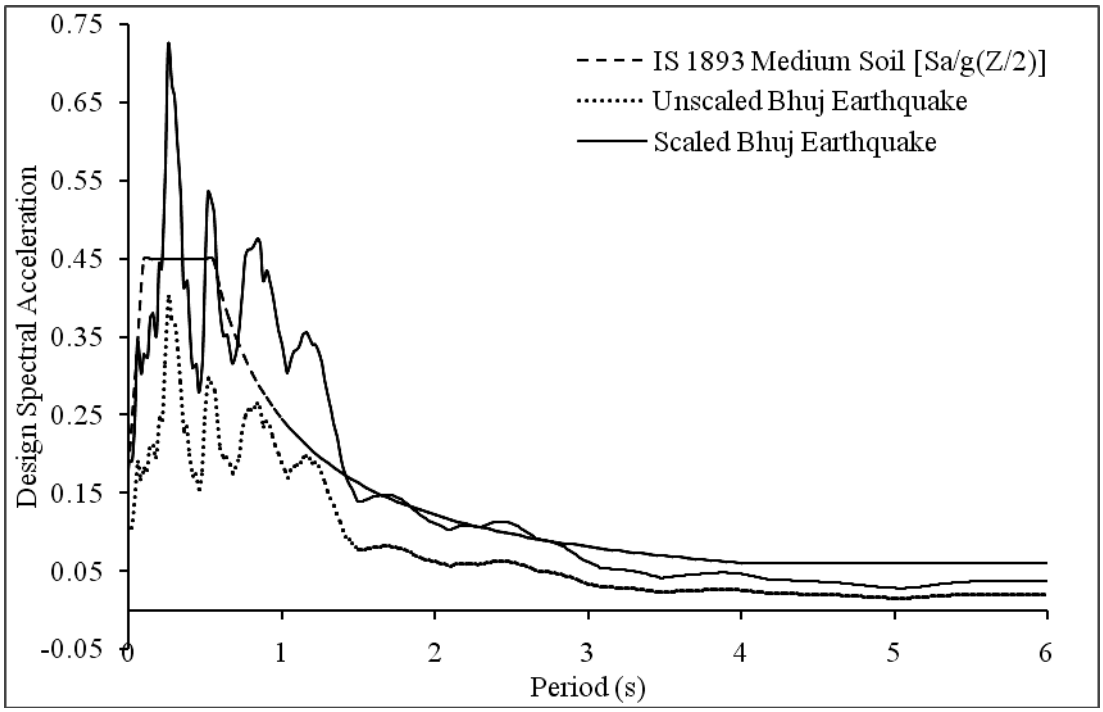

Figure 24 Spectra of Bhuj earthquake compared with design spectra of IS 1893 (2002)

The scaled ground acceleration (Figure 25) was applied to the base of the structures for Case 3 models. The response quantities obtained from the time history analysis were multiplied by the scalar quantity, I/R where I is the importance factor and R is the response reduction factor (ASCE 7, 2005). Additional information regarding time history analysis of buildings can be found in ASCE 7 (2005) and FEMA450 (2003).

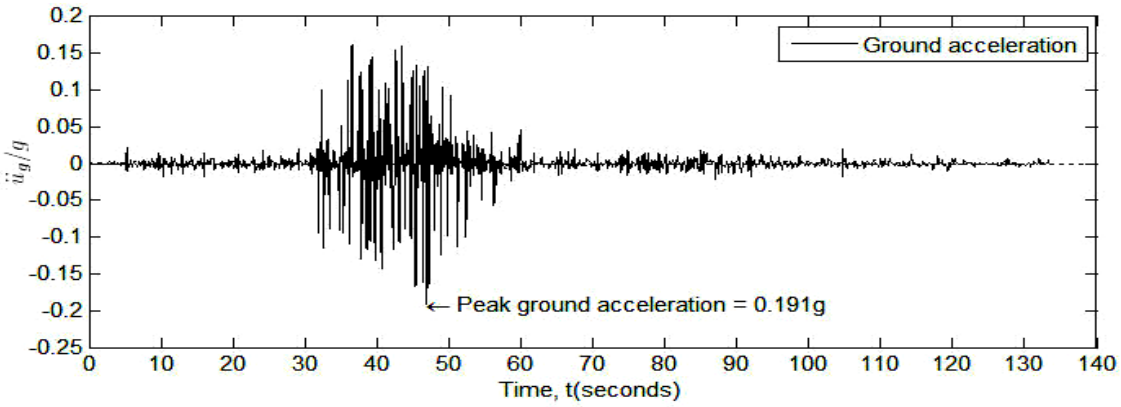

Figure 25 Scaled horizontal ground motion used for time history analysis

It should be noted that the results of linear time history analysis were used only for the comparison of responses among structural systems, not for the subsequent design of structural members.

4.3 Wind load analysis

Indian Standard IS 875: Part 3 (2004) was used for wind load calculation. Though the building in this study met the height to least lateral dimension ratio of less than 5, it did not satisfy the natural frequency of vibration of more than 1 Hz, as required by the code, to qualify for static analysis. This has demanded the dynamic effect of wind be taken into account. The detailed background to the wind loading on structure is provided in Section 3.4.4 under Literature Review.

Basic wind speed of 47 m/s, representing 50-year return period, terrain category 3, and damping of 2 percent of the critical (IS 875, 2004) were adopted for the calculation of wind pressure on the building. High-rise buildings are susceptible to the dynamic effects of wind. In order to account for the dynamic effects of wind, the static wind pressure was converted to the dynamic wind pressure by multiplying it with dynamic response factor. The fundamental natural frequencies required for the computation of dynamic response factors were directly computed as an inverse of corresponding time period given in Table 8 instead of using the approximate formula from IS 875: Part 3 (2004).

Under the action of wind, high-rise buildings oscillate simultaneously in the along-wind, cross-wind and torsional directions. However, the guidance to account for torsional affects is limited because of its complex nature. Many codes do not even account for cross-wind effects. Though IS 875: Part 3 (2004) has provisions to account for cross-wind effect, yet it does not have provisions for combining cross-wind effect with along-wind effect. These are required to be considered together because cross-wind occurs as a consequence of along-wind.

Therefore, for the combination of along-wind and cross-wind, AS/NZS 1170.2 (2002) was referred since it contains expression for the combination of along-wind and cross-wind responses as well as some guidelines for the combination of loads instead of responses. The latter option was used in this study since the former combination was not easily adaptable to the subsequent design of structural members. Thus, the following combination rules were used for the simultaneous application of along-wind and cross-wind onto the structures.

1) Mean along-wind load + 0.75 (peak-mean) along-wind ± 0.75 (peak-mean) cross-wind

2) Mean along-wind load + 1.0(peak-mean) along-wind

The procedures for computation of lateral forces due to along-wind and cross-wind are provided in Section C.1.1 and C.1.2 of Appendix C.

However, only the along-wind forces for different structural systems are reported on Figure 26 for Case 2 models. Typical calculations using the detailed procedures are demonstrated for rigid frame system in Section C.2 of Appendix C for Case 3 model.

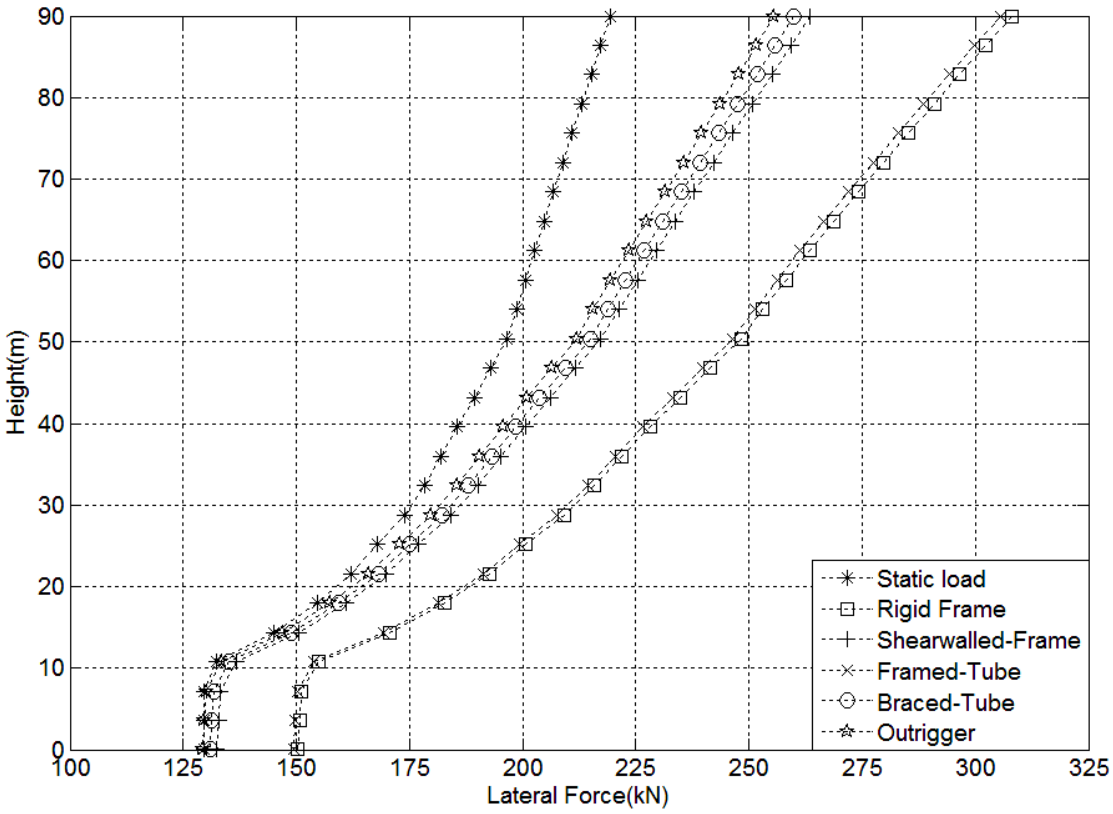

Figure 26 Static wind load and dynamic (along-wind) load for structural systems (Case 2 models)

Since second-order effect due to gravity load can be substantial especially in high-rise buildings, P-Delta effect was considered in all the analytical models during the analysis. For this purpose, full dead load plus 50% of live load was included as gravity load. The detailed background to the need for the inclusion of P-Delta effect simultaneously with lateral loads is included in Section 3.4.5 under Literature Review.

The same load combination, stipulated in the preceding paragraph, was used for determining the mass of the building for the computation of vibration properties of structural systems. Vibration properties of the building include natural periods, natural frequencies and the corresponding mode shapes.

5. Interpretation of Results

Global behaviour of the structure is normally described in terms of the responses such as story shear, story moment, deflection, drift, and roof acceleration. Towards this end, the results of the analysis such as the period of vibration, story shear, story moment, story displacement, and story drift due to wind and earthquake loads are presented and discussed under the Results and Discussions. In particular, behaviour of different structural systems in terms of responses quantities from wind and response spectrum analysis are compared.

6. Comfort Criteria

For most high-rise buildings, serviceability considerations may govern the design. One of them is the comfort criteria, generally expressed in terms of acceleration limits. For a linear fundamental mode of vibration, the maximum horizontal acceleration occurs at the roof level, that is at the top of the building. Hence, the assessment of horizontal acceleration at roof level is adequate to evaluate the comfort criteria.

The horizontal acceleration in the along-wind and cross-wind directions for the 5-year and 10-year return period were computed using Eq. (C12) and Eq. (C13) in Section C.1.4 and C.1.5 of Appendix C along with the structural properties in Table 7 for Case 3 models. Serviceable wind of 31.02 m/s (0.66 x 47 m/s) and 34.78 m/s (0.74 x 47 m/s) were used for 5-year return period and 10-year return period respectively. The factors 0.66 and 0.74 correspond to conversion factor for 5-year and 10-year return period respectively for deriving serviceable wind from ultimate wind as per ASCE 7 (2005).

In Table 7, linear mass refers to the mass per unit meter along the height of the building, structural density is defined as the total mass of the building divided by the volume of the building, and fundamental natural frequency is computed as an inverse of fundamental natural period of vibration given in Table 8. The calculation of horizontal acceleration is demonstrated in Section C.3 of Appendix C for rigid frame system for Case 3 model. The results of the roof acceleration due to serviceable wind for different structural systems are given in Table 17.

Table 7 Structural properties for the computation of horizontal acceleration (Case 3 models)

Structural Systems	Linear mass, m_0 (kg/m)	Structural Density (kg/m^3)	Fundamental natural frequency (Hz)
Rigid Frame	237476	326	0.24
Shearwalled-Frame	214966	295	0.37
Framed-Tube	236022	324	0.23
Braced-Tube	232874	319	0.39
Outrigger	215726	296	0.41

7. Quantity Analysis for Structural Systems

7.1 Structural design

Based on the results of gravity load, response spectrum and wind load analysis, the detailed design of structural members of structural systems for the Case 3 models were carried out in accordance with IS 456 (2000). The size of the columns, beams and other structural members were checked for various load combinations for gravity, wind and earthquake load to arrive at the final size given in Table 3 and Table 4. The amount of steel required for the structural members were maintained in between the minimum and maximum requirements. For columns, in most cases, the

steel reinforcement around 4 percent was maintained near the base of the building. However, the forces got reduced very fast away from the base of the building, and as a result, minimum reinforcements were adopted in columns for upper part of the buildings. Thickness of shearwalls was kept same throughout the height of the building, although it was not required from the design point of view. The same thickness of shearwall was needed to provide support for floor beams.

Although some variation of cost was expected with the variation of steel reinforcement and size of sections, parametric study on the variation of steel and section was not carried out because of practical consideration. Too much refinement of structural members is unrealistic and not desirable from practical aspect. Thus, certain uniformity of sections was maintained considering the practical aspects of construction. But the design was carried for each structural member, and the quantity of materials reported in Section 6 of Results and Discussions, and Section D.1 of Appendix D is the sum of the material quantities of each member.

7.2 Quantity of structural materials

Based on the design, the quantity of concrete and steel were estimated for each structural system. Separate quantity of materials was determined for floor slabs, beams, columns, shearwalls and bracings (Appendix Table D1 and Appendix Table D2). Quantity of concrete and steel required for each structural system is given in Table 18. Foundation and other non-structural materials have been omitted from the estimations.

7.3 Cost of structural materials

The material rates specified in Bhutan Schedule of Rates (BSR, 2007) were used for the estimation of structural materials. The use of characteristic strength of concrete of 35 MPa at 28 days is new to construction industries in Bhutan, and the cost of concrete for this strength is not covered by the above document. This has necessitated the unit cost of concrete be derived based on the concrete mix design.

Thus, the concrete mix for 35 MPa concrete was designed using the Indian Standard 10262 (1982) to arrive at quantities of cement, sand, crushed aggregate and water required to produce 1 m^3 of concrete. The details of the mix design can be found in Section D.2 of Appendix D.

Based on the item rates provided in BSR (2007), the rate for 1 m^3 of concrete was worked out. Cost of transportation from the probable place of origin of materials to the place of destination was included in the rate analysis. Using these rates, the cost of concrete and steel for each structural system was calculated and reported in Table 18.

RESULTS AND DISCUSSIONS

Based on the results obtained from the numerical analysis, the behaviour of different structural systems in terms of fundamental natural period, mode of vibration, story shear, story moment, story deflection, story drift ratio, maximum horizontal acceleration at roof level, and the cost of materials are compared in the following pages.

First the results of the eigenproblem are presented. This is followed by the presentation of seismic responses of different structural systems. In it, the responses from response spectrum analysis and linear time history analysis are discussed in detail. Responses from wind analysis are discussed next, followed by the comparison of wind and response spectrum analysis results. Subsequently, the human comfort criterion in terms of horizontal acceleration at the roof level, and the costs of material for the structural systems are compared.

1. Natural Periods of Vibration

The fundamental natural periods of vibration of structural systems along with the percentage difference for three cases of models are shown in Table 8. For this purpose, full dead load along with 50 percent live load was considered for the computation of mass of the structure. Mass of the structure was obtained by dividing the above load combination by the acceleration due to gravity of 9.81 m/s^2. Mass has the unit of $kN\text{-}s^2/m$ in vibration problem. Vibrations in all the models were dominated by the translational modes. Further, the inclusion of P-Delta effect during the analysis had resulted in slight lengthening of periods.

While some variation of fundamental natural period of vibration among the structural systems for three Cases is noted, the reasons are not easily discernable. With the exception of rigid frame and outrigger system, the general trend is the decrease of fundamental natural period of vibration, T_1 over the three cases of models. This is because the fundamental natural period, T_1 is controlled by the beam-to-

column stiffness ratio, ρ (Chopra, 2001). This is not explicitly evident from Eq.(7), but is inherently embedded in the stiffness of the system. As ρ (beam-to-column stiffness ratio) increases, fundamental natural period of vibration, T_1 decreases.

Table 8 Fundamental natural period of vibration, T_1

Structural Systems	Periods (seconds)			Difference in percent	
	Case 1 models	Case 2 models	Case 3 models	Case 1 and Case 2 models	Case 2 and Case 3 models
Rigid Frame	4.24	4.39	4.23	+3.5%	-3.6%
Shearwalled-Frame	2.75	2.74	2.73	-0.4%	-0.4%
Framed-Tube	5.75	4.29	4.26	-25.4%	-0.7%
Braced-Tube	2.61	2.61	2.57	0%	-1.5%
Outrigger	2.42	2.44	2.44	+0.8%	0%

For shearwalled-frame system, the reduction of column sizes in Case 2 has resulted in the increase of ρ, and hence the decrease of T_1 in Case 2. Since the column sizes were further reduced above 15th story in Case 3, it has further resulted in the reduction of T_1 in Case 3. For the framed-tube system, since the same section of structural members was used in Case 1 models irrespective of structural systems, it has resulted in a period of 5.75 seconds due to it being very flexible. Because of the increase in size of peripheral beams and columns in Case 2, the overall effect is the increase of stiffness of the structural system, thereby resulting in the sharp decrease of T_1 in Case 2. As the column sizes were reduced above 15th story for Case 3, it further resulted in the decrease of T_1. Although, column sizes were altered for braced-tube system in Case 2 (i.e. some column sections were increased and some were decreased), the resulting frame stiffness has coincidentally remained unaltered as indicated by the same T_1 for Case 1 and Case 2. But the slight decrease of T_1 in Case 3 is attributed to the increase of ρ because of the reduction of column sizes above 15th story. For rigid-frame, because of the drastic reduction of column sizes in Case 2 and

sole reliance on columns for the lateral resistance, there is a reduction of overall stiffness of the system, hence the increase in T_1. However, outrigger system appears to defy the general trend. This could be due to the effect of outrigger truss at roof level. However, the variation is negligible.

For the structural systems considered in this study, approximate equations such as Eq. (A1) from the standard (IS 1893, 2002) predicted fundamental period of 2.19 seconds for rigid frame structural systems. Similarly, Eq.(A2) predicted fundamental period of 1.56 seconds for other structural systems. It is interesting to observe that all periods from rational analysis (Table 8) are higher than the values given by approximate formulae in codes. For instance, fundamental period from rational analysis is longer by 93 percent for rigid frame and 75 percent for shearwalled-frame system. While the codal formulae include only depth or height of the structures, the rational analysis considered both mass and stiffness of the structures. As such, size of structural members as well as proportion of live load to be included along with the dead load, would affect the periods. However, these factors are not considered by the approximate period formulae in codes. This would result in same periods irrespective of the size of structural members and loads considered. On the other hand, rational analysis would result in periods that are more accurate.

To observe the influence of higher modes of vibration on the response of the structural systems, the natural periods and the corresponding eight modes of vibration for Case 3 models are plotted on Figure 27. Since the building in this study is symmetric in both mass and stiffness, it has resulted in symmetric mode of vibration that have directions 90 degrees apart and equal periods for two consecutive modes with the exception of braced-tube system. For braced-tube system, though the plan is symmetric, the overall system is not symmetric due to asymmetric arrangement of diagonal bracing. Although the structural systems are different, yet the natural periods obtained were very similar in some structural systems. Hence they got superimposed in the plot.

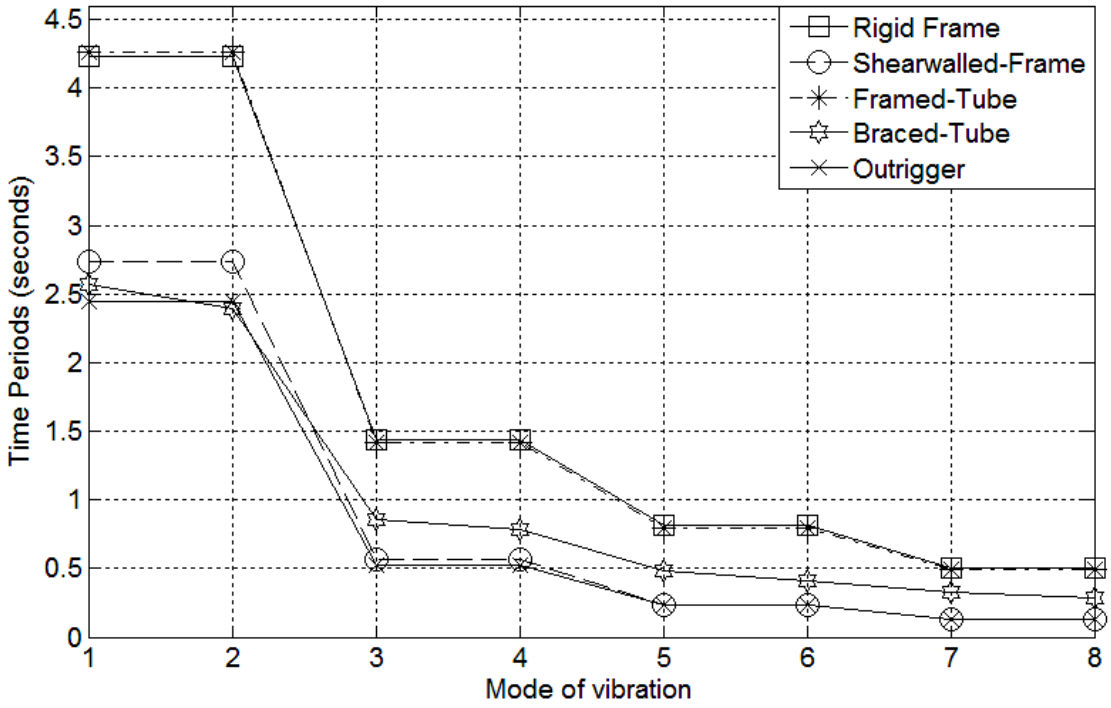

Figure 27 Influence of higher modes on the response (Case 3 models)

Considerable influence from higher modes can be expected for shearwalled-frame, outrigger and braced-tube systems as indicated by low natural periods for higher modes. The lower modal periods would result in corresponding higher design horizontal seismic coefficient, A_h (Eq.(11), Figure 9) and hence higher modal lateral forces, so long as natural period is above 0.1 seconds.

Another factor that affects the modal response is the modal participation factor, P_k given by Eq.(A7) of Appendix A. Modal participation factor (P_k) of mode k of vibration is the amount by which mode k contributes to the overall vibration of the structure. It decreases with the increase in mode of vibration. Modal participation factor are found higher, especially for higher modes of vibrations, for shearwalled-frame, outrigger and braced-tube when compared to the rigid frame and framed-tube. As evident from Eq.(A8) of Appendix A, both design horizontal seismic coefficient, A_k and modal participation factor, P_k influences the corresponding response of mode k. Hence, they are required to be considered simultaneously.

2. Seismic Responses of different Structural Systems

2.1 Responses from response spectrum analysis

Peak story moment, story shear, displacement and story drift ratio from response spectrum analysis are plotted on Figure 28, Figure 29 and Figure 30 for all Cases.

2.1.1 Story moment and story shear

The variation of peak story moment and peak story shear for shearwalled-frame and outrigger systems are marked by the irregularity over the height of the building (Figure 28, Figure 29 and Figure 30). For these structural systems, considerable influence from higher modes of vibrations was observed (Section B.2 of Appendix B). The reason for the snaky plot of story shear for shearwalled-frame and outrigger systems is demystified in terms of modal story shear in Section B.2 of Appendix B. In shearwalled structures, the modal base shear from mode 3 and mode 4 were higher than the modal base shear from mode 1 and mode 2. This is because the natural periods of mode 3 and mode 4 were about 0.5 seconds which correspond to the maximum spectral coefficient in Figure 9, thus resulting in higher modal lateral forces for these modes. Also, during analysis, the peak base shear from response spectrum analysis was found slightly higher than the base shear from static analysis for shearwalled-frame and outrigger. All these suggest that the static analysis alone might not be sufficient to fully unveil the behaviour of this type of structures.

The increase of bending moment towards the base of the building in outrigger system is the result of inclusion of outrigger truss at the roof level. It also caused difference in story shear around mid-height of the building. Further, it was observed that outrigger truss attracts huge shear force in the corewall at the location of outrigger truss.

The rigid frame and framed-tube systems have both the story moment and story shear lower than those of shearwalled-frame, braced-tube and outrigger systems. The superposition of story shear and story moment plots for rigid frame and framed-tube system for Case 2 and Case 3 models is purely incidental. Although there is significant difference in the structural framing, yet it has resulted in the similar plot and hence got superimposed. This consequence may be attributed to the similar time period and corresponding mode of vibration (Figure 27). However, the differences are revealed in Section 6 where the cost of different structural systems is compared. Base shear and base moment for three cases of models are shown in Table 9.

Table 9 Base shear and base moment from response spectrum analysis

Structural System	Base Shear (kN) x10^3			Base Moment (kNm) x10^5		
	Case 1	Case 2	Case 3	Case 1	Case 2	Case 3
Rigid Frame	4.689	4.289	4.260	2.775	2.562	2.505
Shearwalled-Frame	8.075	7.833	7.822	3.149	3.034	2.998
Framed-Tube	4.336	4.323	4.256	2.820	2.558	2.509
Braced-Tube	6.772	6.578	6.520	3.707	3.580	3.540
Outrigger	8.099	7.805	7.790	3.531	3.353	3.299

Note: Case 1, Case 2 and Case 3 refers to corresponding analytical models

As observed in Table 9, both the base shear and the base moment decreased from Case 1 to Case 3 models. For base shear, it decreased by 9.1% for rigid frame, 3.1% for shearwalled-frame,1.8% for framed-tube, 3.7% for braced-tube and 3.8% for outrigger. For base moment, it decreased by 9.7% for rigid frame, 4.8% for shearwalled-frame, 11% for framed-tube, 4.5% for braced tube and 6.6% for outrigger systems. This shows that the decrease is greater for base moment than for base shear.

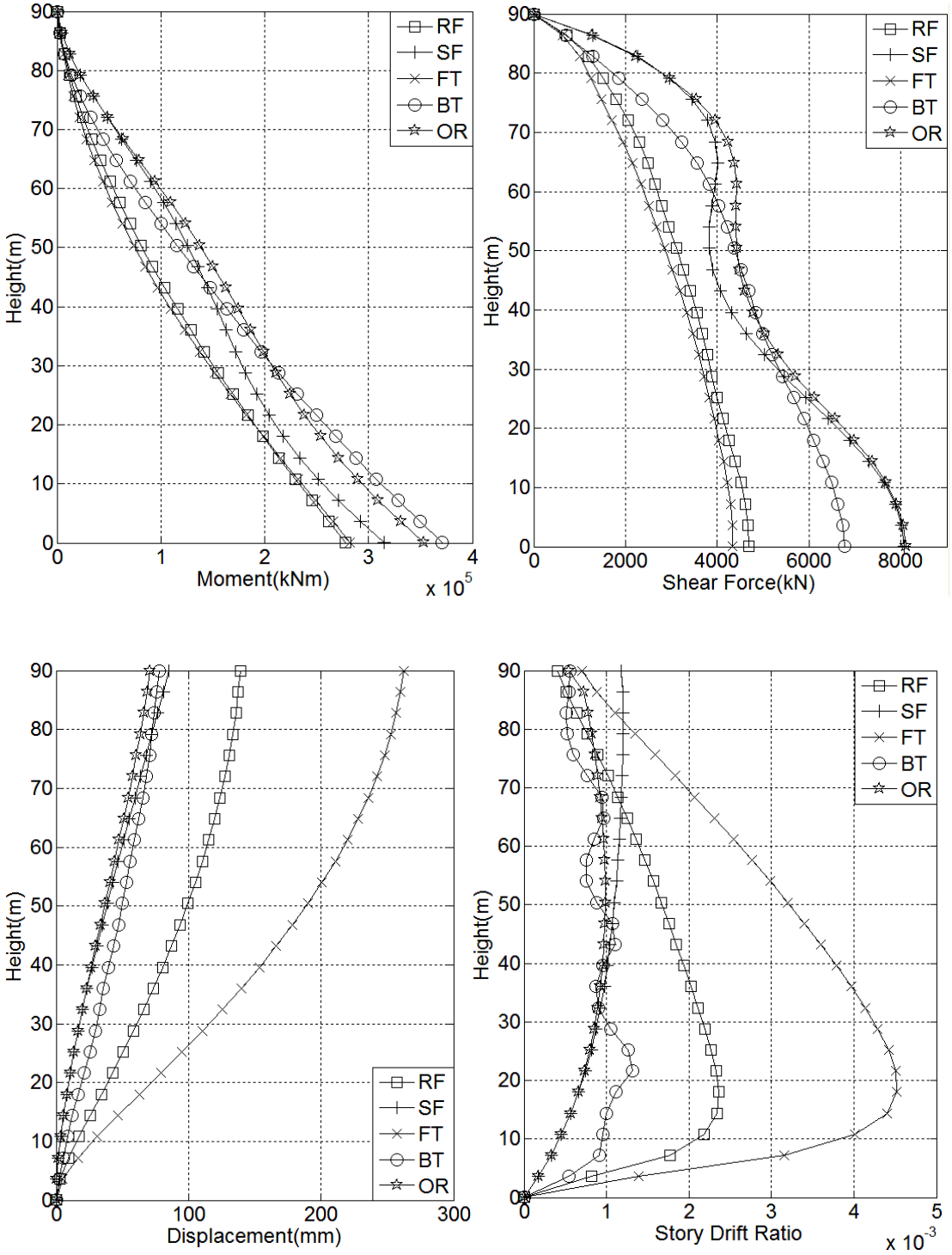

Figure 28 Peak story moment, story shear, displacement and story drift ratio from response spectrum analysis (Case 1 models)

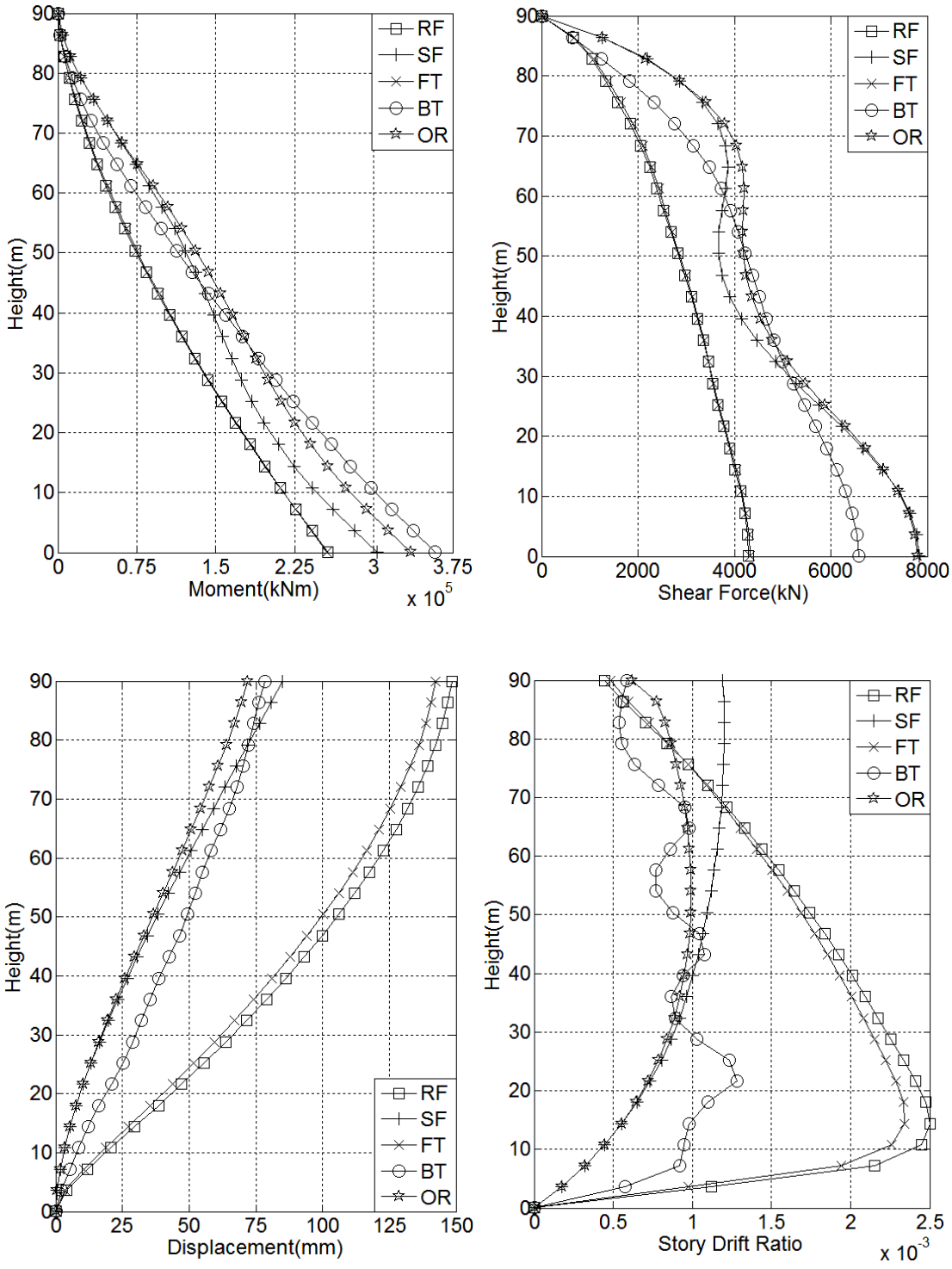

Figure 29 Peak story moment, story shear, displacement and story drift ratio from response spectrum analysis (Case 2 models)

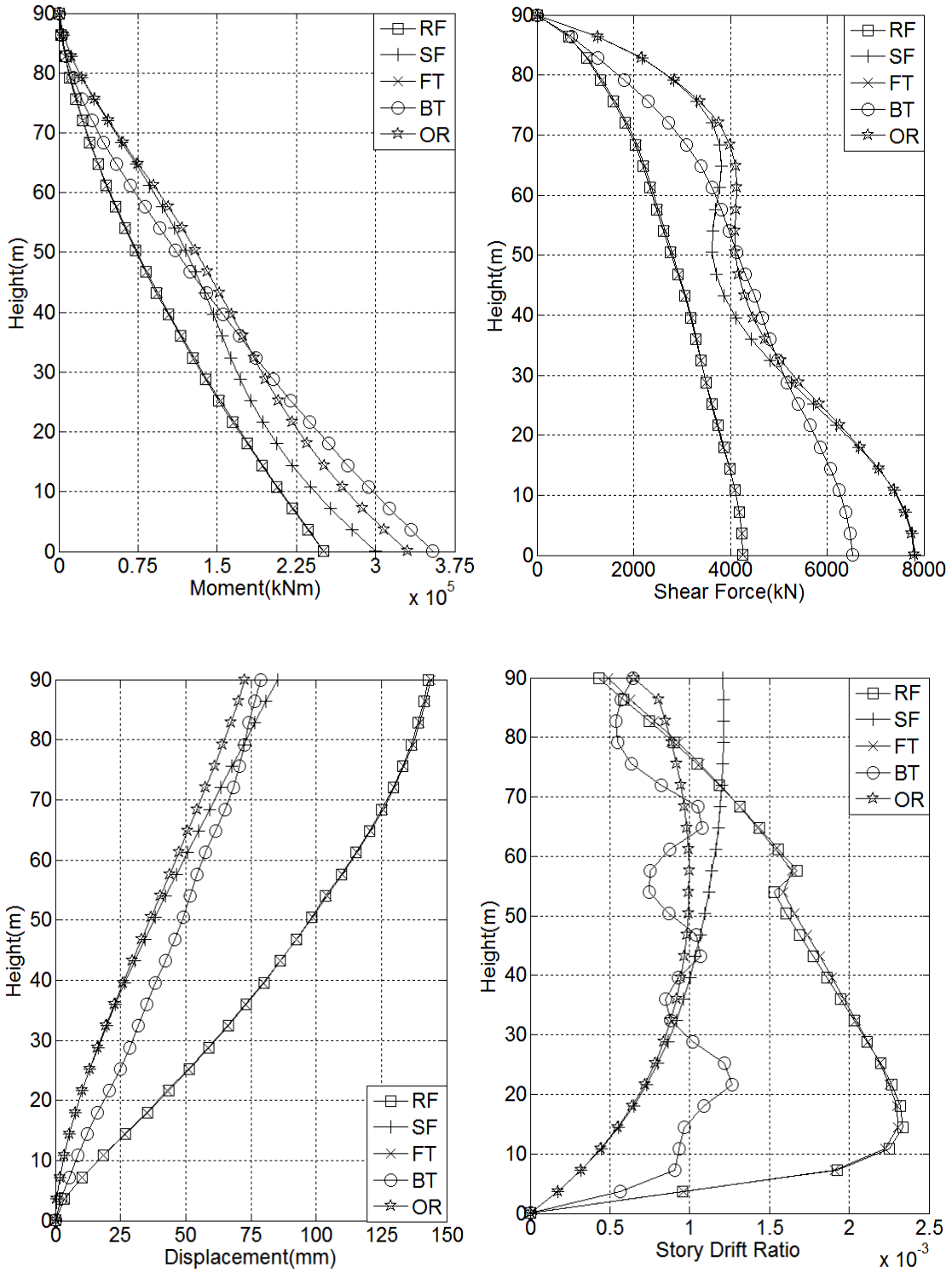

Figure 30 Peak story moment, story shear, displacement and story drift ratio from response spectrum analysis (Case 3 models)

2.1.2 Peak story displacement and drift ratio

The variation of displacement for shearwalled-frame and outrigger systems is more uniform and linear compared to other structural systems over the height of the building (Figure 28, Figure 29 and Figure 30).

The variation of story drift ratio for rigid frame and framed-tube system is drastic for first four storys. Thereafter, story drift decreases gradually to the top of the building. In other words, the drift is concentrated towards the base of the building in this type of structural systems. Abrupt changes can be observed in story drift ratio from 15^{th} story to 16^{th} story for Case 3 models. This is because, for Case 3 models, the columns sections were reduced from 16^{th} story upwards. This abrupt jump in story drift ratio is absent in the plot of Case 1 and Case 2 models since same sections were used throughout the building height. It is interesting to note that the impact of reduction of column sizes above 15^{th} story was depicted only by the drift ratio.

Story drift ratio for shearwalled-frame increases gradually from the base till the mid-height. Thereafter, it is almost constant up to the top of the building. Similar is the case for outrigger system except that story drift ratio gradually decreases upward of mid-height of building. Braced-tube system depicted peculiar behaviour in terms of drift. In this case, the increase of story drift is dramatic for first 3 storys. Thereafter, it continuously varied till the top of building. Further the variation oscillates about the certain value. This unique wavy-plot may be attributed to the presence of diagonal bracing along the periphery of the building. It is also to be noted that there is no sudden jump in story drift ratio for shearwalled-frame, braced-tube and outrigger systems, indicating that they are less likely to be affected by the reduction of column sections.

Roof displacement and maximum story drift ratio for three cases of models are shown in Table 10.

Table 10 Roof displacement and maximum drift ratio from response spectrum analysis

Structural System	Roof Displacement (mm)			Maximum Story Drift ratio $x10^{-3}$		
	Case 1	**Case 2**	**Case 3**	**Case 1**	**Case 2**	**Case 3**
Rigid Frame	139.0	148.6	142.8	2.366	2.502	2.335
Shearwalled-Frame	85.2	84.9	85.2	1.197	1.201	1.213
Framed-Tube	262.5	142.5	143.9	4.523	2.343	2.306
Braced-Tube	78.2	78.3	78.7	1.311	1.281	1.267
Outrigger	71.0	71.9	72.5	0.986	0.993	0.997

Note: Case 1, Case 2 and Case 3 refers to corresponding analytical models

As observed from Table 10, the general trend is the increase of roof deflection from Case 2 to Case 3 with the exception of rigid frame. The increase is brought about by the reduction in stiffness in the upper part of the building for Case 3 models. However, the reduction of deflection in Case 3 for rigid frame is the result of increase of column section below 15^{th} story which enhanced the global stiffness of the structure. For Case 1 models, same sections were used throughout the building, which made framed-tube very flexible. This has resulted in roof deflection of 262.5 mm.

2.2 Responses from time history analysis

While the response spectrum analysis provided only the peak values of the responses, time history analysis provided not only the peak values along with the time of occurrence of peak values, but also provided detailed history of the response quantities for the prescribed duration. Peak values along with the time of occurrence are marked in the individual plot in Figure 31 and Figure 32. As evident from these figures, the predominant responses are concentrated roughly in between 30 to 70 seconds, corresponding to the predominant input ground acceleration in Figure 23.

2.2.1 Base shear and base moment

The base shear and base moment from time history analysis are plotted on Figure 31 and Figure 32 for different structural systems. Both these response quantities differ from those of response spectrum analysis (Table 11). This is expected since the response quantities obtained from the time history analysis are based on the actual ground motion, which is characterized by jaggedness. Jagged characteristic of ground motion is reflected in the plot of design horizontal acceleration spectra of scaled Bhuj earthquake in Figure 24.

Both the base shear and base moment for rigid frame and framed-tube systems are lesser than those from response spectrum analysis. This is expected because the design response spectra for scaled Bhuj earthquake in Figure 24 are lower than that of IS 1893 for a period above 2.7 seconds. For other structural systems, the responses do not follow any unique trend but the values are closer to those from response spectrum analysis. The reason, again, can be inferred from the plot of Figure 24, whereby the design response spectra of the scaled Bhuj earthquake is much closer to IS 1893 curve for a period between 2 and 3 seconds. Since the shearwalled-frame, braced-tube and outrigger systems have fundamental periods between 2 and 3 seconds, the analysis yielded more accurate results for these systems.

The occurrence of peak responses also differs widely. Generally, peak responses for the shearwalled-frame, braced-tube and outrigger systems occurred early compared to the rigid frame and framed-tube systems. Further, the occurrence of peak base moment preceded the occurrence of peak base shear in all the structural systems. This point to the important fact that peak of all responses does not occur at the same time. Moreover, the occurrence of peak responses depends on the type of structural systems.

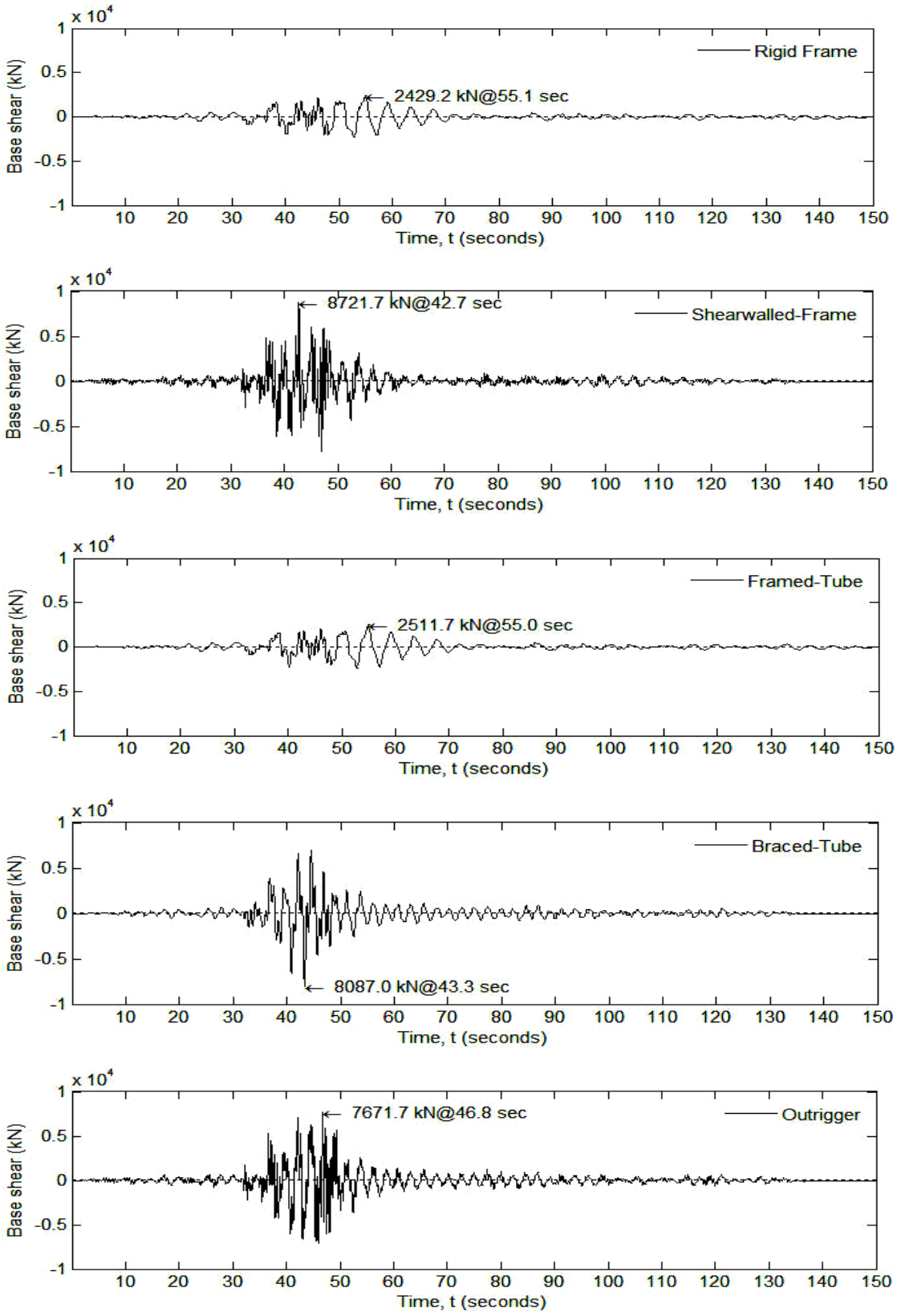

Figure 31 Base shear history for different structural systems (Case 3 models)

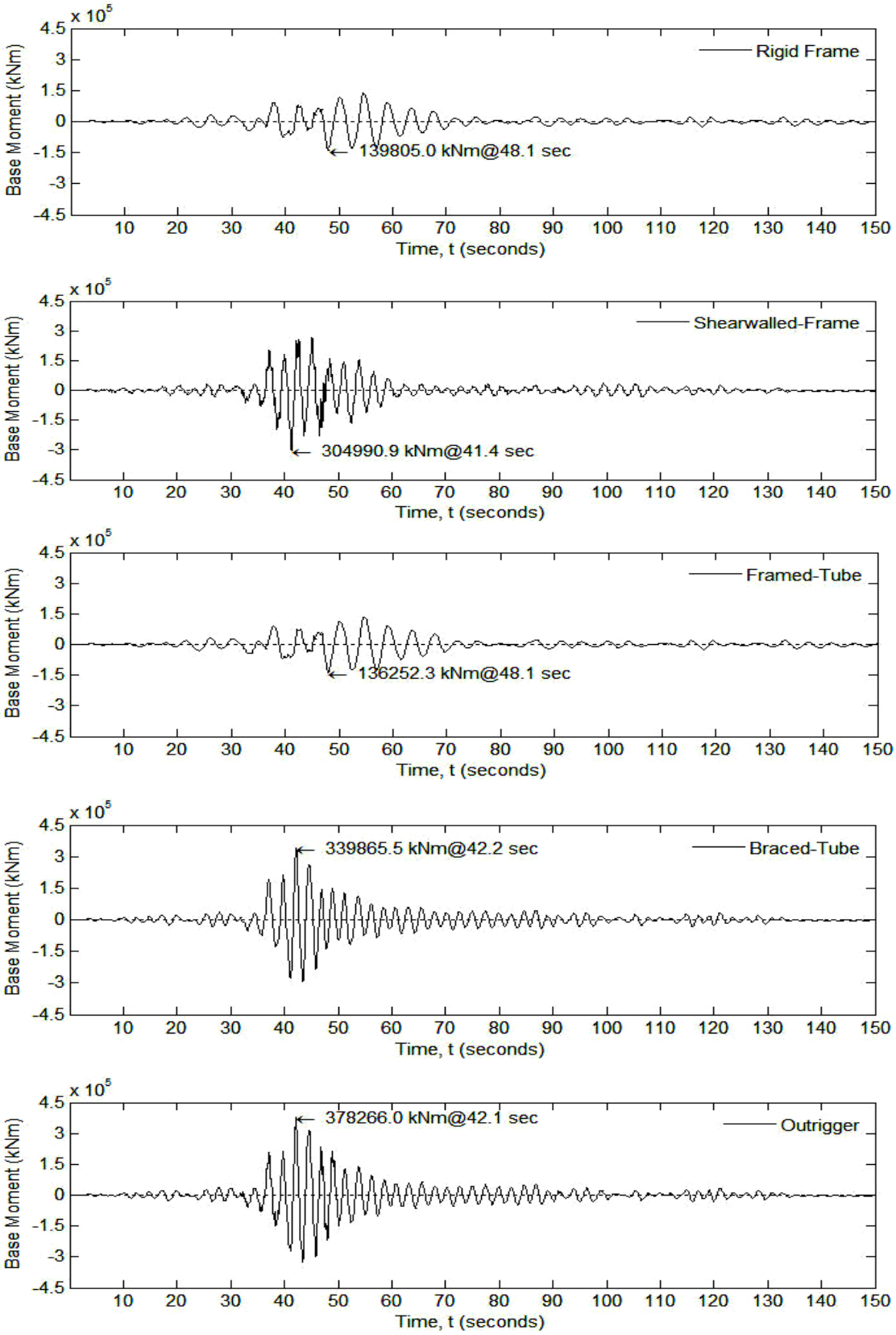

Figure 32 Base moment history for different structural systems (Case 3 models)

Table 11 Comparison of base shears and base moments from response spectrum and time history analysis for Case 3 models

Structural System	Base Shear (kN) x10^3		Base Moment (kNm) x10^5	
	Response Spectrum	Time History	Response Spectrum	Time History
Rigid Frame	4.260	2.43	2.505	1.40
Shearwalled-Frame	7.822	8.72	2.998	3.05
Framed-Tube	4.256	2.51	2.509	1.36
Braced-Tube	6.520	8.09	3.540	3.40
Outrigger	7.790	7.67	3.299	3.78

2.2.2 Displacements

Peak displacement at different height of the buildings are extracted from the results of time history analysis and presented in Table 12.

For shearwalled-frame, braced-tube and outrigger systems, the displacement at 25th story agrees reasonably well with the displacements from response spectrum analysis given in Table 10. The reason, again, can be inferred from the plot of Figure 24, whereby the design response spectra of the scaled Bhuj earthquake is much closer to IS 1893 curve for a period between 2 and 3 seconds. On the other hand, the displacements for rigid frame and framed-tube systems are much lower compared to those from response spectrum analysis. This is because the design response spectra for scaled Bhuj earthquake in Figure 24 are lower, and significantly deviate from that of IS 1893 for a period above 2.7 seconds.

Also, it was noticed that the occurrence of peak displacements over the height of building for a particular structural system was nearly at the same time,

separated only by a fraction of seconds. However, it differed among structural systems.

Table 12 Peak displacements from time history analysis (Case 3 models)

Structural System	Maximum Horizontal Displacements (in mm)				
	5th story	**10th story**	**15th story**	**20th story**	**25th story**
Rigid Frame	19.92	40.25	56.53	71.76	83.91
Shearwalled-Frame	7.68	23.49	42.67	62.43	82.60
Framed-Tube	20.42	41.44	57.34	70.91	82.08
Braced-Tube	18.94	37.05	51.67	64.93	73.86
Outrigger	8.57	25.81	45.76	64.96	80.70

3. Wind Responses of different Structural Systems

Story moment, story shear, displacement and drift ratio from the along-wind load analysis are plotted on Figure 33, Figure 34 and Figure 35.

3.1 Story moment and story shear

The variation of story moment and story shear over the height of the building from wind load analysis is smooth and uniform, with values for shearwalled-frame, braced-tube and outrigger systems lesser than those of rigid frame and framed-tube systems. The smooth plot may be attributed to the fact that the wind responses are based on the fundamental mode of vibration only. The higher modes are considered to have negligible influence on the responses in the case of wind.

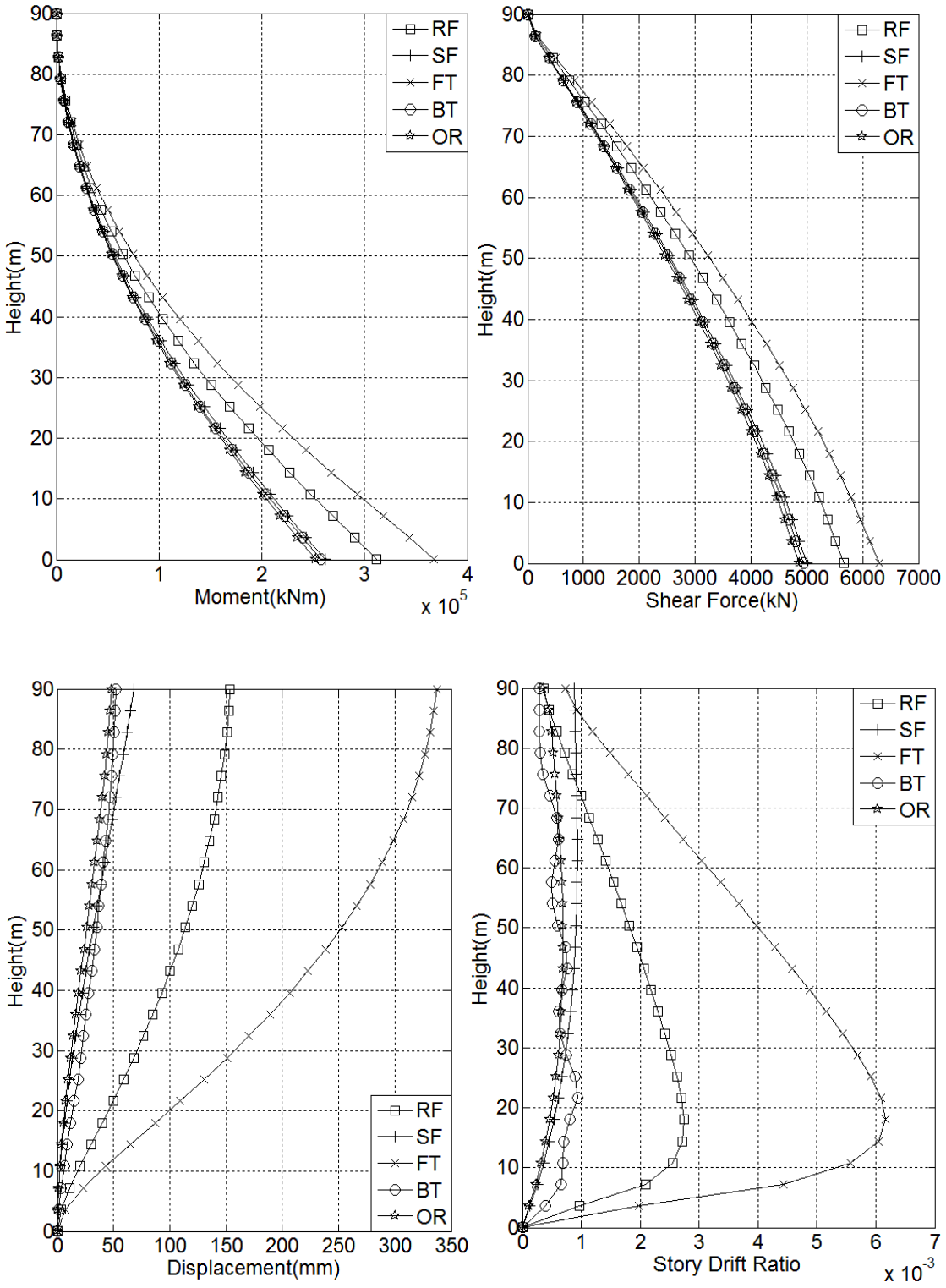

RF-Rigid Frame; SF-Shearwalled-Frame; FT- Framed-Tube; BT-Braced-Tube; OR-Outrigger

Figure 33 Story moment, story shear, displacement and story drift ratio for along-wind load (Case 1 models)

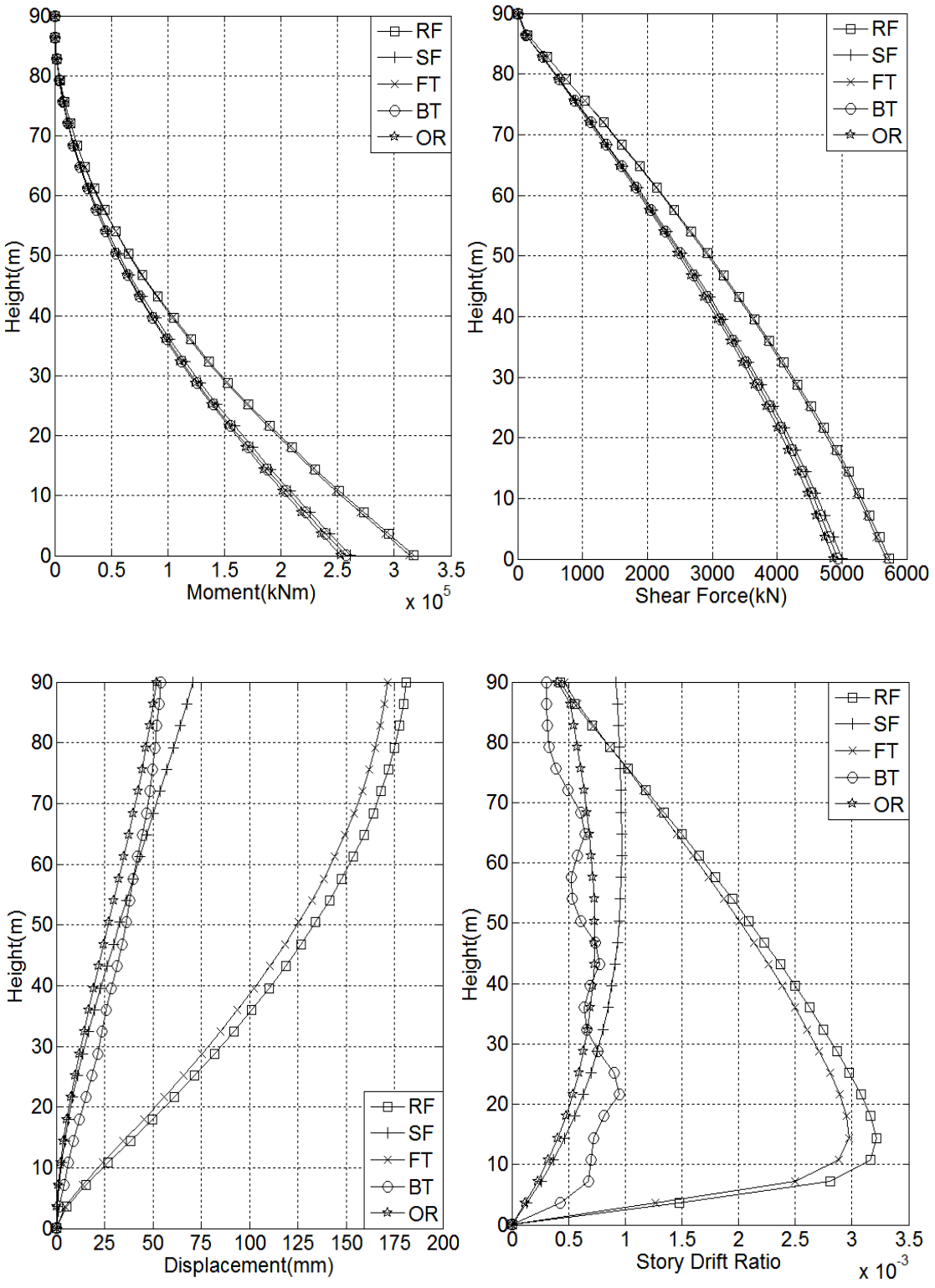

RF-Rigid Frame; SF-Shearwalled-Frame; FT- Framed-Tube; BT-Braced-Tube; OR-Outrigger

Figure 34 Story moment, story shear, displacement and story drift ratio for along-wind load (Case 2 models)

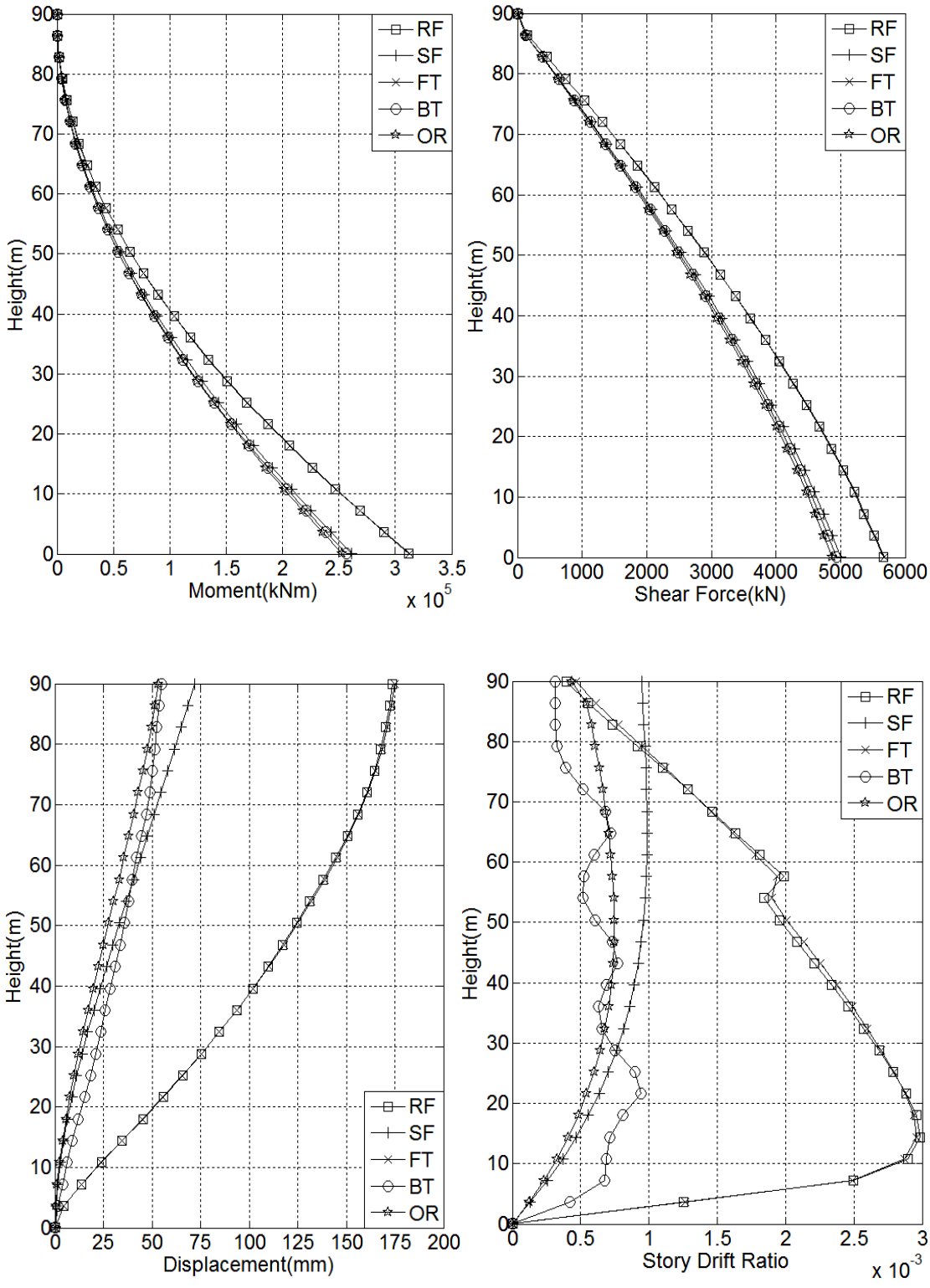

Figure 35 Story moment, story shear, displacement and story drift ratio for along-wind load (Case 3 models)

The fact the story shear and story moment from wind is higher for rigid frame and framed-tube systems compared to those of other systems, is directly attributed to the fundamental period of vibration of the building. Lateral forces due to dynamic effects of wind are proportional to the fundamental period of vibration. Since rigid frame and framed-tube systems have higher fundamental natural period of vibration, this has resulted in higher dynamic forces due to wind. Hence, this in turn has resulted in the higher story shear and story moment in these structural systems.

The plot of story moment and story shear for rigid frame and framed-tube is identical and appear to be superimposed since the fundamental time period (Table 8) used for the computation of wind load are almost same for Case 3. Some difference may, however, be seen in the plot of Case 1 and Case 2 models. Base shear and base moment for three cases of models are presented in Table 13.

Table 13 Base shear and base overturning moment for along-wind load

Structural System	Base Shear (kN) x10^3			Base Moment (kNm) x10^5		
	Case 1	Case 2	Case 3	Case 1	Case 2	Case 3
Rigid Frame	5.668	5.729	5.663	3.119	3.170	3.115
Shearwalled-Frame	5.005	5.000	4.998	2.615	2.611	2.610
Framed-Tube	6.291	5.687	5.675	3.677	3.133	3.123
Braced-Tube	4.942	4.942	4.930	2.577	2.577	2.569
Outrigger	4.861	4.870	4.871	2.524	2.529	2.529

Note: Case 1, Case 2 and Case 3 refers to corresponding analytical models

3.2 Story displacement and story drift ratio

The plot profile of story displacement and story drift ratio (Figure 33, Figure 34 and Figure 35) show considerable differences among structural systems. The variation of displacement for shearwalled-frame and outrigger systems is more uniform and linear compared to other structural systems over the height of building.

For rigid frame and framed-tube systems, the drift is concentrated towards the base of the building. The effect of the reduction of column sizes can be observed only in these structural systems in which abrupt changes in the story drift can be noticed near 15th story (Figure 35). It is also interesting to note that the impact of reduction of column sizes above 15th story was depicted only by the drift ratio.

Story drift ratio for shearwalled-frame increases gradually from the base till the mid-height. Thereafter, it is almost constant up to the top of the building. Similar is the case for outrigger system except that story drift ratio gradually decreases upward of mid-height of building. Due to the presence of diagonal bracing, braced-tube system has drift continuously varying till the top of building. Further the variation oscillates about the certain value. It is also to be noted that there is no sudden jump in story drift ratio for shearwalled-frame, braced-tube and outrigger systems, indicating that they are less likely to be affected by the reduction of column sections.

Roof displacement and maximum story drift ratio for three cases of models are shown in Table 14. Because the dynamic wind loads are proportional to the fundamental period of the building, the roof displacement among three Cases follow the trend similar to fundamental period tabulated in Table 8.

Table 14 Roof displacement and drift ratio for along-wind load

Structural System	**Roof Displacement (mm)**			**Maximum Story Drift ratio x10^{-3}**		
	Case 1	**Case 2**	**Case 3**	**Case 1**	**Case 2**	**Case 3**
Rigid Frame	153.6	181.2	173.8	2.742	3.215	2.983
Shearwalled-Frame	68.4	70.8	72.0	0.934	0.969	0.989
Framed-Tube	337.1	171.5	175.1	6.159	2.972	2.960
Braced-Tube	52.5	54.3	54.8	0.938	0.947	0.942
Outrigger	48.4	51.8	53.1	0.692	0.732	0.747

4. Comparison of Wind and Earthquake Responses

The comparison and the discussions given hereunder are restricted to the response quantities from response spectrum analysis and the dynamic effects due to wind.

Important response quantities such as base shear, base moment, maximum displacement and maximum drift ratio from wind and response spectrum analysis are tabulated in Table 15 and Table 16 for Case 3 models. Similar comparison can be made while referring to Table 9, Table 10, Table 13 and Table 14.

4.1 Story moment and story shear

The plot profiles of story shear and story moment from response spectrum (Figure 28, Figure 29 and Figure 30) and along-wind load analysis (Figure 33, Figure 34 and Figure 35) show significant differences for different structural systems.

Plot profiles for three cases of models along with Table 15 permit several observations. Peak story moment and story shear from seismic analysis are in general characterized by the irregular variation over the height of the building whereas the story moment and shear from the wind analysis are smooth and uniform over the height of the building. This is because seismic responses are influenced by the higher modes of vibration whereas the wind responses are based on the fundamental mode of vibration. Shearwalled-frame, outrigger and braced-tube are more affected by the higher modes compared to rigid frame and framed-tube systems. This reasoning can be inferred from the similarity of the plot profile of story shear and story moment for seismic and wind for the rigid frame and the framed-tube systems.

Unlike the seismic responses wherein story moment and story shear varied widely among the structural systems, for wind responses, story moment and story shear can be distinctively grouped into two: those of rigid framed and framed-tube systems, and those of shearwalled-frame, braced-tube and outrigger systems.

Structural systems having lower fundamental periods (shearwalled-frame, braced-tube and outrigger) have higher seismic story shear and story moment compared to structural systems having higher fundamental periods (rigid frame and framed-tube). On the other hand, the story shear and story moment from wind are higher for rigid frame and framed-tube systems. This is because for seismic analysis lower period results in higher base shear and base moment (Figure 9). Since shearwalled-frame, braced-tube and outrigger systems are stiffer than the rigid frame and framed-tube system, they attract more seismic forces. On the other hand, dynamic effects of wind are proportional to the fundamental period of vibration. Since the rigid frame and framed-tube systems are flexible compared to other systems in this study, and hence higher fundamental periods, it has resulted in higher base shear and base moment for wind.

Table 15 Comparison of base shear and base moments for Case 3 models

Structural Systems	Base Shear (kN) x10^3		Base Moment (kNm) x10^5	
	Seismic	Wind	Seismic	Wind
Rigid Frame	4.260	5.663	2.548	3.115
Shearwalled-Frame	7.822	4.998	2.998	2.615
Framed-Tube	4.242	5.675	2.501	3.122
Braced-Tube	6.520	4.930	3.540	2.569
Outrigger	7.790	4.870	3.299	2.529

As observed in Table 15, wind base shear is greater than seismic base shear by 32.9% for rigid frame, and 33.8% for framed-tube. Similarly, wind base moment is larger than seismic base moment by 22.3% for rigid frame, and 24.8% for framed-tube. On the other hand, seismic base shear is greater than wind base shear by 56.5% for shearwalled-frame, 32.3% for braced-tube, and 60% for outrigger. Similarly, seismic base moment is larger than wind base moment by 14.6% for shearwalled-frame, 37.8% for braced-tube, and 30.4% for outrigger system. The

important observation to be made here is that the rigid frame and framed-tube have higher base shear and base moment from wind while shearwalled-frame, braced-tube and outrigger have higher base shear and base moment from seismic load.

4.2 Displacement and drift ratio

Except for the magnitude, the displacement and story drift ratio for seismic (Figure 28, Figure 29 and Figure 30) and wind (Figure 33, Figure 34, Figure 35) analysis show great deal of similarity in every aspects. This is possible because the higher modes of vibration have less effect on the deflection and story drift compared to the moments and shears.

Table 16 shows that the seismic deflection and drift are always larger than those of wind for shearwalled-frame, braced-tube and outrigger systems, while it is just the opposite for rigid frame and framed-tube systems. Wind displacement is greater than seismic displacement by 21.7% for both for rigid frame and framed-tube. On the other hand, seismic displacement is larger than wind displacement by 18.3% for shearwalled-frame, 43.6% for braced-tube, and 36.5% for outrigger systems.

Table 16 Comparison of roof displacement and drift ratios for Case 3 models

Structural Systems	**Roof Displacement (mm)**		**Maximum Story drift ratio x10^{-3}**	
	Seismic	**Wind**	**Seismic**	**Wind**
Rigid Frame	142.8	173.8	2.335	2.983
Shearwalled-Frame	85.2	72.0	1.213	0.989
Framed-Tube	143.9	175.1	2.306	2.960
Braced-Tube	78.7	54.8	1.267	0.942
Outrigger	72.5	53.1	0.997	0.747

4.3 Influence of fundamental natural period on lateral forces

Although the fundamental natural periods determined from rational analysis (Table 8) were used to compute both the seismic and wind forces in this study, many codes (IS 1893, 2002; IS 875: Part 3, 2004; ASCE 7, 2005) provide equations for approximate fundamental natural period. For instance, the IS 875: Part 3 provides fundamental time period for moment resisting frame as $T=0.1n$, where n is the number of storys, and for other types of structures as $T = 0.09h / \sqrt{d}$, in which h is the height of building and d is the dimension of building parallel to the wind.

The major difference between the seismic and wind forces is that the seismic forces are inversely proportional to the fundamental period while the dynamic forces due to wind are directly proportional to the fundamental time period of the structure.

The approximate periods given in the codes are mainly aimed at obtaining the conservative forces due to earthquake. Hence, the use of codal time period would admittedly provide higher base shear and results in safe design for seismic load. This has been further proven to be true from the seismic responses obtained from the dynamic analysis, wherein the structural systems having lower fundamental period (shearwalled-frame, braced-tube and outrigger) have higher seismic base shear and base moment (Table 15).

On the contrary, the use of codal fundamental period might result in underestimation of lateral forces due to wind since period calculated from codal formulae are always lesser than the periods from rational analysis. The effect of fundamental period on the magnitude of lateral wind force is self-evident from Figure 26. Because the longer periods results in higher forces for dynamic wind, the responses of rigid frame and framed-tube system for wind were significantly higher than seismic responses.

Thus, it is important to chose correctly the fundamental period for the computation of dynamic load due to wind. This is especially applicable for tall buildings in which dynamic effects of wind are significant.

5. Roof Accelerations for Structural Systems

The magnitude of horizontal acceleration induced by the wind is one form of assessing the human comfort criteria in high-rise buildings. The expressions for horizontal acceleration given by Eq. (C12) and Eq. (C13) in Section C.1.4 and C.1.5 of Appendix C are based on the assumption that the building vibration under the effect of wind is predominantly of first mode. Thus, for a linear fundamental mode of vibration, the maximum horizontal acceleration occurs at the roof level, that is at the top of the building. Hence, the assessment of horizontal acceleration at roof level is adequate to evaluate the comfort criteria.

The horizontal acceleration in the along-wind and cross-wind directions for the 5-year and 10-year return period were computed using Eq. (C12) and Eq. (C13) (Section C.1.4 and C.1.5 of Appendix C) for Case 3 models. Serviceable wind of 31.02 m/s and 34.78 m/s for 5-year return period and 10-year return period respectively were used.

The horizontal acceleration in the along-wind and cross-wind direction at the top of building for Case 3 models are given in Table 17. The approximate allowable limits from Figure 13 are also tabulated for comparison. The example calculation of horizontal acceleration for the rigid frame system can be found in Section C.3 of Appendix C. Section 6 of Research Methodology maybe referred for the background relating to the calculation of horizontal accelerations.

Table 17 permits few observations. Firstly, the cross-wind acceleration is always higher than along-wind acceleration for all structural systems. This indicates that the cross-wind response has important influence on the human comfort criteria. Secondly, the acceleration for rigid frame and framed-tube systems are considerably

higher than those of other structural systems, indicating that long period structures (or flexible structures) would be seriously affected by the horizontal acceleration due to wind. Thirdly, when the values of horizontal accelerations are compared with human perception levels in Table 2, it shows that for values in the range of 0.1 to 0.25 m/s^2, considerable motion can be expected at the roof level. Generally dampers are used to minimize building motions induced by wind.

Table 17 Horizontal accelerations at roof level due to wind (Case 3 models)

Structural Systems	5-year wind[1]		10-year wind[2]		Allowable limits	
	Along-wind (m/s^2)	Cross-wind (m/s^2)	Along-wind (m/s^2)	Cross-wind (m/s^2)	5-year wind (m/s^2)	10-year wind (m/s^2)
Rigid Frame	0.046	0.121	0.065	0.166	0.16	0.18
Shearwalled-Frame	0.034	0.106	0.048	0.141	0.13	0.15
Framed-Tube	0.047	0.122	0.067	0.168	0.16	0.18
Braced-Tube	0.029	0.096	0.042	0.127	0.13	0.15
Outrigger	0.030	0.101	0.043	0.134	0.13	0.15

[1] 5-year wind refers to the wind with return period of 5 years

[2] 10-year wind refers to the wind with return period of 10 years

6. Material Cost for Structural Systems

Cost is another important factor that determines the efficiency of structural systems. To this effect, the structural members for each structural system were designed according to IS 456 (2000). The quantity of steel and concrete required for each structural systems was then estimated and produced in Table 18. This quantity of materials includes the concrete and steel required for columns, beams, floor slabs, structural walls, bracing and outrigger truss. Individual material quantity for floor slabs, beams, columns, shearwalls and bracings can be found in Appendix Table D1 and Appendix Table D2.

Based on the item rates provided in BSR (2007), the rate for 1 m^3 of concrete was worked out as Nu. 4359/m^3 for Thimphu, the capital of Bhutan. For steel, the rate is Nu. 32.8/kg. Details can be found in Section D.3 of Appendix D. Using these rates, the cost of concrete and steel for each structural system is computed and shown in Table 18. The cost difference relative to rigid frame system is also computed in terms of percentage. The total cost of the structural system is plotted in Figure 36. The detailed background to the cost estimation of structural systems can be found in Section 7 under Research and Methodology.

Table 18 Cost of structural materials

Structural Systems	Concrete (m^3)	Steel (kg)	Cost of Concrete (Nu. in millions)[1]	Cost of Steel (Nu. in millions)	Total Cost difference %
Rigid Frame	5,257	436,215	22.92	14.31	0
Shearwalled-Frame	5,335	452,872	23.26	14.85	2.4
Framed-Tube	5,148	560,457	22.44	18.38	9.6
Braced-Tube	4,920	572,978	21.45	18.79	8.1
Outrigger	5,349	454,201	23.32	14.90	2.7

[1] USD $1.00 = Nu. 38

As noted in the Table 18, the distribution of concrete material among the structural systems is more or less uniform due to the inherent uniformity in sections adopted for the analytical modelling. However, some differences can be noticed in the distribution of steel among the structural systems. This is expected because the member forces are bound to be different in different structural systems. Even within the particular structural system, member forces can vary with the height above the base of the building.

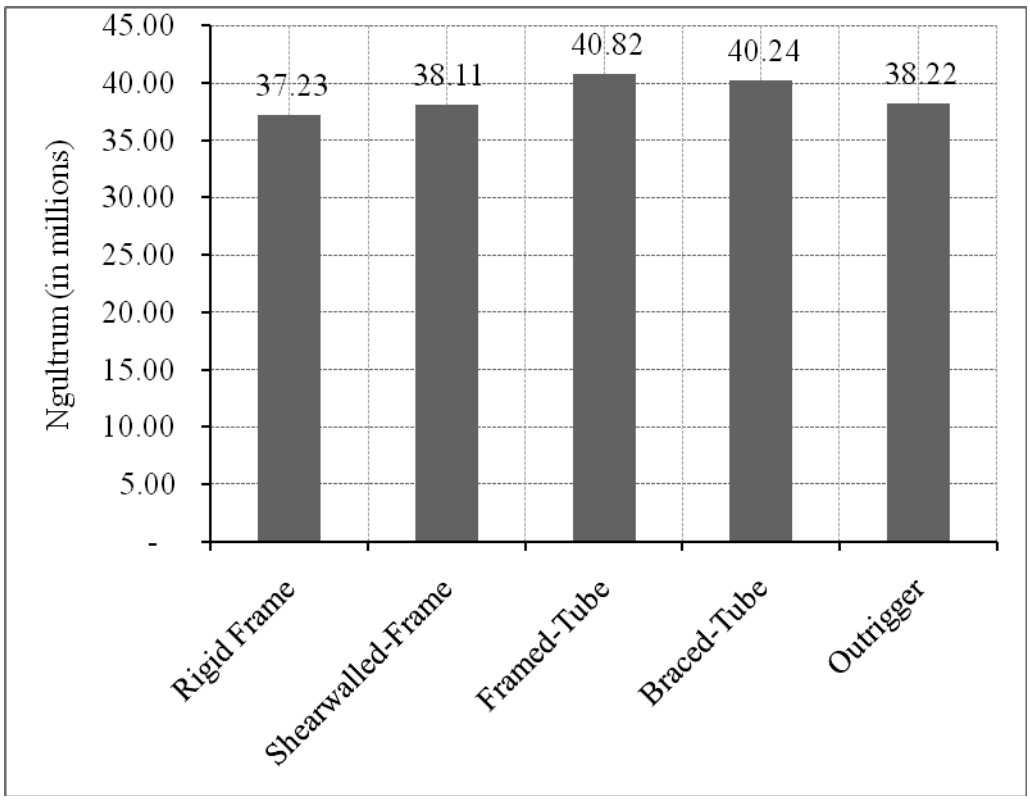

Figure 36 Material cost of structural systems

From the viewpoint of structural behaviour, as noted in preceeding pages, rigid frame and framed-tube systems have similar behaviour in every respect, but in terms of cost, the cost of frame-tube is higher than rigid frame system by almost 10%. Behaviour of braced-tube system is also found to be excellent but it is the second-most expensive. Shearwalled-frame and outrigger are quite competitive relative to rigid frame system. It is to be mentioned that for comparison purposes, the costs given in Table 18 are accurate enough to depict the relative cost of structural systems.

7. Influence of various factors on Structural Systems

In Figure 37, different quantities such as cost of materials, horizontal acceleration at roof level, plan density index, and wind and seismic deflection at roof level are normalized with respect to those of rigid frame system to observe how each

parameter vary for different structural systems. Rigid frame system was adopted as baseline since it had the least cost.

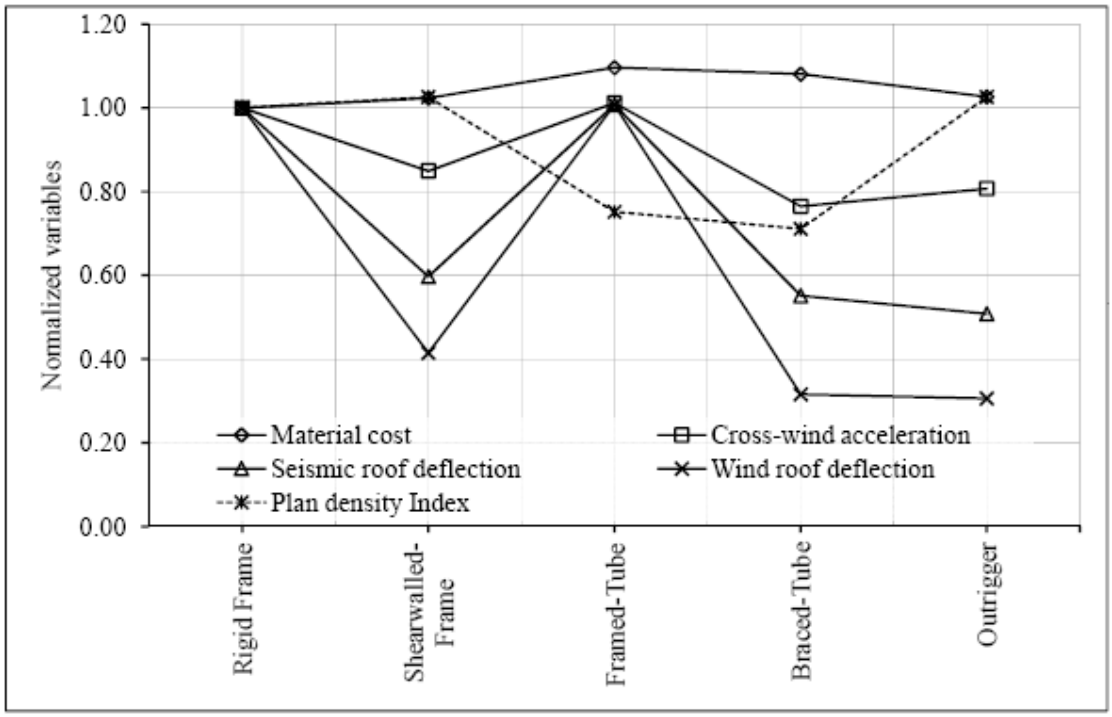

Figure 37 Comparison of different normalized variables for structural systems

The structural plan density index is defined as the total area of all vertical structural elements divided by the gross floor area of the footprint of the building at the ground level. It ranges from 1.93% to 2.78% for the structural systems of Case 3 models, with 2.71% for rigid frame, 2.78% for shearwalled-frame and outrigger, 2.04% for framed-tube, and 1.93% for braced-tube system.

As observed from Figure 37, to deduce the conclusion with regard to the efficiency of structural system is a difficult task, especially when many factors are to be considered in judging the efficiency. Nevertheless, rigid frame system seems to outperform other structural system in terms of cost. However, it must be understood that its performance in the serviceability limits are not so good compared to other structural systems. Shearwalled-frame and outrigger appears to perform well both in terms of cost and serviceability criteria, but the outrigger attracts huge shear force in

shearwalls at the location of outrigger truss as observed during the analysis. Moreover, they have the highest plan density index of 2.8 percent among the structural systems. Framed-tube system is not a likely choice for being the most expensive and poor performance in serviceability limit states. Likewise, braced-tube system may not be readily accepted for obvious reason of being the eyesore to the architects. However, considering the overall aspects, it is still the rigid frame or shearwalled-frame system, found by many, to be appropriate for the medium-height buildings.

However, in reality, other factors might influence the choice of structural systems. Often the human desire to construct elegant tall structures transcends all other factors.

CONCLUSIONS AND RECOMMENDATIONS

Conclusions

The behaviour of five types of structural systems namely: rigid frame, shearwalled-frame, framed-tube, braced tube and outrigger systems under the effect of earthquake and wind were investigated by incorporating each structural system into the hypothetical 25-story reinforced concrete building.

Seismic analysis using equivalent lateral force procedure, response spectrum and linear time history analysis, and dynamic effects due to wind were considered to obtain response quantities such as story shear, story moment, story displacement and story drift. These response quantities along with horizontal acceleration and the cost of structural materials were used to compare and assess the performance among different structural systems.

Based on the present study, following conclusions are drawn:

1. Mode of vibration is predominantly of translation for all structural systems owing to the symmetrical plan of the building. Mode of vibration is also symmetric with equal natural periods for two consecutive modes with the exception of braced-tube system. For braced-tube systems, because of the mutistory diagonal bracing on the four faces of the building, it resulted in slight differences of periods for two consecutive modes.

2. Rational analysis yielded higher fundamental period of vibration compared to the period given by the approximate period formulae in the standards. In the current study, the observed period elongation for rigid frame system is 93% and shearwalled-frame is 75% for case 3 models. Employment of periods in seismic codes does not therefore provide uniform levels of safety for different structural systems.

3. The lateral force increases with the increase in fundamental period for wind while it decreases with the increase in fundamental period for earthquake. Because rigid frame and framed-tube systems have higher fundamental periods, they are governed by the wind load. On the other hand, shearwalled-frame, braced-tube and outrigger systems have lower fundamental periods, they are governed by the earthquake. Hence, the use of same fundamental period from codes does not guarantee the same level of safety for both wind and earthquake. The approximate time period in the codes are appropriate only for seismic analysis because of their inherent conservativeness built into them.

4. For seismic analysis, story shear and story moment are significantly affected by the higher modes of vibration compared to the story displacement and drift. The effect is more pronounced for shearwalled-frame, braced-tube and outrigger systems.

5. Shearwalled-frame and outrigger systems showed uniform distribution of drift with height compared to rigid frame and framed-tube systems in which the maximum drift is concentrated near the base of building. This also indicates that if structural systems tend to be flexible, then shear deformation tends to predominate.

6. The influence on the responses of structural systems due to the reduction of column cross-section towards upper part of building is observed only for drift in rigid frame and framed-tube systems.

7. Cross-wind accelerations are higher than the along-wind accelerations for all structural systems. Further, the horizontal accelerations for rigid frame and framed-tube are greater than other systems. This shows that the human comfort criteria are significant especially for structures having longer periods.

8. Among five structural systems considered in this study, cost analysis showed that rigid frame system is the cheapest followed by the shearwalled-frame system. On the other end, framed-tube system is the most expensive with material

cost higher by roughly 10% above rigid frame system although their behaviour is nearly identical.

Recommendations

Based on this work, following recommendations are made:

1. Good judgement is necessary when using fundamental period of vibration for computing dynamic effects due to wind on building. This is because the lateral dynamic forces due to wind are proportional to the fundamental period of the building. The use of approximate time periods given in many codes might underestimate wind forces on building since they are mainly aimed at obtaining conservative forces due to earthquake.

2. It is important to undertake dynamic analysis especially for seismic actions since it unfolds important characteristics of the behaviour of structural systems that are not revealed by static analysis. However, it should be paralleled by the static analysis for benchmarking purposes.

3. For further work of similar nature to the one in this study, one may consider the following:

1) Effect of non-structural components on the building responses
2) Effect of flexibility of support
3) Inclusion of more types of structural systems
4) Effect of elastic modulus, E on seismic and wind responses. Is it justified to use $E = 5000\sqrt{f_{ck}}$, while the strength of concrete in a building is actually higher than f_{ck}?
5) Use of other floor framing types
6) Effect of different ground motions on structural systems
7) Nonlinear analysis to include the hysteretic behaviour of materials

8) Cost of structural systems may include formwork, non-structural components, foundations, labour and so on to obtain overall picture of the influence of the cost on structural systems

LITERATURE CITED

ACI 318. 2005. **Building Code Requirements for Structural Concrete and Commentary**. American Concrete Institute, Detroit, USA.

ASCE 7. 2005. **Minimum Design Loads for Buildings and Other Structures**. American Society of Civil Engineers, Reston, Virginia, USA.

AS/NZS 1170.2. 2002. **Structural Design Actions, Part 2: Wind Actions**. Australian / New Zealand Standard, Sydney, Australia.

BSR. 2007. **Bhutan Schedule of Rates (Civil)**. Standards and Quality Authority, Ministry of Works and Human Settlement, Royal Government of Bhutan.

Chopra, A.K. 2001. **Dynamics of Structures: Theory and Applications to Earthquake Engineering**. 2nd Edition, Prentice-Hall of India, Private Ltd., New Delhi.

Cook, R.D., D.S. Malkus, M.E. Plesha and R.J. Witt. 2002. **Concepts and Applications of Finite Element Analysis**. 4th Edition. John Wiley & Sons, Inc., USA.

FEMA 450. 2003. **NEHRP Recommended Provisions for Seismic Regulations for New Buildings and other Structures**. Building Seismic Safety Council, Federal Emergency Management Agency, Washington (DC).

Gunel, M.H. and H. E. Ilgin. 2007. A Proposal for the Classification of Structural Systems of Tall Buildings. **Building and Environment**. 42: 2667-2675.

IS 10262. 1982. **Recommended Guidelines for Concrete Mix Design**. Bureau of Indian Standards, New Delhi.

IS 875. 1987. **Code of Practice for Design Loads (other than Earthquake) for Buildings and Structures (Part 1 and Part 2)**. Bureau of Indian Standards, New Delhi.

IS 456. 2000. **Plain and Reinforced Concrete-Code of Practice**. Bureau of Indian Standards, New Delhi.

IS 1893. 2002. **Criteria for Earthquake Resistant Design of Structures (Part 1)**. Bureau of Indian Standards, New Delhi.

IS 875. 2004. **Wind Loads on Buildings and Structures-Proposed Draft and Commentary (Part 3)**. IITK-GSDMA Code Project Report Nos. IITK-GSDMA- Wind02-V5.0 and IITK-GSDMA-Wind04-V3.0, Department of Civil Engineering, IIT Roorke, India. Available Source: http://www.nicee.org

Kim, H., D. Lee and C.K. Kim. 2005. Efficient Three-dimensional Seismic Analysis of a High-rise Building Structure with Shear walls. **Engineering Structures**. 27(6): 963-976.

Lam, N.T.K., B.A. Gaull and J.L. Wilson. 2007. Calculation of Earthquake Actions on Building Structures in Australia. **Electronic Journal of Structural Engineering-Special Issue**. p22-40.

LATBSDC. 2005. An Alternative Procedure for Seismic Analysis and Design of Tall Buildings located in the Los Angeles Region – A Consensus Document. **Los Angeles Tall Buildings Structural Design Council**, Los Angeles, USA.

Liu, G.R. and S.S. Quek. 2003. **The Finite Element Method: A Practical Course**. 1st Edition. Butterworth-Heinemann, Elsevier Science Ltd., England.

MacLeod, I.A. 1970. Shear Wall-Frame Interaction – A Design Aid. **Portland Cement Association,** Illinois, USA.

Malhotra, P.K. 2003. Strong-Motion Records for Site-Specific Analysis. **Earthquake Spectra**. 19(3): 557-578.

Mendis, P., T. Ngo, N. Haritos, A. Hira, B. Samali and J. Cheung. 2007. Wind Loading on Tall Buildings. **Electronic Journal of Structural Engineering-Special Issue**. p41-54.

Moehle, J., Y. Bozorgnia and T.Y. Yang. 2007. The Tall Buildings Initiative. **Structural Engineers Association of California**, SEAOC Convention Proceedings, California, USA.

Paulay, T. and M.J.N. Priestley. 1992. **Seismic Design of Reinforced Concrete and Masonry Buildings**. John Wiley & Sons, Inc. USA.

Sadjadi, R., M.R. Kianoush and S. Talebi. 2007. Seismic Performance of Reinforced Concrete Moment Resisting Frames. **Engineering Structures**. 29(9): 2365-2380.

Scott, D., N. Hamilton and E. Ko. 2005. Structural Design Challenges for Tall Buildings. **Structure Magazine**. p20-23. Available Source: http:// www.structuremag.org

Simiu, E. and R.H. Scanlan. 1996. **Wind Effects on Structures: Fundamentals and Applications to Design.** 3rd Edition. John Wiley & Sons, Inc., New York.

Smith, B.S. and A. Coull. 1991. **Tall Building Structures: Analysis and Design**. John Wiley & Sons, Inc. USA.

SP6. 1964. **Handbook for Structural Engineers – Structural Steel Sections**. Bureau of Indian Standards, New Delhi.

Taranath, B.S. 1988. **Structural Analysis and Design of Tall Buildings**. McGraw-Hill International Editions, Singapore.

Taranath, B.S. 1998. **Steel, Concrete and Composite Design of Tall Buildings**. 2nd Edition. McGraw-Hill, New York.

Wilson, E.L. 2002. **Three Dimensional Static and Dynamic Analysis of Structures – A Physical Approach with Emphasis on Earthquake Engineering.** 3rd Edition. Computers and Structures, Inc. Berkeley, California, USA.

Zhou, Y., T. Kijewski and A. Kareem. 2003. Aerodynamic Loads on Tall Buildings: Interactive Databse. **Journal of Structural Engineering**. 129(3):394-404.

Zils, J. and J. Viise. 2003. An Introduction to High-Rise Design. **Structure Magazine**. p12-16. Available Source: http://www.structuremag.org

APPENDICES

Appendix A

Seismic Analysis

A.1 Seismic Analysis based on Indian Standard IS 1893 (2002) Criteria for Earthquake Resistant Design of Structures – Part 1 General Provisions and Buildings

IS 1893 (2002) provides both static and dynamic analysis for seismic design of building. Step-by-step procedure for static analysis based on equivalent lateral force procedure and the dynamic analysis based on response spectrum method are outlined in Section A.1.1 and Section A.1.2 below.

A.1.1 Static analysis

Step-by-step procedures to determine static lateral forces on the structure are as follows:

Step 1. Compute the fundamental natural period of the structures, using either the approximate formula from standard or based on rational analysis. Approximate fundamental natural period of vibration (T_a), in seconds, of a moment-resisting frame building is given by (IS 1893, 2002):

$$T_a = 0.075h^{0.75} \quad \text{for RC framed building without brick infill panels} \tag{A1}$$

$$T_a = \frac{0.09h}{\sqrt{d}} \quad \text{all other buildings} \tag{A2}$$

where

h = Height of the building in m

d = Base dimension of the building at ground level, in m, along the considered direction of the lateral force

Step 2. Compute the design horizontal seismic coefficient, A_h using the formula:

$$A_h = \frac{ZI}{2R}\left(\frac{S_a}{g}\right) \tag{A3}$$

where

Z = Zone factor, equal to 0.10, 0.16, 0.24, 0.36 corresponding to seismic zone II, III, IV and V

I = Importance factor, equal to either 1.0 (for general buildings) or 1.5 (for important buildings)

R = Response reduction factor, whose value ranges from 1.5 to 5 corresponding to least ductile to most ductile building system

S_a/g = Spectral acceleration coefficient, read from Figure 9 corresponding to fundamental natural period computed in Step 1, and damping ratio, ζ

Step 3. Compute the design seismic base shear (V_b) by:

$$V_b = A_h W \tag{A4}$$

where

W = Seismic weight of the building equal to full dead load plus fraction of live load (25% of live load for residential building and 50% of live load for commercial buildings)

A_h = Design horizontal seismic coefficient

Step 4. Determine the design lateral force on the structure from the design base shear calculated in Step 3 using the equation:

$$Q_i = V_b \frac{W_i h_i^2}{\sum_{j=1}^{n} W_j h_j^2} \tag{A5}$$

where

Q_i = Design lateral force at floor i

W_i = Seismic weight of floor i

h_i = Height of floor i measured from base

n = Number of storys in the building

Step 5. Perform static analysis based on the load calculated in Step 4.

A.1.2 Dynamic analysis

Step-by-step method to determine the building responses due to earthquake using Response Spectrum Method are as follows:

Step 1. Solve eigenproblem (which involves solving matrix Eq.(7)) to extract mode shapes (ϕ_n), modal frequencies (f_n) or time period (T_n) of each mode.

Step 2. Compute the modal mass (M_k) and modal participation factor (P_k) of mode k.

$$M_k = \frac{\left[\sum_{i=1}^{n} W_i \phi_{ik}\right]^2}{g\sum_{i=1}^{n} W_i \left(\phi_{ik}\right)^2} \tag{A6}$$

$$P_k = \frac{\sum_{i=1}^{n} W_i \phi_{ik}}{\sum_{i=1}^{n} W_i \left(\phi_{ik}\right)^2} \tag{A7}$$

where

W_i = Seismic weight of floor i

ϕ_{ik} = Mode shape coefficient at floor i in mode k

g = Acceleration due to gravity

Step 3. Compute the lateral force at each floor in each mode using:

$$Q_{ik} = A_k \phi_{ik} P_k W_i \tag{A8}$$

where

Q_{ik} = Lateral force at floor i in mode k

A_k = Design horizontal acceleration spectrum value as per Eq. (A3) using

the natural period of vibration (T_k) of mode k, and damping ratio, ζ_k

W_i = Seismic weight of floor i

Step 4. Perform static analysis for each mode for modal lateral forces computed Step 3, to obtain various responses (axial force, bending moment, shear, deflection, etc). Alternatively, story shear (V_{ik}) acting in story i in mode k can be obtained from:

$$V_{ik} = \sum_{j=i+1}^{n} Q_{ik} \tag{A9}$$

Step 5. Obtain peak responses in story i due to all modes considered by combining those due to each mode using the modal combination rule: *square-root-of-sum-of-squares* (SRSS) given by Eq.(13) or *complete quadratic combination* (CQC) rule given by Eq.(14).

A.2 Scaling Methods for Ground Motions

A few methods that are employed for the scaling of ground motion records to match with either site-specific response spectrum or standard response spectrum are given below.

A.2.1 Spectrum intensity method

In this method, the ground motion is scaled by the factor SI_c/SI_n where SI_c and SI_n are the areas under the code velocity spectrum and the velocity spectrum of the selected accelerogram, respectively. Originally, George W. Housner has defined the velocity spectrum as the area under the pseudo-velocity spectrum between periods of 0.1 to 2.5 seconds for damping, ζ of 5 percent. This is mathematically represented by:

$$SI = \int_{0.1}^{2.5} S_v(\xi = 0.05, T)dT \tag{A10}$$

where SI is the spectrum intensity and S_v is the pseudo-velocity spectrum. Knowing the pseudo-acceleration spectrum (S_a), pseudo-velocity spectrum (S_v) can be easily derived from the relations given by (Chopra, 2001; Malhotra, 2003)

$$S_a\left(\frac{T}{2\pi}\right)^2 = S_d = S_v\left(\frac{T}{2\pi}\right) \tag{A11}$$

where S_d is the spectral displacement.

A.2.2 ASCE 7 and FEMA method

ASCE 7 (2005) states "ground motions shall consist of pairs of appropriate horizontal ground motion acceleration components that shall be selected and scaled from individual recorded events. Appropriate ground motions shall be selected from events having magnitudes, fault distance, and source mechanisms that are consistent with those that control the maximum considered earthquake. For each pair of horizontal ground motion components, a square root of the sum of the squares (SRSS) spectrum shall be constructed by taking the SRSS of the 5 percent damped response spectra for the scaled components. Each pair of motions shall be scaled such that for each period between 0.2T and 1.5T, the average of the SRSS spectra from all horizontal component pairs does not fall below 1.3 times the corresponding ordinate of the design response spectrum by more than 10 percent." Further details can be found in ASCE 7 (2005) and FEMA 450 (2003). This method is applicable to selected set of ground motions.

A.2.3 Malhotra's method

Malhotra (2003) has presented a procedure to select and scale strong-motion records for site-specific analysis. Two methods of scaling of ground motions are given: one for closer, smaller event and the other for distant, larger event.

For a closer, smaller event, the scaling factor is given by:

$$\alpha = \frac{S_a(0.2s)}{S_{a,\max}} \tag{A12}$$

And for a distant, larger event, the scaling factor is given by:

$$\alpha = \frac{S_a(1s)1s}{S_{a,\max}T_3} \tag{A13}$$

where S_a(0.2s) and S_a(1s) are the pseudo-spectral acceleration read from site-specific response spectrum or standard response spectrum corresponding to the time period within the bracket. $S_{a,max}$ is the maximum pseudo-spectral acceleration, and T_3 is the time period corresponding to the point where acceleration region meets the velocity region in the Newmark-Hall smooth spectrum of the selected ground motion. $S_{a,max}$ and T_3 for some selected strong-motion records are given by Malhotra (2003).

A.3 Ground Motion used for this study

Ground motion records of Bhuj earthquake was recorded by the Indian Institute of Technology, Roorke, India at Ahmedabad station, situated at the hypocentral distance of 239 km. The details of the ground motion can be found at the *website http://db.cosmos-eq.org*. The time history plot of ground acceleration, ground velocity and ground displacement are given in Figure 23. Malhotra's scaling method was used for this study since it yielded better results compared to spectrum intensity method.

Malhotra (2003) has provided $S_{a,max}$ = 0.262g and T_3 = 0.520 seconds for this earthquake. Eq. (A13) was adopted for the scaling of ground motion since this earthquake can be classified as distant larger event as its magnitude is greater than 7.

Since the country of Bhutan does not have any record of seismic activities to generate the site-specific response spectra, the seismic designs were solely based on the standard response spectrum given in IS 1893 (2002). Thus, any ground motion that are to be used for time history analysis, should be chosen to be compatible with

the standard response spectrum. The detailed compatibility check required for selecting the ground motion from the past records to match with the standard response spectrum or site-specific response spectrum are given elsewhere (Malhotra, 2003).

From the response spectra plot of IS 1893 (2002), S_a(1s) = 1.36g for medium soil. However, the response spectra given in IS 1893 (2002) and shown in Figure 9 needs to be scaled down using Eq. (A3) to arrive at the design response spectrum since comparison of actual ground motion is always made with respect to design response spectrum (ASCE 7, 2005). So, S_a(1s) = 1.36g(Z/2) = 1.36g(0.36/2) = 0.2448g. The background to this manipulation is described in Section 3.4.3 of Literature Review. Normally I/R factor in Eq. (A3) is applied to the response quantities (bending moment, shear, deflection, etc) instead of applying at the beginning of analysis.

Hence the scaling factor to match the ground motion with the design spectrum is given by:

$$\alpha = \frac{0.2448g}{0.262g(0.520)} = 1.8$$

The scaled ground motion is given in Figure 25.

Appendix B

Verification of Finite Element Results

B.1 Size of Shell Elements for Analytical Modeling of Shearwalls

Shell elements were used to model the concrete shearwall. Appendix Figure B1 shows the part of the shearwall and the associated number of shell elements that was used for the model.

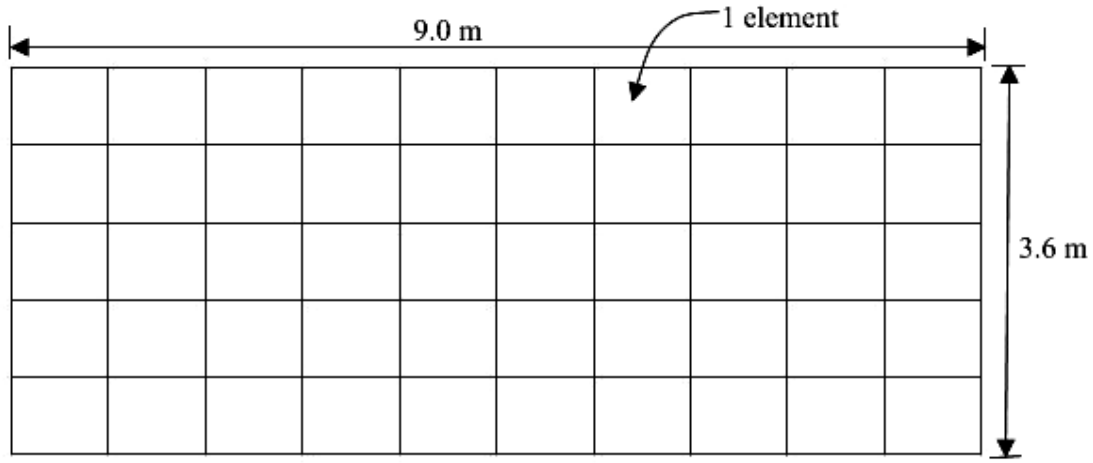

Appendix Figure B1 Analytical model of shearwall with 10 x 5 shell elements per story

Before arriving at the decision to use 10 x 5 shell elements for the shearwall, parametric test was conducted with the variation of number of shell elements both horizontally and vertically, and noting the variation of responses. It was essential to choose right amount of shell elements that reasonably simulate the behaviour of shearwall without compromising on the computer speed. Appendix Table B1 shows the parametric test runs.

To observe how fast the response quantities are converging towards the true value, the responses quantities are normalized with respect to final values and plotted on Appendix Figure B2. It can be observed that the rate of convergence is faster for base shear and base moment compared to deflection. It is also to be noted that even with the use of 2 x 1 elements, the difference in base shear and moments are within 1% , while for deflection it is within 2% of the final value.

Appendix Table B1 Parametric test program for determining size of shell elements

No. of elements		No. of Nodes	No. of DOFs	Seismic[1]			Along-wind
Hori-zontal	Ver-tical			Peak Base shear (kN)	Peak Base Moment (kNm)	Peak Roof Deflection (mm)	Roof Deflection (mm)
2	1	6	36	7872.77	302410.175	84.39	70.715
4	2	15	90	7833.46	300746.346	84.873	71.495
6	3	28	168	7826.55	300337.682	85.002	71.706
8	4	45	270	7823.43	300055.406	85.101	71.868
10	5	66	396	7821.54	299823.359	85.187	72.008

[1] Results from response spectrum analysis

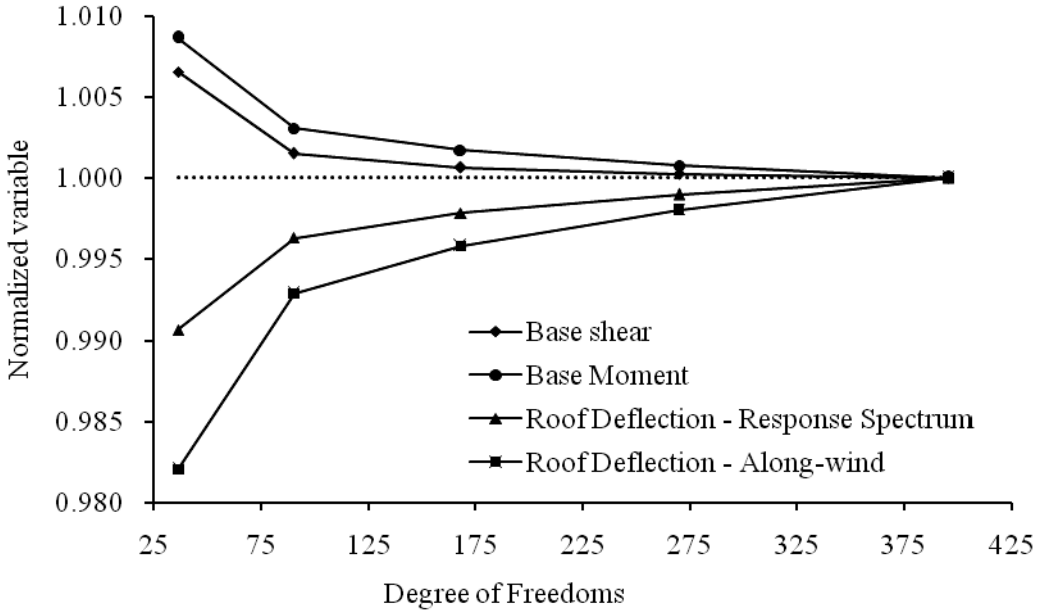

Appendix Figure B2 Variation of base shear, base moment and deflection with degree of freedoms

B.2 Story Shear for Shearwalled-frame System

Observing the unique plot of story shear in the case of shearwalled-frame system (Figure 28, Figure 29 and Figure 30), further study was carried out to find out the cause of such plot. Mode shapes and relevant parameters were extracted from the analysis, and the story shear for each mode was manually calculated. It was found that, mode 1, mode 3, mode 5 and mode 7 contributed to the total story shear in x-direction. Contribution from mode 2, mode 4, mode 6 and mode 8 were almost nil in x-direction, and are not produced here. Similarly, in the orthogonal direction, contributions to the total story shear were from mode 2, mode 4, mode 6 and mode 8.

Appendix Figure B3 shows the modal story shears. Because of its simplicity, SRSS rule was used to combine each mode to find the total story shear shown in Appendix Figure B4. However, the story shears given in main body of the thesis are a result of CQC combinations.

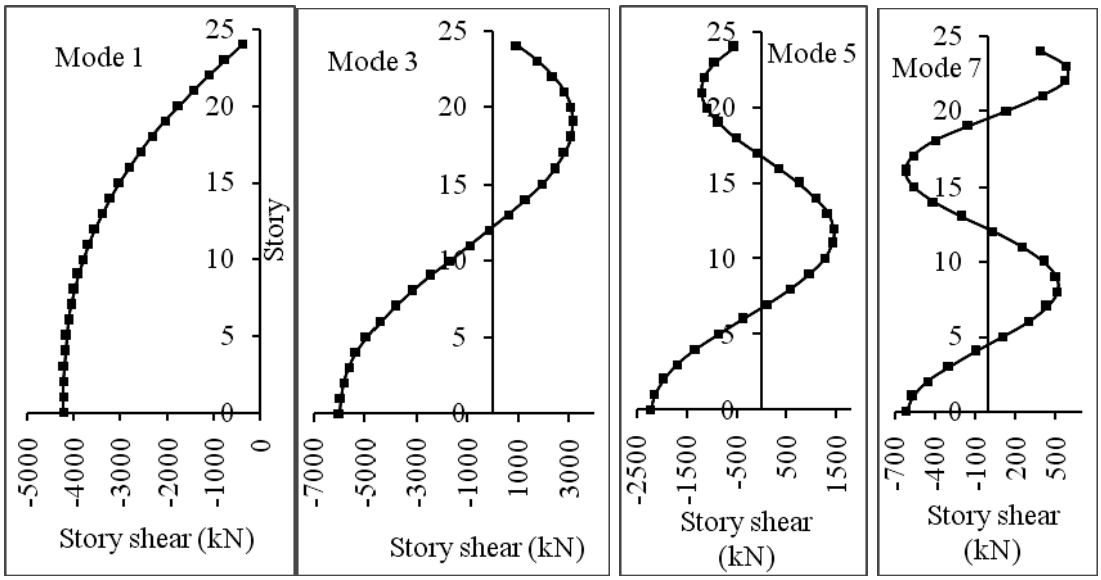

Appendix Figure B3 Modes and the corresponding story shears for shearwalled-frame system

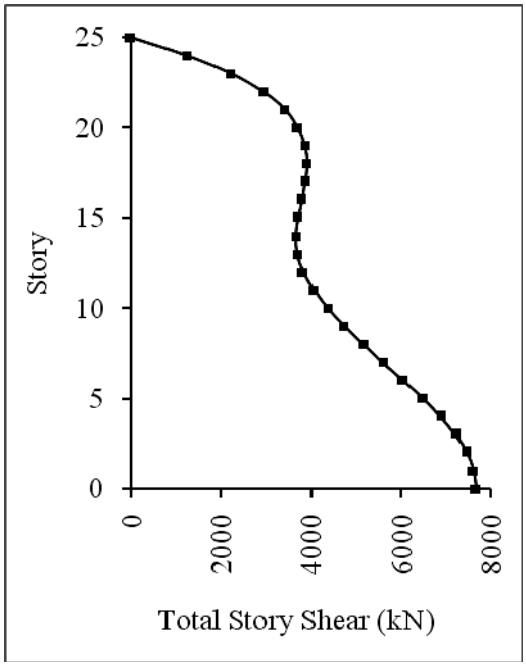

Appendix Figure B4 Total story shear for shearwalled-frame system

Appendix C

Dynamic Effects of Wind and Related Calculations

C.1 Excerpts from Indian Standard IS 875: Part 3 (2004) Wind loads on buildings and structures-Proposed draft and commentary

The procedures and necessary equations required for the computation of along-wind loading, cross-wind loading, and the corresponding horizontal acelerations are provided below.

C.1.1 Computation of along-wind load

Along-wind load on a structure at any height z is given by:

$$F_z = C_f A_e p_z C_{dyn} \tag{C1}$$

where

F_z = Along-wind equivalent static load on the structure at any height z corresponding to strip area A_e,

C_f = Force coefficient for the building from Appendix Figure C1

A_e = Effective frontal (strip) area considered for the structure at height z

$p_z = 0.6V_z^2$, wind pressure in N/m^2 at height z

$V_z = V_b(k_1k_2k_3k_4)$, design wind speed at height z

V_b = Basic wind speed (m/s) assumed as 47 m/s for this study

k_1 = Probability factor (risk coefficient) equal to 1.0 for all general buildings (Table 1; IS 875: Part 3)

k_2 = Terrain roughness and height factor (Appendix Table C1)

k_3 = Topography factor, equal to 1.0 for flat terrain or ground

k_4 = Importance factor for cyclonic regions, equal to 1.0 for general structures

C_{dyn} = Dynamic response factor given by:

$$C_{dyn} = \frac{1 + 2I_h\sqrt{g_v^2 B_s + \dfrac{H_s g_R^2 SE}{\beta}}}{\left(1 + 2g_v I_h\right)} \tag{C2}$$

I_h = Turbulence intensity, obtained from Appendix Table C2 by setting z equal to h,

h = Average roof height of building above the ground

g_v = Peak factor for the upwind velocity fluctuations, which is taken as 3.5

B_s = Background factor, which is a measure of the slowly varying background component of the fluctuating response, caused by low frequency wind speed variations, given as follows:

$$B_s = \frac{1}{1+\frac{\sqrt{\left[36(h-s)^2+64b_{sh}^2\right]}}{2L_h}} \tag{C3}$$

H_s = Height factor for the resonant response

$= 1+(s/h)^2$, s is the height above the ground at which action effects are to be calculated

g_R = Peak factor for resonant response (1 hour period) given by:

$$g_R = \sqrt{\left[2\ln(3600 f_0)\right]} \tag{C4}$$

S = Size reduction factor given as follows:

$$S = \frac{1}{\left[1+\frac{4f_0 h(1+g_v I_h)}{V_h}\right]\left[1+\frac{4f_0 b_{oh}(1+g_v I_h)}{V_h}\right]} \tag{C5}$$

E= (π/4) times the spectrum of turbulence in the approaching wind stream, given as follows:

$$E = \frac{\pi N}{\left(1+70N^2\right)^{5/6}} \tag{C6}$$

β = Ratio of structural damping to critical damping of a structure; for reinforced concrete building, β=0.02 (Table 32; IS 875: Part 3, 2004)

b_{sh} = Average breadth of the structure between heights s and h

L_h = Measure of the integral turbulence length scale at height h

$= 100(h/10)^{0.25}$

f_0 = First mode natural frequency of vibration of a structure in the along-wind direction in Hertz

b_{oh} = Average breadth of the structure between heights 0 and h

N = Reduced frequency

$= f_0 L_h[1+(g_v I_h)]/V_h$

V_h = Design wind speed at height h

Appendix Table C1 k_2 factors to obtain design wind speed variation with height in different terrains

Height (z) *(m)*	**Terrain and height multiplier *(k_2)***			
	Terrain Category 1	**Terrain Category 2**	**Terrain Category 3**	**Terrain Category 4**
10	1.05	1.00	0.91	0.80
15	1.09	1.05	0.97	0.80
20	1.12	1.07	1.01	0.80
30	1.15	1.12	1.06	0.97
50	1.20	1.17	1.12	1.10
100	1.26	1.24	1.20	1.20
150	1.30	1.28	1.24	1.24
200	1.32	1.30	1.27	1.27
250	1.34	1.32	1.29	1.28
300	1.35	1.34	1.31	1.30
350	1.37	1.36	1.32	1.31
400	1.38	1.37	1.34	1.32
450	1.39	1.38	1.35	1.33
500	1.40	1.39	1.36	1.34

NOTE: For intermediate values of height z and terrain category, use linear interpolation.

Appendix Table C2 Turbulence Intensity (I_z)

Height (z) m	Terrain category 1	Terrain category 2	Terrain category 3	Terrain category 4
10	0.157	0.183	0.239	0.342
15	0.152	0.176	0.225	0.342
20	0.147	0.171	0.215	0.342
30	0.140	0.162	0.203	0.305
40	0.133	0.156	0.195	0.285
50	0.128	0.151	0.188	0.270
75	0.118	0.140	0.176	0.248
100	0.108	0.131	0.166	0.233
150	0.095	0.117	0.150	0.210
200	0.085	0.107	0.139	0.196
250	0.080	0.098	0.129	0.183
300	0.074	0.092	0.121	0.173
400	0.068	0.082	0.108	0.155
500	0.058	0.074	0.098	0.141

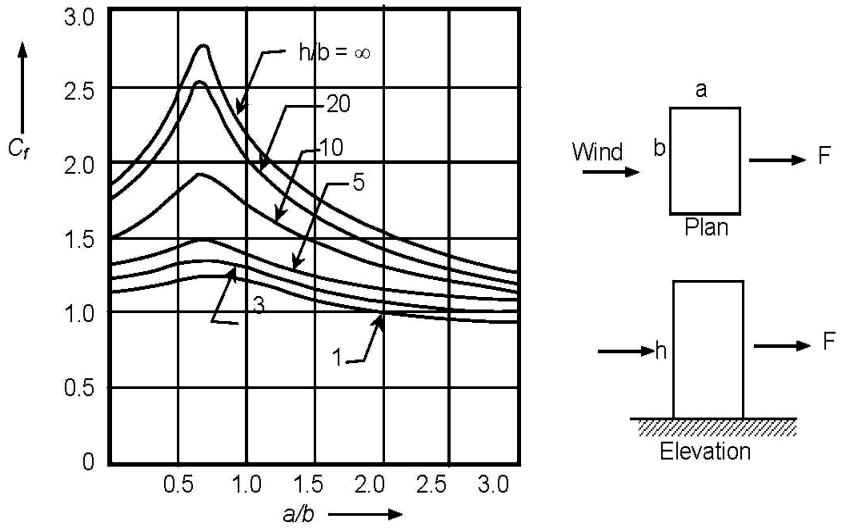

Appendix Figure C1 Force coefficients, C_f for rectangular clad building in uniform flow

C.1.2 Computation of cross-wind load

The equivalent cross-wind static force per unit height (W_e) as a function of z (in N/m) is as follows:

$$W_e(z) = 0.6V_h^2 dC_{dyn} \tag{C7}$$

where d is the lateral dimension of the building parallel to the wind stream, and

$$C_{dyn} = 1.5g_R\left(\frac{b}{d}\right)\frac{K_m}{(1+g_v I_h)^2}\left(\frac{z}{h}\right)^k\sqrt{\frac{\pi C_{fs}}{\beta}} \tag{C8}$$

where

K_m = Mode shape correction factor for cross-wind acceleration
$= 0.76+0.24k$

k = Mode shape power exponent for the fundamental mode of vibration assumed as 1.0 for this study.

C_{fs} = Cross-wind force spectrum coefficient generalized for a linear mode shape

g_R,g_v, I_h and β are defined in Section C.1.1.

C.1.3 Cross-wind force spectrum coefficient, C_{fs}

Values of cross-wind force spectrum coefficient (C_{fs}) generalized for a linear mode shape are either read from the Appendix Figure C2 or calculated from the expressions (C10) and (C11) based on the reduced velocity (V_n).

The reduced velocity, V_n is calculated as

$$V_n = \frac{V_z}{f_0 b(1+g_v I_h)} \tag{C9}$$

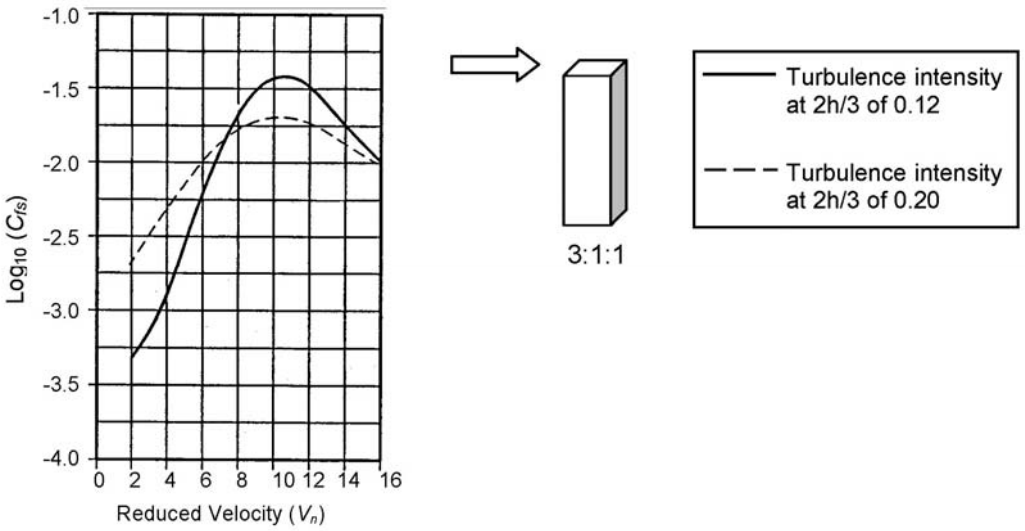

Appendix Figure C2 Cross-wind force spectrum coefficient for a 3:1:1 square section

Alternate to the Appendix Figure C2, C_{fs} can be calculated from the following expressions

$$\log_{10} C_{fs} = 0.000353V_n^4 - 0.0134V_n^3 + 0.15V_n^2 - 0.345V_n - 3.109 \qquad \text{(C10)}$$

for I_z =0.12 (at 2/3 of height), and

$$\log_{10} C_{fs} = 0.00008V_n^4 - 0.0028V_n^3 + 0.0199V_n^2 + 0.13V_n - 2.985 \qquad \text{(C11)}$$

for I_z =0.20 (at 2/3 of height)

C.1.4 Peak along-wind acceleration

The peak acceleration, $\ddot{x}_h$ at the top of a tall building in the along-wind direction is obtained from the following expression:

$$\ddot{x}_h = \frac{6}{m_0 h^2} \frac{g_R I_h \sqrt{\frac{SE}{\beta}}}{(1+2g_v I_h)} \left[\sum_{z=0}^{h} C_f p_z A_e z \right] \quad \text{(C12)}$$

where m_0 is the average mass per unit height (kg/m).

The acceleration at any height may be obtained by considering it to vary linearly with height.

C.1.5 Peak cross-wind acceleration

The peak cross-wind acceleration, $\ddot{y}_h$ at the top of a tall building is given by the following expression:

$$\ddot{y}_h = \frac{0.90 b g_R}{m_0} \left[\frac{V_h}{1+g_v I_h} \right]^2 K_m \sqrt{\frac{\pi C_{fs}}{\beta}} \quad \text{(C13)}$$

Definitions for all variables are same as those in Section C.1.1 except that the expression of g_R is modified in the following manner to compare for 10-minute wind given in Figure 13:

$$g_R = \sqrt{2 \ln(600 f_0)} \quad \text{(C14)}$$

C.2 Lateral Load due to Dynamic Effects of Wind - Example Calculations

Since the fundamental frequency of the building was less than 1 Hz for all the models, dynamic analysis was needed. The calculation procedure is demonstrated for the rigid frame system for Case 3 model. The width of the strip area is taken as the full width of the building in this calculation.

Wind and building data:
Basic wind speed, V_b = 47 m/s
Terrain category 3 (IS 875: Part 3, Sec 5.3.2.1)

Building: width, b = 27 m; depth, a = 27 m; height, h= 90 m

Design Factors:

Risk coefficient factor, k_1 =1.0 (IS 875: Part 3, Sec 5.3.1, Table 1)

Terrain and Height factor, k_2 varies with height (Appendix Table C1)

Topography factor, k_3 = 1.0 (IS 875: Part 3, Sec 5.3.3.1)

Cyclonic region factor, k_4 = 1.0 (IS 875: Part 3, Sec 5.3.4)

Design wind pressure:

Design wind speed, $V_z = V_b$ (k_1 x k_2 x k_3 x k_4)

= 47 (1.0 x k_2 x1.0 x 1.0)

= 47k_2 (m/s)

Design wind pressure, $p_z = 0.6V_z^2$

Along-wind load calculation

Lateral force due to wind in the along-wind direction is given by the Eq. (C1).

For a/b = 27/27 =1.0, h/b = 90/27 = 3.33, C_f = 1.35 (Appendix Figure C1)

Dynamic response factor calculations:

h = 90 m, b_{oh} = 27 m, d = 27 m

L_h =100(90/10)$^{0.25}$ = 173.205 m

f_0 =1/T = 1/4.23 = 0.236 Hz, β = 0.02 (IS 875: Part 3, Table 31)

For base floor (s=0)

$$B_s = \frac{1}{1+\frac{\left[36(90-0)^2+64x27^2\right]^{0.5}}{2x173.205}} = 0.373$$

$H_s = 1 + (0/90)^2 = 1$, V_h = 55.65 m/s at h = 90 m

$$g_R = \sqrt{2\ln(3600x0.236)} = 3.673$$

I_h = 0.170 (from Appendix Table C2, corresponding to Terrain category 3)

g_v = 3.5 (Section C.1.1)

$$S = \frac{1}{\left[1+\frac{4x0.236x90(1+3.5x0.170)}{55.65}\right]\left[1+\frac{4x0.236x27(1+3.5x0.170)}{55.65}\right]} = 0.1679$$

$$N = \frac{0.236x173.205(1+3.5x0.170)}{55.65} = 1.1736$$

$E = \pi N/(1+70N^2)^{5/6} = 0.0812$

$$C_{dyn} = \frac{1+2x0.17\left[3.5^2 x0.373+\frac{1x3.673^2 x0.1679x0.0812}{0.02}\right]^{0.5}}{(1+2x3.5x0.170)} = 1.033$$

Using the above procedure, along-wind forces over the height of the building is obtained, and produced in Appendix Table C3.

Cross-wind load calculation

The cross-wind static force is given by the expression(C7).

$K_m = 0.76 + 0.24k = 1.00$ for k = 1 (linear mode)

For z = h, $V_n = 55.65/[0.236x27(1+3.5x0.170)] = 5.47$

$I_h = 0.183$ (at 2/3 of height of building, i.e. at 60 m above ground)

Using the expressions (C10) and (C11) or from Appendix Figure C2, we have

$\text{Log}_{10} C_{fs} = -2.3851$, $C_{fs} = 0.00412$ for $I_z = 0.12$ (at 2/3 of height)

$\text{Log}_{10} C_{fs} = -2.0651$, $C_{fs} = 0.00861$ for $I_z = 0.20$ (at 2/3 of height)

$\therefore C_{fs} = 0.00767$ for $I_z = 0.183$ (at 2/3 of height) after the interpolation.

$$C_{dyn} = 1.5x3.673\left(\frac{27}{27}\right)\frac{1}{(1+3.5x0.183)^2}\left(\frac{z}{90}\right)^1\sqrt{\frac{\pi x0.00767}{0.02}} = 0.02497z$$

Using the above procedure, cross-wind lateral forces over the height of the building is obtained, and reproduced in Appendix Table C3.

Appendix Table C3 Along-wind and cross-wind load for rigid frame system (Case 3 model) – Example calculations

Height (m)	Height factor, k	V_z (m/s)	p_z (kN/m^2)	Along-wind				Cross-wind	
				B_s	H_s	C_{dyn}	Force (kN)	C_{dyn}	Force (kN)
0.0	0.910	42.77	1.098	0.373	1.000	1.033	74.37	0.000	0.00
3.6	0.910	42.77	1.098	0.382	1.002	1.035	149.08	0.090	16.22
7.2	0.910	42.77	1.098	0.390	1.006	1.038	149.52	0.180	32.43
10.8	0.920	43.22	1.121	0.399	1.014	1.042	153.25	0.269	48.65
14.4	0.963	45.25	1.229	0.408	1.026	1.046	168.70	0.359	64.86
18.0	0.994	46.72	1.310	0.418	1.040	1.051	180.68	0.449	81.08
21.6	1.018	47.85	1.374	0.428	1.058	1.057	190.54	0.539	97.29
25.2	1.036	48.69	1.423	0.438	1.078	1.063	198.52	0.628	113.51
28.8	1.054	49.54	1.472	0.448	1.102	1.070	206.82	0.718	129.72
32.4	1.067	50.16	1.510	0.459	1.130	1.078	213.52	0.808	145.94
36.0	1.078	50.67	1.540	0.471	1.160	1.086	219.49	0.898	162.15
39.6	1.089	51.17	1.571	0.482	1.194	1.095	225.68	0.988	178.37
43.2	1.100	51.68	1.603	0.494	1.230	1.104	232.09	1.077	194.58
46.8	1.110	52.19	1.634	0.507	1.270	1.113	238.72	1.167	210.80
50.4	1.121	52.67	1.664	0.519	1.314	1.123	245.33	1.257	227.01
54.0	1.126	52.94	1.682	0.531	1.360	1.134	250.15	1.347	243.23
57.6	1.132	53.21	1.699	0.544	1.410	1.144	255.11	1.437	259.44
61.2	1.138	53.48	1.716	0.556	1.462	1.155	260.20	1.526	275.66
64.8	1.144	53.75	1.734	0.568	1.518	1.167	265.41	1.616	291.87
68.4	1.149	54.02	1.751	0.579	1.578	1.178	270.72	1.706	308.09
72.0	1.155	54.29	1.769	0.589	1.640	1.190	276.13	1.796	324.30
75.6	1.161	54.57	1.786	0.598	1.706	1.201	281.62	1.885	340.52
79.2	1.167	54.84	1.804	0.606	1.774	1.213	287.17	1.975	356.73
82.8	1.172	55.11	1.822	0.611	1.846	1.225	292.78	2.065	372.95
86.4	1.178	55.38	1.840	0.615	1.922	1.236	298.42	2.155	389.16
90.0	1.184	55.65	1.858	0.616	2.000	1.247	152.05	2.245	202.69

The same load calculation was repeated for other structural systems for three Cases of models, thus amounting to 15 such tabulated calculations. For brevity, other tables have been excluded from here. It is also worthy to note that only a portion of cross-wind force was applied to the building according to the reasons highlighted in Section 3.4.4 of Literature Review.

C.3 Horizontal Acceleration for Case 3 models - Example Calculations

Calculation procedures for the horizontal acceleration at roof level are demonstrated using the rigid frame structural system for Case 3 model.

Mass per unit height, m_0 = 237476 kg/m
Fundamental natural frequency of the building, f_0 = 1/4.23 = 0.236 Hz
$g_R = [2 \ln(600x0.236)]^{0.5} = 3.148$ (10-minute wind)
g_v = 3.5 (Section C.1.1)

C.3.1 Along-wind acceleration

Turbulence Intensity, I_h = 0.170
Serviceable wind speed, V_s = 0.66 x 47 m/s (0.66 from Table C6-7; ASCE 7, 2005)
= 31.02 m/s (for 5-year return period)
Serviceable wind speed at height, h =90 m, V_h = 36.73 m/s

$$S = \frac{1}{\left[1+\frac{4x0.236x90(1+3.5x0.170)}{36.73}\right]\left[1+\frac{4x0.236x27(1+3.5x0.170)}{36.73}\right]} = 0.101$$

$$N = \frac{0.236x173.205(1+3.5x0.170)}{36.73} = 1.778$$

$E = \pi N/(1+70N^2)^{5/6} = 0.0618$

Appendix Table C4 Calculation of $\sum C_f p_z A_e Z$

Height (m)	**k_2**	**V_z (m/s)**	**p_z (N/m^2)**	**A_e (m^2)**	**$C_f p_z A_e Z$ (Nm)**
0.0	0.910	28.23	478.10	48.6	0.0
3.6	0.910	28.23	478.10	97.2	2.259E+05
7.2	0.910	28.23	478.10	97.2	4.517E+05
10.8	0.920	28.53	488.24	97.2	6.919E+05
14.4	0.963	29.87	535.19	97.2	1.011E+06
18.0	0.994	30.83	570.44	97.2	1.347E+06
21.6	1.018	31.58	598.32	97.2	1.696E+06
25.2	1.036	32.14	619.66	97.2	2.049E+06
28.8	1.054	32.70	641.38	97.2	2.424E+06
32.4	1.067	33.10	657.55	97.2	2.796E+06
36.0	1.078	33.44	670.92	97.2	3.169E+06
39.6	1.089	33.77	684.43	97.2	3.557E+06
43.2	1.100	34.11	698.08	97.2	3.957E+06
46.8	1.110	34.44	711.86	97.2	4.372E+06
50.4	1.121	34.76	725.05	97.2	4.795E+06
54.0	1.126	34.94	732.52	97.2	5.191E+06
57.6	1.132	35.12	740.03	97.2	5.593E+06
61.2	1.138	35.30	747.58	97.2	6.004E+06
64.8	1.144	35.48	755.17	97.2	6.421E+06
68.4	1.149	35.66	762.79	97.2	6.846E+06
72.0	1.155	35.83	770.46	97.2	7.279E+06
75.6	1.161	36.01	778.16	97.2	7.720E+06
79.2	1.167	36.19	785.90	97.2	8.168E+06
82.8	1.172	36.37	793.68	97.2	8.623E+06
86.4	1.178	36.55	801.50	97.2	9.087E+06
90.0	1.184	36.73	809.35	48.6	4.779E+06

$$\sum_{z=0}^{h} C_f p_z A_e z = 1.083x10^8 \text{ Nm}$$

$$\ddot{x}_h = \frac{6}{237476x90^2}\frac{3.148x0.170\sqrt{\frac{0.101x0.0618}{0.02}}}{(1+2x3.5x0.170)}\left[1.083x10^8\right] = 0.046 \text{ m/s}^2$$

$$= 4.7 \text{ milli-g}$$

C.3.2 Cross-wind horizontal acceleration

$K_m = 0.76 + 0.24k = 1.00$ for k = 1 (linear mode)

For z = h, $V_n = 36.73/[0.236x27(1+3.5x0.170)] = 3.61$

$I_h = 0.183$ (at 2/3 of height of building, i.e. at 60 m above ground)

Using the expressions (C10) and (C11) or using the Appendix Figure C2, we have

$\text{Log}_{10} C_{fs} = -2.9701$, $C_{fs} = 0.00107$ for $I_z = 0.12$ (at 2/3 of height)

$\text{Log}_{10} C_{fs} = -2.3745$, $C_{fs} = 0.00422$ for $I_z = 0.20$ (at 2/3 of height)

$\therefore C_{fs} = 0.00356$ for $I_z = 0.183$ (at 2/3 of height) after the interpolation

$$\ddot{y}_h = \frac{0.90x27x3.148}{237476}\left[\frac{36.73}{1+3.5x0.183}\right]^2 1\sqrt{\frac{\pi x0.00356}{0.02}} = 0.121 \text{ m/s}^2$$

$$= 12.3 \text{ milli-g}$$

Similar procedures had been followed to compute the horizontal acceleration for the other structural systems under the effect of wind, and are produced in Table 17.

Appendix D

Quantity Analysis of Structural Materials

D.1 Quantity of Structural Materials for five Structural Systems

Quantity of structural materials required for the five structural systems are summarized in the following tables.

Appendix Table D1 Quantity of structural materials for main structural members

Structural Systems	Concrete			Reinforcement				
				Columns		Beams		Slabs
	Columns (m^3)	Beams (m^3)	Slabs (m^3)	Main rebar (kg)	Column Ties (kg)	Main rebar (kg)	Beam Stirrups (kg)	Rebar (kg)
Rigid Frame	1559	1819	1879	118177	12517	165052	47388	93080
Shearwalled-Frame	683	1646	1879	89343	6105	128415	39861	136640
Framed-Tube	1211	2055	1882	160878	9317	210938	50652	128673
Braced-Tube	1134	1819	1882	163536	9012	137056	41493	126258
Outrigger	683	1646	1879	81187	6147	132873	28784	136775

Appendix Table D2 Quantity of structural materials for additional structural members

Structural Systems	Concrete (m^3)	Steel (kg)	Rebar (kg)	Ties (kg)	Remarks
Shearwalled-Frame	1127	-	52508	-	Shearwall
Braced-Tube	85	68148	25588	1887	Diagonal bracing
Outrigger	1127	-	56583	-	Shearwall
	15	9657	1818	377	Outrigger truss

D.2 Mix Design for M35 grade Concrete as per IS10262 (1982) Indian Standard Recommended Guidelines for Concrete Mix Design

Mix design for M35 grade of concrete, having moderate workability (slump range 50 mm~75 mm).

Step 1. Design stipulations

Characteristic compressive strength required in the field at 28 days	35 N/mm^2
Maximum size of aggregate	20 mm (angular)
Degree of workability	0.90 compacting factor
Degree of quality control	Good
Type of exposure	Severe (Table 3; IS 456)

Step 2. Test data for materials

Cement	53 grade (OPC)
Specific gravity of cement	3.15
Specific gravity of fine aggregate	2.6
Specific gravity of coarse aggregate	2.6
Fraction of aggregate sizes	
Coarse aggregate	
20 mm	70%
10 mm	30%
Fine aggregate	Grading Zone I

Normally, the Grading zone for fine aggregate, percent composition of different size of coarse aggregate are established based on the sieve analysis. Likewise, specific gravity of cement, sand and coarse aggregate are determined from the laboratory test. For the sake of this study, the above values are adopted.

Step 3. Target mean strength of concrete

The target mean strength of the concrete is given by the following formula

$$\overline{f}_{ck} = f_{ck} + 1.65\sigma \qquad \text{(D1)}$$

where

$\overline{f}_{ck}$ = Target average compressive strength at 28 days

f_{ck} = Characteristic compressive strength at 28 days

σ = Standard deviation, equal to 5 N/mm^2 (Table 8; IS 456, 2000)

Thus, for M35 grade concrete is

$$\overline{f}_{ck} = 35 + 1.65\text{x}5$$

$$= 43.3 \text{ N/mm}^2$$

Step 4. Determine water cement ratio

From Figure 1 of IS10262 (1982), using strength curve F (which roughly corresponds to the OPC 53 grade), the free water cement ratio required for the target mean strength of 43.3 N/mm^2 = 0.43. This value is less than the maximum value of 0.45 allowed by IS 456 (2000) for durability requirement.

From Table 4 of IS10262 (1982), for 20 mm nominal maximum size aggregate and compaction factor of 0.8, water content per cubic meter of concrete = 186 kg
Add 3% water for incremental compaction factor of 0.1 (i.e. 3% of 186 kg = 5.58 kg)
∴ Water demand = 186 + 5.58 = 191.58 kg

∴ Cement content = mass of water/water cement ratio

$$= 191.58/0.43$$

$$= 445.53 \text{ kg/m}^3$$

This is more than the minimum requirement of 340 kg/m^3 as per Table 5 of IS 456 (2000) and less than the maximum allowable cement content of 450 kg/m^3 (IS 456, 2000).

Step 5. Determine coarse and fine aggregate

From Table 4 of IS10262 (1982), for 20 mm nominal maximum size aggregate and sand conforming to grading Zone II, compaction factor of 0.8, and w/c ratio of 0.6, sand content as percentage of total aggregate by absolute volume =35%

Adjustment of fine aggregate required for the conditions other than the conditions used for deriving the Table 4 of IS10262 (1982)

Fine aggregate (sand) conforming to grading zone I	+1.5%
Decrease of water cement ratio (0.6-0.43)	-3.4%
(0.05 decrease of water content @ -1% sand reduction)	
∴Net sand content (% of total aggregate by absolute volume)	33.1%

Total aggregate content per unit volume of concrete is calculated from the following equations:

$$V = \left[W + \frac{C}{S_c} + \frac{1}{p}\frac{f_a}{S_{fa}} \right] \frac{1}{1000} \text{ , and} \qquad \text{(D2)}$$

$$V = \left[W + \frac{C}{S_c} + \frac{1}{(1-p)}\frac{c_a}{S_{ca}} \right] \frac{1}{1000} \qquad \text{(D3)}$$

where

V = Absolute volume of fresh concrete, which is equal to gross volume (m^3) minus the volume of entrapped air,

W = Mass of water (kg) per m^3 of concrete,

C = Mass of cement (kg) per m^3 of concrete,

S_c = Specific gravity of cement,

p = Ratio of fine aggregate to total aggregate by absolute volume,

f_a, c_a = Total masses of fine aggregate and coarse aggregate (kg) per m^3 of concrete respectively, and

S_{fa}, S_{ca} = Specific gravities of saturated surface dry fine aggregate and coarse aggregate respectively.

Entrapped air as percent of volume of wet concrete = 2% (Table 3; IS10262, 1982).

Using Equations (D2) and (D3), we have

$$0.98\ m^3 = \left[191.58 + \frac{445.53}{3.15} + \frac{1}{(0.331)}\frac{f_a}{2.6}\right]\frac{1}{1000} \quad \text{, and}$$

$$0.98\ m^3 = \left[191.58 + \frac{445.53}{3.15} + \frac{1}{(1-0.331)}\frac{c_a}{2.6}\right]\frac{1}{1000}$$

Thus, we get

Total mass of fine aggregate, f_a = 556.79 kg

Total mass of coarse aggregate, c_a = 1125.36 kg

Thus, for 1 m^3 of concrete of M35 grade, the quantity of materials required is

Cement	446 kg
Water	192 litre
Sand	557 kg
Crushed stone (20 mm downwards)	1125 kg

For this study, use of mineral admixture as well as chemical admixture has been omitted. The inclusion of admixture would demand sophisticated analysis, and the composition of concrete would certain be altered from what is derived above.

D.3 Rate of Materials

Based on the BSR (2007), rate of cement, sand and crushed stones are given in Appendix Table D3. The rate for steel is 32.8 per kilogram. These rates are inclusive of the transportation cost from the probable place of origin of materials to the place of destination, Thimphu, the capital city of Bhutan. The place of origin for materials is assumed as Phuentsholing, a town near the Indian border and is 179 km away from Thimphu, the capital city of Bhutan.

Appendix Table D3 Cost estimation for unit volume (1 m^3) of concrete

Items	Rate per kg	Materials (kg)	Cost of Materials (Nu.)[1]
Cement	5.59	446	2493.14
Sand	0.30	557	167.10
Crushed stone	1.51	1125	1698.75
		Total	**4358.99**

[1] USD$1.00 = Nu. 38

CURRICULUM VITAE

NAME : Mr. Rinchen

BIRTH DATE : 4th September, 1972

BIRTH PLACE : Wengkhar, Mongar, Bhutan

EDUCATION :

YEAR	INSTITUTE	DEGREE/DIPLOMA
1999	Sydney University	B.Eng. (Civil Engineering)
2008	Kasetsart University	M.Eng. (Civil Engineering)

POSITION/TITLE : Civil Engineer

WORK PLACE : Ministry of Works and Human Settlement, Thimphu, Bhutan